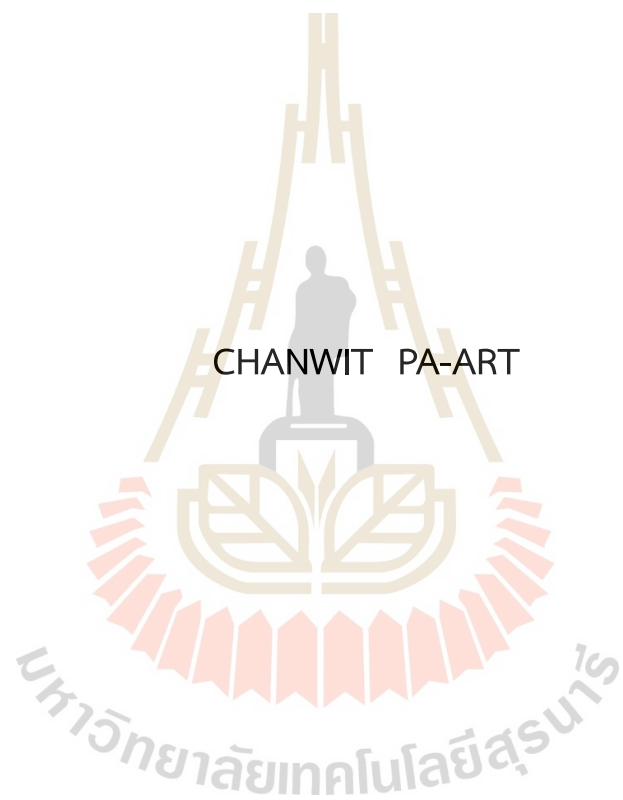


STUDY OF MECHANICAL PROPERTIES OF 3D PRINTED
CARBON-BASED COMPOSITE RESIN



A Thesis Submitted in Partial Fulfillment of the Requirements for the
Degree of Master of Science in Physics
Suranaree University of Technology
Academic Year 2022

การศึกษาคุณสมบัติเชิงกลของเรซินผสมสารประกอบคาร์บอนที่พิมพ์ด้วย
เครื่องพิมพ์สามมิติ



นายชาญวิทย์ พาอาจ

วิทยานิพนธ์นี้เป็นส่วนหนึ่งของการศึกษาตามหลักสูตรปริญญาวิทยาศาสตรมหาบัณฑิต

สาขาวิชาฟิสิกส์

มหาวิทยาลัยเทคโนโลยีสุรนารี

ปีการศึกษา 2565

STUDY OF MECHANICAL PROPERTIES OF 3D PRINTED
CARBON-BASED COMPOSITE RESIN

Suranaree University of Technology has approved this thesis submitted in partial fulfillment of the requirements for a Master's Degree.

Thesis examination committee



(Assoc. Prof. Dr. Panomsak Meemon)

Chairperson



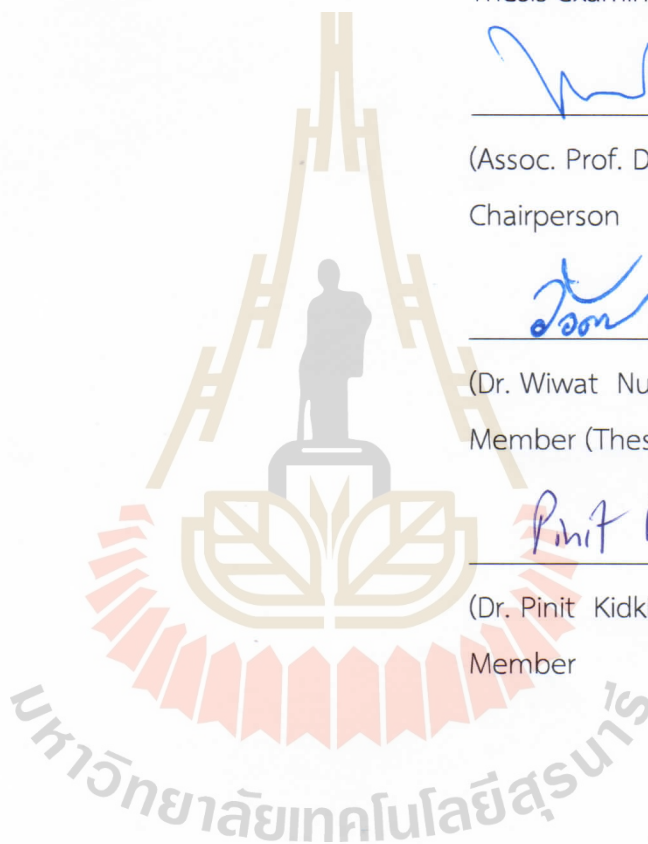
(Dr. Wiwat Nuansing)

Member (Thesis advisor)



(Dr. Pinit Kidkhunthod)

Member



(Assoc. Prof. Dr. Yupaporn Ruksakulpiwat)

Vice Rector for Academic Affairs
and Quality Assurance



(Prof. Dr. Santi Maensiri)

Dean of Institute of Science

ชาญวิชญ์ พาอาจ : การศึกษาคุณสมบัติเชิงกลของเรซินผสมสารประกอบคาร์บอนที่พิมพ์ด้วย
เครื่องพิมพ์สามมิติ (STUDY OF MECHANICAL PROPERTIES OF 3D PRINT CARBON-
BASED COMPOSITE RESIN) อาจารย์ที่ปรึกษา : อาจารย์ ดร.วิวัฒน์ นวลสิงห์, 121 หน้า

คำสำคัญ: การพิมพ์สามมิติ, การพิมพ์แบบเสริมความแข็งแรง, สารประกอบคาร์บอน, คุณสมบัติเชิงกล

การพิมพ์สามมิติมีบทบาทสำคัญในหลากหลายอุตสาหกรรม เนื่องจากเป็นเทคโนโลยีที่ช่วยสร้างชิ้นงานได้อย่างรวดเร็วและยืดหยุ่น แต่ข้อจำกัดสำคัญของเรซินที่ใช้ในกระบวนการพิมพ์สามมิติแบบแอลซีดี (LCD 3D Printing) คือ สมบัติเชิงกลที่ยังไม่แข็งแรงเพียงพอสำหรับการใช้งานที่ต้องรับแรงมาก การพัฒนาสารเติมแต่งเพื่อปรับปรุงสมบัติเชิงกลของเรซินจึงเป็นหัวข้อที่ได้รับความสนใจอย่างมาก วิทยานิพนธ์ฉบับนี้มุ่งเน้นการศึกษาคุณสมบัติและประสิทธิภาพของ ไรดิออกไซด์ (rGO) และ วัสดุลำคาร์บอนนาโนทิวบ์ (MWCNT) ซึ่งเป็นวัสดุคาร์บอนที่มีคุณสมบัติโดดเด่น เช่น ความแข็งแรงและความยืดหยุ่นสูง ในการใช้เป็นสารเติมแต่งเพื่อเสริมสมบัติเชิงกลของเรซินสำหรับการพิมพ์สามมิติ วัตถุประสงค์ของวิทยานิพนธ์นี้คือ เพื่อศึกษาผลลัพธ์ที่ได้จากการผสม rGO และ MWCNT ในอัตราส่วน 0.1% w/w โดยคุณสมบัติเชิงกลที่ทำการศึกษาคือมอดูลัสของยัง (Young's modulus) และค่าความทนต่อแรงดึง (maximum tensile strength) ของชิ้นงานที่พิมพ์จากเครื่องพิมพ์สามมิติ การทดสอบแรงดึงดำเนินการตามมาตรฐาน ASTM D638 type V ผลการวิจัยพบว่าชิ้นงานที่ใช้เรซินเสริมสาร rGO และ MWCNT มีค่ามอดูลัสของยังและค่าความทนต่อแรงดึงเพิ่มขึ้นเมื่อเปรียบเทียบกับเรซินทั่วไป ผลลัพธ์เหล่านี้แสดงให้เห็นว่าสารประกอบคาร์บอนนาโนทั้งสองชนิดมีศักยภาพสูงในการเพิ่มสมบัติเชิงกลของชิ้นงานที่พิมพ์ด้วยเครื่องพิมพ์สามมิติได้อย่างมีประสิทธิภาพ ผลการทดลองนี้สามารถนำไปต่อยอดเพื่อการวิจัยและพัฒนาเกี่ยวกับวัสดุเพื่อการเสริมประสิทธิภาพหรือการใช้วัสดุคาร์บอนอื่นๆได้ในอนาคต

สาขาวิชาฟิสิกส์
ปีการศึกษา 2565

ลายมือชื่อนักศึกษา ชาญวิชญ์ พาอาจ
ลายมือชื่ออาจารย์ที่ปรึกษา วิวัฒน์ นวลสิงห์

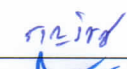
CHANWIT PA-ART : STUDY OF MECHANICAL PROPERTIES OF 3D PRINT CARBON-BASED COMPOSITE RESIN. THESIS ADVISOR : WIWAT NUANSING, Ph.D. 121 PP.

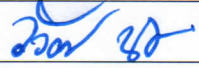
Keyword: 3D printing; reinforced printing; carbon composite; mechanical properties

3D printing is an important technology in many industries because it allows for quick and flexible production of parts. However, resins used in LCD 3D printing often lack the mechanical strength needed for high load-bearing applications. Adding materials to improve the mechanical properties of these resins has become a key area of research. This study examines the use of reduced graphene oxide (rGO) and multi-wall carbon nanotube (MWCNT) as additives. These carbon-based nanomaterials are known for their high strength and flexibility. The research focuses on adding 0.1% w/w of rGO or MWCNT to resin to enhance its mechanical properties. The mechanical properties studied include the Young's modulus and maximum tensile strength of 3D-printed samples. Tensile testing was performed using the ASTM D638 type V standard. The results show that resin with rGO or MWCNT has higher Young's modulus and maximum tensile strength compared to regular resin. This demonstrates that these carbon-based nanomaterials can effectively improve the mechanical properties of 3D-printed parts. The findings confirm that rGO and MWCNT are promising additives for strengthening resins used in LCD 3D printing. Future research could focus on refining the additive ratios and exploring other carbon-based materials to achieve even better results.

School of Physics

Academic Year 2022

Student's Signature _____ 

Advisor's Signature _____ 

ACKNOWLEDGEMENT

I would like to express my deepest gratitude to my thesis advisor, Dr. Wiwat Nuansing, for their unwavering guidance, invaluable insights, and constant encouragement throughout this research journey. Their expertise and support have been instrumental in shaping this thesis.

I extend my heartfelt thanks to the members of my thesis committee, Assoc. Prof. Dr. Panomsak Meemon and Dr. Pinit Kidkhunthod, for their valuable feedback and constructive suggestions that helped improve the quality of this work.

I am also thankful to the research team at Advance Material Physics lab, whose collaboration and assistance were integral to the successful execution of the experiments and data analysis.

Furthermore, I wish to acknowledge the financial support provided by Science Achievement Scholarship of Thailand, SAST, which enabled the completion of this research.

Finally, I am grateful to my family and friends for their unwavering encouragement and understanding, which kept me motivated during the challenging phases of this thesis.

Chanwit Pa-art

CONTENTS

	Page
ABSTRACT IN THAI.....	I
ABSTRACT IN ENGLISH.....	II
ACKNOWLEDGEMENT.....	III
CONTENTS.....	IV
LIST OF FIGURES.....	VI
LIST OF ABBREVIATIONS.....	IX
CHAPTER	
I INTRODUCTION.....	1
1.1 Background and motivation.....	1
1.2 Research objectives.....	2
II LITERATURE REVIEW.....	3
2.1 LCD 3D printing.....	3
2.2 Reduced graphene oxide.....	5
2.3 Carbon nanotubes.....	6
2.4 Tensile testing.....	7
III METHODOLOGY.....	12
3.1 Materials, instruments and printing conditions.....	12
3.1.1 Materials and instruments.....	12
3.1.2 Printing conditions.....	12
3.2 Material characterization.....	15
3.3 Resin and composite resin preparation.....	15
3.4 Tensile testing.....	16
IV RESULT AND DISCUSSION.....	19

CONTENTS (Continued)

	Page
4.1 Material characterization and analysis.....	19
4.1.1 Reduced graphene oxide (rGO).....	19
4.1.2 Multi-walled carbon nanotubes (MWCNT).....	21
4.2 Preliminary experiments.....	22
4.3 Printed samples characteristics.....	24
4.4 Mechanical properties.....	27
4.4.1 Mechanical properties of normal resin.....	28
4.4.2 Mechanical properties of 0.1%w rGO composite resin.....	30
4.4.3 Mechanical properties of 0.1%w MWCNT composite resin.....	32
4.4.4 Elongation at break.....	33
V CONCLUSION.....	37
REFERENCES.....	40
APPENDICES	43
APPENDIX A THE STRESS-STRAIN CURVE OF EACH CONDITION.....	44
APPENDIX B PUBLICATION AND PRESENTATION.....	115
CURRICULUM VITAE.....	121

LIST OF FIGURES

Figure	Page
2.1 Demonstration of LCD resin printer while printing each layer.....	4
2.2 The stress-strain curve obtained through experimental testing, specifically a tensile test.....	10
3.1 A schematic representing the dimensions of the ASTM D638 Type V model used for tensile testing.....	14
3.2 The 3D model CAD schematic illustrates the dimensional representation of the ASTM D638 Type V model used for tensile testing in mm.....	14
3.3 The samples were printed in three different orientations, x, y, and z orientations.....	15
3.4 The diagram illustrates the experimental process employed for the carbon-based added resin.....	16
3.5 During the analysis of the stress-strain curve, the calculation of Young's modulus involves determining the slope of the linear elastic region. Additionally, valuable data concerning the elongation at break can be obtained by evaluating the tensile stress percentages from the curve.....	18
4.1 The SEM image of rGO, captured at an EHT of 3 kV with a magnification of 1000x, reveals a clumped structure rather than the expected flat sheet morphology (left). The EDS spectrum of rGO indicates an elemental composition of 5.39 wt% carbon, 40.15 wt% oxygen, and 6.46 wt% sulfur (right).....	19

LIST OF FIGURES (Continued)

Figure	Page
4.2	22
<p>The SEM image of MWCNT, captured at an EHT of 3 kV with a magnification of 5000x, show that the MWCNTs are not present as isolated single tubes but instead form grouped, thread-like bundles (left). The EDS analysis indicates that the MWCNTs are composed of 98.6 wt% carbon and 1.4 wt% oxygen (right).....</p>	
4.3	23
<p>The preceding samples encountered issues with shear forces and fracture occurred around the grip area rather than at the neck region.....</p>	
4.4	24
<p>The previous grip (left) had a smooth surface contact in contrast to the current grip (right), which features a rough texture.....</p>	
4.5	25
<p>After the grip change, the samples demonstrated a consistent pattern, with fracture occurring exclusively around the neck region in all the tested samples. The Figure provided illustrates the 8s neat resin samples after undergoing tensile testing.....</p>	
4.6	26
<p>The overshoot effect is evident in the y orientation samples from 4s to 20s exposure time. Although the 4s and 8s samples presented minor issues, the 12s, 16s, and 20s samples exhibited more prominent overshooting, even after recalibrating the 3D printer using three layers of A4 paper.....</p>	
4.7	27
<p>The calibration process of the Elegoo Mars 3 3D printer can be demonstrated effectively by employing three pieces of A4 papers.....</p>	
4.8	29
<p>The maximum tensile strength of the neat resin is displayed in MPa units, corresponding to the exposure time for the x, y, and z orientations.....</p>	
4.9	29
<p>The Young's modulus of the neat resin is displayed in GPa units, corresponding to the exposure time for the x, y, and z orientations.....</p>	

LIST OF FIGURES (Continued)

Figure	Page
4.10 The maximum tensile strength of the 0.1% w/w rGO composite resin is displayed in MPa units, corresponding to the exposure time for the x, y, and z orientations.....	31
4.11 The Young's modulus of the 0.1% w/w rGO composite resin is displayed in GPa units, corresponding to the exposure time for the x, y, and z orientations.....	31
4.12 The maximum tensile strength of the 0.1% w/w MWCNT composite resin is presented in units of MPa, corresponding to the exposure time for each of the x, y, and z orientations.....	32
4.13 The Young's modulus of the 0.1% w/w MWCNT composite resin is presented in units of GPa, corresponding to the exposure time for each of the x, y, and z orientations.....	33
4.14 The plot represents the elongation at break corresponding to the exposure time for each orientation of the neat resin samples. The data reveals that the maximum percent elongation observed was $4.28 \pm 0.73\%$, while the minimum was $2.15 \pm 0.31\%$	34
4.15 The plot represents the elongation at break corresponding to the exposure time for each orientation of the 0.1% added rGO resin samples.....	35
4.16 The plot illustrates the elongation at break for the 0.1% added MWCNT resin samples, corresponding to the exposure time for each orientation.....	35

LIST OF ABBREVIATIONS

3D	Three Dimension
ASTM	American Society for Testing and Materials
CAD	Computer-aided Design
CNT	Carbon Nanotube
DLP	Digital Light Projector
E	Young's Modulus
FDM	Fused Deposition Modeling
GO	Graphene Oxide
IPA	Isopropyl Alcohol
LCD	Liquid Crystal Display
LED	Light-emitted Diode
MWCNT	Multi-walled Carbon Nanotube
MTS	Maximum Tensile Strength
rGO	Reduced Graphene Oxide
SLA	Stereolithography Apparatus
SWCNT	Single-walled Carbon Nanotube
TS	Tensile Strength
UV	Ultraviolet

CHAPTER I

INTRODUCTION

1.1 Background and motivation

3D printing, also known as additive manufacturing, is a process of creating three-dimensional objects from three-dimensional digital design. This technology has the potential to enhance processes in designing, prototyping, and manufacturing products in a wide range of fields, including engineering, architecture, medicine, and art (Shahrubudin, N., Lee, T. C. and Ramlan, R. (2019)). With 3D printing, complex geometric shapes and details can be produced with high precision and accuracy, making it a powerful tool for innovation and creativity.

The 3D printing process involves building an object layer by layer, using a variety of materials such as plastics, resins, metals, and living cells (Abdollahi, S., Davis, A., Miller, J. H. and Feinberg, A. W. (2018)). The digital design is first converted into cross-sectional slices by slicing software, which are then fed into the 3D printer. The printer then builds the object by depositing material layer by layer until the final product is complete. (Lee, J.-Y., An, J. and Chua, C. K. (2017))

There are various types of 3D printing, one of them is LCD 3D printing LCD 3D printing, also known as MSLA (mask stereolithography), is a type of 3D printing technology that uses a liquid crystal display (LCD) to selectively cure a layer of resin to form a 3D object. It is a type of resin-based 3D printing, which uses liquid photopolymer resins that solidify when exposed to light.

The LCD 3D printing process commences with the preparation of a digital model using 3D modeling software. Subsequently, the digital model undergoes slicing, where it is divided into numerous thin layers, thereby establishing the foundation for the subsequent printing stages. The hardware components of the LCD 3D printer, comprising

the LCD panel, light source, resin vat, and build platform, are meticulously calibrated and readied for the printing operation.

However, this method is limited to the use of UV-curable resins, which can be more fragile than other types of materials. While resin can be formulated to have desired properties, such as stiffness, flexibility, or transparency, the range of available materials is still limited compared to other types of 3D printing methods. This work focuses on enhancing mechanical properties, such as tensile strength and Young's modulus, of a standard resin with carbon-based nanomaterial, graphene, and carbon nanotube. Graphene is a single layer of carbon atoms arranged in a hexagonal lattice. Carbon nanotubes are cylindrical carbon molecules that have a diameter of a few nanometers (typically between 1 and 100 nanometers) and can be several micrometers long. These materials are known as strong and lightweight materials, making them useful for a range of applications.

To enhance the mechanical properties of the UV resin, carbon-based nanomaterial was added to liquid resin. After the carbon-based material has been dispersed in the resin, the mixture can be used in a 3D printer to create a printed object. To investigate the effectiveness of the addition of carbon-based material, this study used tensile testing to determine improvements in mechanical properties. Specifically, the tensile strength and Young's modulus of the standard resin and the carbon-based composite resin.

1.2 Research objectives

1.2.1 To compare the mechanical properties, such as tensile strength and Young's modulus, of a standard resin with carbon-based composite resin.

1.2.2 To determine the best 3D-printing conditions for composite resin.

1.2.3 To investigate the effect of the concentration of the carbon-based composite material in the resin on the mechanical properties of the printed objects.

CHAPTER II

LITERATURE REVIEW

2.1 LCD 3D printing

From all photocuring 3D printing techniques, such as Stereolithography (SLA), Digital Light Projection (DLP), and Liquid Crystal Display (LCD) 3D printing, the biggest differences are the light source and imaging systems. While SLA 3D printing uses a laser diode and DLP technologies use a projector to cure resin layer by layer, in LCD 3D printing, the liquid crystal display (LCD) panel serves as the light source. The high resolution of the LCD panel allows for greater precision in producing fine details and complex shapes in the printed product, which is a significant advantage. However, one limitation of LCD 3D printing is the potential for lower print quality due to the pixel of the LCD panel, which may result in lower surface finish and resolution compared to SLA or DLP printing.

In addition to the printing accuracy, the major difference between DLP and LCD 3D printing is the light intensity. The light intensity is an important factor for photopolymerization which determines the speed of printing and curing degree. In LCD 3D printing, the light source is diffused and less intense than in DLP printing, which can result in less precise curing and potentially lower print quality.

During the printing process, the LCD panel serves as the primary interface for displaying the initial layer of the sliced digital model onto the resin surface contained within the vat, as demonstrated in Figure 1.1 (Mohamed, M. G. A., Kumar, H., Wang, Z., Martin, N., Mills, B. and Kim, K. (2019)). By selectively masking the pixels, the LCD panel allows for the controlled emission of UV light, which in turn initiates a photopolymerization reaction within the resin. As a result of this reaction, the liquid resin undergoes a conversion into a solid state, conforming to the pattern delineated by the displayed layer.

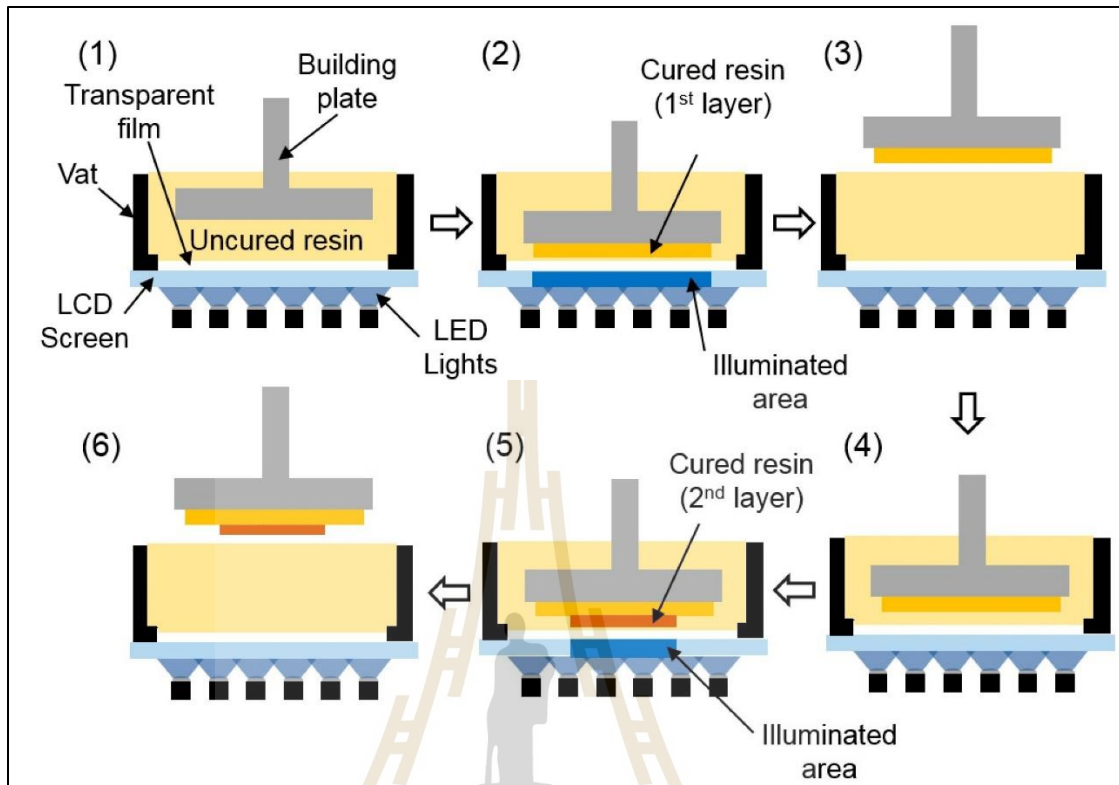


Figure 2.1 Demonstration of LCD resin printer while printing each layer. (1) The printing process begins with the resin vat being filled with uncured resin. (2) The building plate, initially positioned lower but remaining untouched to the transparent film, establishes a gap that corresponds to the thickness of the first layer to be printed. The LCD screen, serving as the light source, selectively illuminates the predetermined areas of the resin vat that correspond to the desired shape and structure of the first layer. (3) The building plate is then lifted, separating it from the transparent film and the solidified first layer. This movement creates space for the subsequent layer to be printed. (4) Following the lifting of the building plate, it is lowered again to the desired distance from the transparent film creating the gap for the formation of the second layer. (5) The process of LCD illumination, building plate lifted, and subsequent layer formation is repeated. (6) This involves the continuous repetition of layer formation, building plate movement, and layer solidification until the final object is fully constructed. (Modified from Mohamed, M. G. A., Kumar, H., Wang, Z., Martin, N., Mills, B. and Kim, K. (2019)).

To achieve completed three-dimensional products, the build platform, which holds the growing object, descends incrementally. Each incremental descent affords the necessary space for the subsequent layer to be deposited atop the previously solidified layer. This layer-by-layer process ensures the gradual construction of the desired object. Consequently, the LCD panel continuously displays each subsequent layer, while the UV light selectively solidifies the resin, adhering to the corresponding pattern for that specific layer.

Upon the completion of the printing process, which encompasses the successful fabrication and solidification of all layers, the build platform ascends, facilitating the removal of the printed object from the resin vat. Then, post-processing steps may be undertaken to refine the object's properties. Such steps might include a thorough cleansing to eliminate any residual uncured resin or the implementation of additional curing procedures, aiming to optimize the object's final characteristics.

2.2 Reduced graphene oxide

Graphene is a two-dimensional material composed of a single layer of carbon atoms arranged in a hexagonal lattice (Markandan, K. and Lai, C. Q., (2020)). It is considered a wonder material due to its properties, which include high electrical conductivity, thermal conductivity, and mechanical strength (Lim, S. M., Shin, B. S. and Kim, K. (2017)).

One of the most notable properties of graphene is its electrical conductivity. Graphene is an excellent conductor of electricity, and its conductivity is about 100 times greater than copper (Hanon, M., Ghaly, A., Zsidai, L., Szakál, Z., Szabó, I. and Kátai, L. (2021)). It also provides high thermal conductivity, making it a promising material for heat dissipation applications (Maheshwar, S. and Madhuri, S. (2010)). Another important property of graphene is its mechanical strength, yet it is extremely lightweight and flexible. This property makes graphene popular for use in high-performance composites and lightweight materials. However, obtaining large-scale, defect-free graphene sheets is challenging due to limitations in existing synthesis methods.

Graphene oxide (GO) is a derivative of graphene that is produced through a process called oxidation and exfoliation. This process involves treating graphite, which is a three-dimensional carbon-based material found in pencil lead, with strong oxidizing agents, such as a mixture of concentrated sulfuric acid and potassium permanganate. The oxidation introduces various oxygen-containing functional groups, such as epoxides, hydroxyls, and carboxyls, onto the graphene lattice, resulting in the formation of graphene oxide. Graphene oxide possesses unique properties that distinguish it from pristine graphene. It becomes hydrophilic due to the presence of oxygen functional groups, allowing it to disperse well in water and other polar solvents. However, the incorporation of these functional groups disrupts the π -conjugated electron system of graphene, leading to a loss of electrical conductivity and mechanical strength.

To restore some of the exceptional properties of pristine graphene, researchers employ a reduction process to transform graphene oxide into reduced graphene oxide (rGO). The reduction process aims to selectively remove or reduce the oxygen-containing functional groups while preserving the graphene-like structure. This reintroduces sp² carbon-carbon bonds and partially restores the original electronic and mechanical properties of graphene. As a result, rGO exhibits improved electrical conductivity and mechanical strength compared to graphene oxide, making it more suitable for various practical applications.

2.3 Carbon nanotubes

Carbon nanotubes (CNTs) are cylindrical structures made of carbon atoms, with a diameter of a few nanometers and a length that can range from a few micrometers to several millimeters (Harris, P. J. F. (2004)). They can be thought of as a rolled-up sheet of graphene, which is a single layer of carbon atoms arranged in a hexagonal lattice.

There are two main types of carbon nanotubes: single-walled carbon nanotubes (SWCNTs), which consist of a single cylindrical layer of carbon atoms, and multi-walled carbon nanotubes (MWCNTs), which consist of multiple concentric layers of carbon atoms.

SWCNTs and MWCNTs can have different properties, and their potential applications may differ as a result.

Carbon nanotubes have unique mechanical, electrical, and thermal properties that make them attractive for a wide range of applications (Andrews, R. and Weisenberger, M. C. (2004)). They are among the strongest and stiffest materials known to humans, with a tensile strength that is about 100 times greater than steel. They are also excellent electrical conductors, with the ability to carry electric current at very high speeds and over long distances. Additionally, they have high thermal conductivity, making them good conductors of heat.

One of the most promising applications of carbon nanotubes is in electronics. Their exceptional electrical conductivity and small size make them attractive for creating faster and more efficient electronic devices. Researchers are exploring their use in transistors, sensors, and energy storage devices, among other applications. Carbon nanotubes also have potential applications in materials science. They can be used to reinforce polymers, such as plastics and composites, making them stronger and more durable. They can also be used as a conductive additive in adhesives, coatings, and inks.

2.4 Tensile testing

Tensile testing is a standard mechanical testing method used to determine the mechanical properties of a material. During a tensile test, a sample of the material is subjected to a gradually increasing tensile load until it breaks. The load applied to the material is measured, as well as the amount of deformation (strain) that the sample undergoes (Harding, J. and Welsh, L. M. (1983)). These measurements are used to calculate the tensile strength and Young's modulus of the material.

The tensile strength of a material is determined by the maximum load it can withstand before breaking, divided by its cross-sectional area. The equation for tensile strength (TS) is

$$TS = \frac{F_{max}}{A},$$

Where F_{max} is the maximum load or force applied to the specimen during the tensile test and A is the original cross-sectional area of the specimen.

The Young's modulus, also known as elastic modulus, is determined by the ratio of the applied stress (load per unit area) to the resulting strain (change in length divided by the original length) which can be written in the equation below,

$$E = \frac{\sigma}{\epsilon},$$

where E is the Young's modulus, σ is the applied stress, and ϵ is the resulting strain. The Young's modulus is a measure of a material's stiffness or resistance to deformation under an applied load.

Stress is a measure of the force per unit area applied to a material under an external load. It is calculated by dividing the applied force by the original cross-sectional area of the material. The result represents the stress at a specific point in the material and is commonly used in mechanical testing to measure a material's strength and deformation properties. This relation can be written by the equation below,

$$\sigma = \frac{F}{A},$$

Where σ is the stress applied to the specimen, F is the applied force and A is the original cross-sectional area of the specimen.

Strain is a measure of the deformation of a material under load. It is defined as the ratio of the change in length of the material to its original length. It is typically expressed as a decimal or percentage. It can be calculated using this equation,

$$\epsilon = \frac{\Delta L}{L},$$

Where ϵ is the strain, ΔL is the change in length of the specimen and L is the original length of the specimen.

One significant outcome derived from tensile testing is the stress-strain curve, which serves as a graphical portrayal illustrating the relationship between the stress applied to a material and the resultant strain it experiences. This curve plays a pivotal

role in offering valuable insights into the mechanical behavior and properties of a material under varying loading conditions.

From Figure 2.2, when a material is subjected to low levels of stress, it undergoes elastic deformation. This elastic region signifies that the material can revert to its original shape upon stress removal. In this linear relationship between stress and strain, the material adheres to Hooke's Law. The slope of the stress-strain curve in the elastic region corresponds to the material's elastic modulus, which provides an indication of its stiffness and ability to resist deformation.

As stress continues to increase, the material may reach a critical point referred to as the yield point. At this juncture, the material begins to exhibit permanent deformation even after the stress is removed. The yield point signifies the transition from elastic to plastic deformation and is important in understanding the material's behavior.

Beyond the yield point lies the plastic region, wherein further stress application leads to permanent deformation. The stress-strain curve in this region assumes a non-linear form, and the material may experience strain hardening or softening, depending on its composition and properties. This stage may also witness necking, which refers to a localized reduction in cross-sectional area.

The stress-strain curve culminates at the ultimate tensile strength (or maximum tensile strength), which represents the maximum stress a material can withstand before fracturing. This point serves as the peak on the curve, highlighting the material's critical limit. Beyond the ultimate tensile strength, the material undergoes significant deformation and ultimately fails.

At the fracture point, the material experiences sudden and rapid failure, leading to complete separation or rupture of the specimen. This stage is characterized by a dramatic drop in stress, coupled with an abrupt increase in strain.

Through the analysis of the stress-strain curve, various mechanical properties of the material can be determined. These include Young's modulus, which corresponds to the slope of the linear elastic region and signifies the material's stiffness and resistance to deformation. Additionally, the yield strength indicates the stress at which plastic

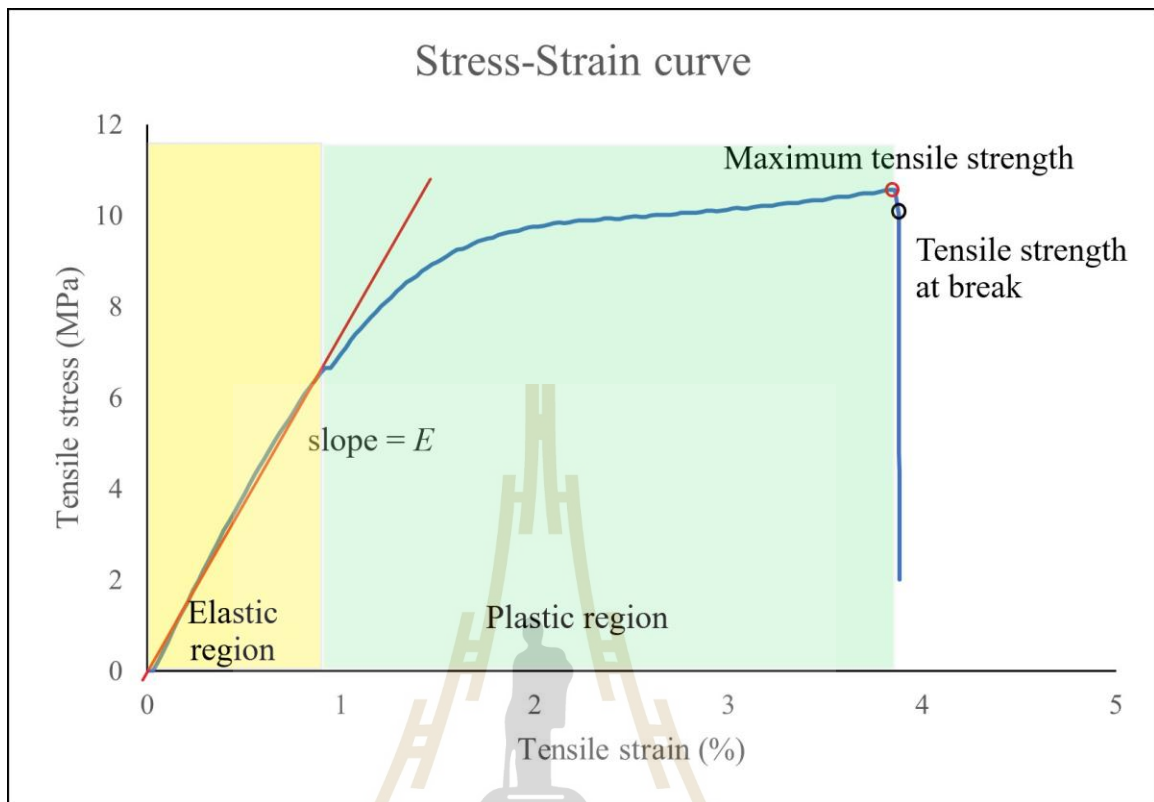


Figure 2.2 The stress-strain curve obtained through experimental testing, specifically a tensile test. In the elastic region, the relationship between stress and strain is linear. The slope of the stress-strain curve in the elastic region represents the material's elastic modulus, which indicates its stiffness. Beyond the yield point, the material enters the plastic region, where further stress leads to permanent deformation. The stress-strain curve in this region is non-linear, and the material experiences strain hardening or softening, depending on its composition and properties. The maximum stress a material can withstand without fracture is known as the maximum tensile strength. It represents the peak point on the stress-strain curve. Once this stress level is reached, the material begins to deform significantly and eventually fails.

deformation commences, while the ultimate tensile strength reflects the maximum stress the material can withstand before fracturing. Ductility refers to the material's ability to

undergo plastic deformation without breaking, and toughness represents the total energy absorption capacity of the material before fracture.

Elongation at break, also known as strain at failure, is a mechanical property that can be derived from the stress-strain curve of a material. When a tensile test is performed on a sample, it undergoes deformation, and the stress-strain curve illustrates the relationship between the applied stress (force per unit area) and the resulting strain (deformation). Elongation at break refers to the maximum amount of strain or deformation that a material can undergo before it breaks or fractures. It represents the percentage increase in length of the sample compared to its original length just before it fails.

To calculate elongation at break from the stress-strain curve, one needs to identify the point on the curve where the sample fractures (breaks). The strain at this point is then measured as the percentage increase in length relative to the original length.

Elongation at break is an essential parameter for evaluating the ductility and flexibility of a material. Materials with high elongation at break can undergo significant deformation before failure, indicating their ability to absorb energy and withstand stretching forces, making them suitable for applications that require resilience and toughness. Conversely, materials with low elongation at break are more brittle and may be more prone to sudden failure under stress.

Tensile testing is an important tool for material characterization, and it is commonly used in industries such as aerospace, automotive, and construction. It can also be used in research and development to study the effects of different materials and processing parameters on mechanical properties.

CHAPTER III

METHODOLOGY

3.1 Materials, instruments and printing conditions

3.1.1 Materials and instruments

The experimental setup for this study involved the utilization of an Elegoo Mars 3 (Shenzhen Elegoo Technology Co.,Ltd) 3D printer to fabricate the samples. The printer offers a printing dimension of 89.6 mm * 143.43 mm * 175 mm for width, length, and height, respectively. In the xy-plane, the printer operates with a screen resolution of 0.035 mm or 35 micrometers, corresponding to 4098 * 2560 pixels. This high resolution is crucial as it directly impacts the quality and level of detail achieved in the printed products.

In this study, the base material utilized was eSUN standard white resin, a product of Shenzhen Esun Industrial Co., Ltd. To enhance the mechanical properties of the resin, we incorporated two nanomaterials, namely reduced graphene oxide (rGO) and multi-wall carbon nanotube (MWCNT), obtained from Graphene Globe Technology Co. Ltd., based in Thailand. The composite resin was prepared with a concentration of 0.1 % by weight (w/w) for both rGO and MWCNT.

3.1.2 Printing conditions

To ensure standardization and comparability, all samples were fabricated in accordance with ASTM D638 type V standards, with the dimensions of the model following 9.53 mm in width, 63.5 mm in length, and 3.2 mm in height. Furthermore, a gauge length's width of 3.18 mm was established around the neck of the model as shown in Figure 3.1 and Figure 3.2.

In this experiment, we conducted a comprehensive exploration of the printing process by systematically varying the exposure time for each printing layer. Specifically,

we employed exposure times of 4, 8, 12, 16, and 20 seconds, allowing us to analyze the impact of these varying durations on the resulting samples.

To ensure a comprehensive assessment of the printed samples, we adopted three distinct orientations: X, Y, and Z, as shown in Figure 3.3. In the X orientation, the width face of the sample was oriented parallel to the printing plate. For the Y orientation, we placed the same face of the sample perpendicular to the printing plate, offering a different perspective for observation. Last, we employed the Z orientation, where the small face of the sample was in contact with the printing plate.

By exploring the printing process using these diverse orientations and varying exposure times, we aimed to gain valuable insights into the influence of printing parameters on the final outcomes and establish a deeper understanding of the optimal settings for achieving desired properties in the printed samples.

Following the completion of the printing process, a meticulous post-printing procedure was implemented to ensure the utmost quality of the samples. The samples underwent a thorough cleaning regime utilizing 99.99% isopropanol (IPA) to meticulously remove any traces of residual uncured resin. This crucial step was undertaken to achieve pristine surfaces and prevent any potential deformations in the printed specimens upon exposure to daylight.

To further enhance the structural stability of the samples, a UV light curing process was subsequently employed. The specimens were exposed to UV light for a precisely controlled duration of 90 seconds. This UV curing step induced cross-linking reactions within the resin, contributing to the solidification and improved mechanical properties of the 3D printed components.

It is noteworthy to mention that, despite the curing process, the predetermined exposure times for each printing layer were maintained without any interference. The selected 90-second curing time was chosen to ensure that it would not compromise or alter the originally varied exposure times, thus preserving the integrity of the experimental setup and allowing for accurate assessment of the impact of exposure time on the final mechanical properties of the 3D printed samples.

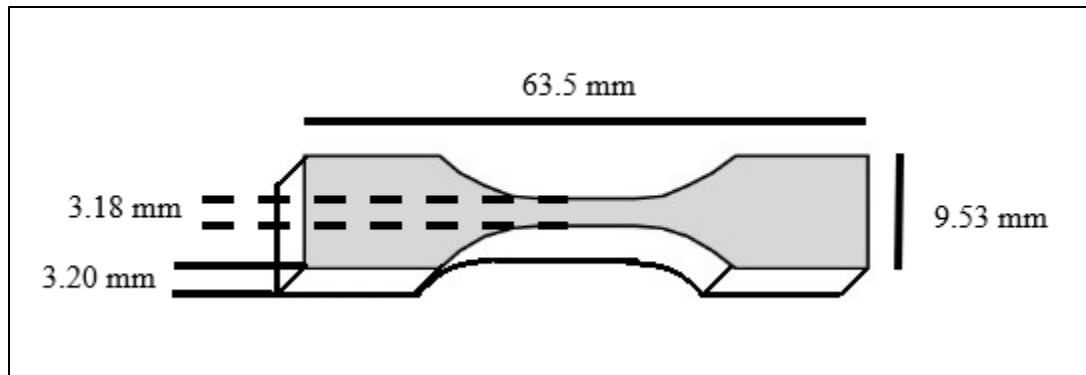


Figure 3.1 A schematic representing the dimensions of the ASTM D638 Type V model used for tensile testing.

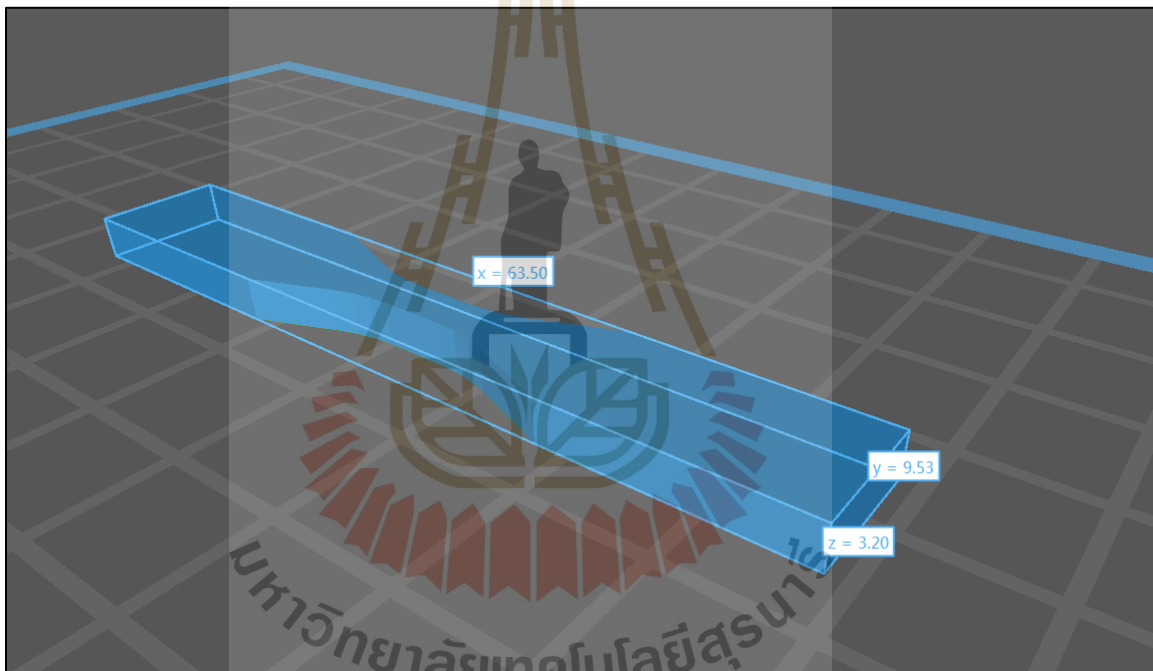


Figure 3.2 The 3D model CAD schematic illustrates the dimensional representation of the ASTM D638 Type V model used for tensile testing in mm.

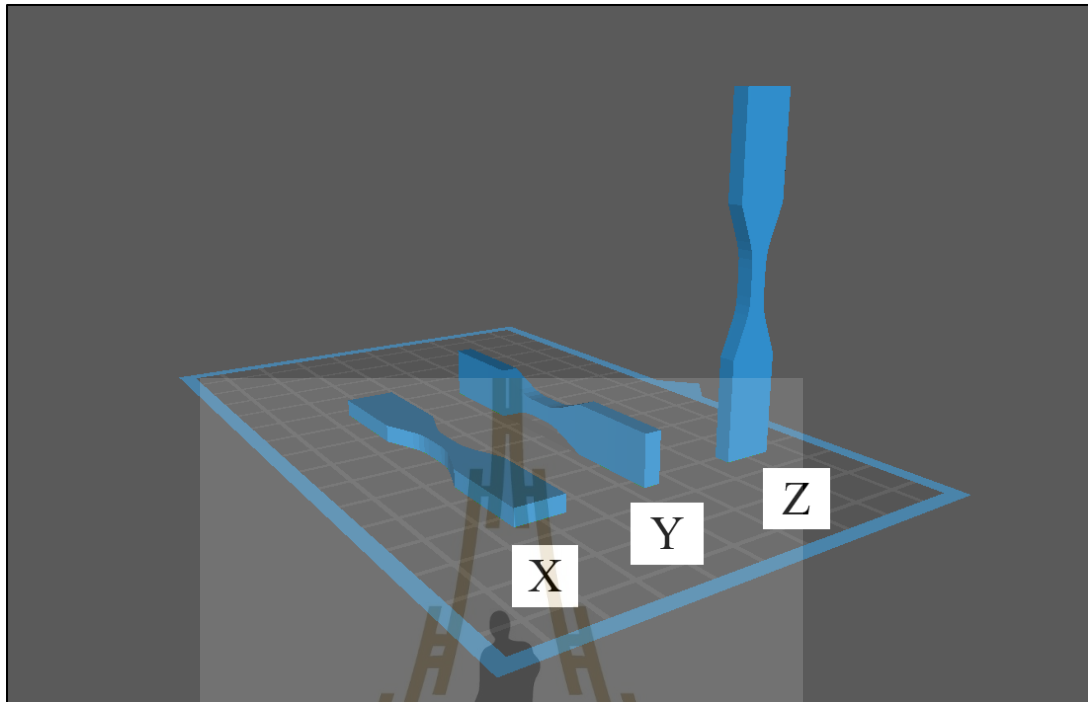


Figure 3.3 The samples were printed in three different orientations, X, Y, and Z orientations.

3.2 Material Characterization

Before mixing the composite resin, reduced graphene oxide (rGO) and multi-wall carbon nanotube (MWCNT) were analyzed to confirm their quality. This analysis used two methods: scanning electron microscopy (SEM). Scanning Electron Microscopy was used to observe the surface structure and shape of the rGO and MWCNT. The images helped identify their size and how well they might mix with the resin. It also helped confirm that the materials were pure and evenly distributed.

3.3 Resin and composite resin preparation

According to the information presented in Figure 3.4, the preparation of the carbon composite resin mixture involved blending 3D resin with carbon-based composite at a concentration of 0.1% w/w. To achieve a homogeneous mixture, the resin was stirred using a magnetic stirrer for a duration of 4 hours. Subsequently, the resin mixture was carefully

introduced into the vat of the Elegoo Mars 3 LCD 3D printer, facilitating the subsequent printing of the designated test specimens.

Following the printing process, a thorough analysis of the results was undertaken to meticulously examine and discern the influence of several crucial factors, namely the concentration of graphene, the exposure time, and the orientation of printing, on the mechanical properties of the 3D printed carbon-based composite specimens. This comprehensive investigation aimed to shed light on the interplay between these influential variables and the resultant mechanical characteristics of the printed specimens, thereby unraveling vital insights for optimizing the fabrication process and enhancing the overall performance of the 3D printed carbon-based composite materials.

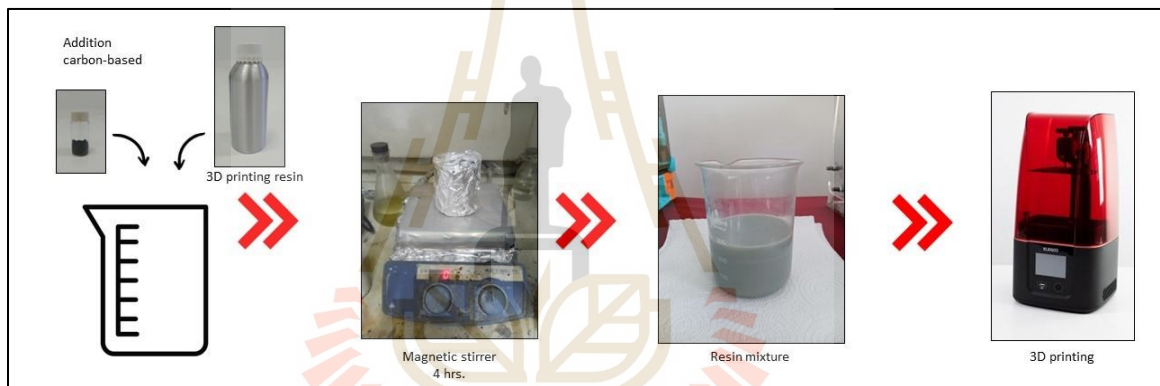


Figure 3.4 The diagram illustrates the experimental process employed for the carbon-based added resin.

3.4 Tensile testing

The tensile testing took place utilizing the Instron 5565 universal tensile machine, located in room F5109 within the F5 building at Suranaree University of Technology. Throughout the testing, a constant pulling speed of 0.1 mm/min was employed, with a maximum load capacity of 5 kN.

Following the completion of the tensile testing, the acquired data will be utilized to plot the stress-strain curve, providing valuable insights into the material's mechanical behavior. By analyzing the linear elastic region of the curve, the slope will be determined, facilitating the calculation of Young's modulus, an essential material property indicative of

its stiffness and elasticity. For each testing condition, a total of 7 specimens were tested to ensure robustness and accuracy, and the desired results were obtained by calculating the average of mentioned 7 sets of stress-strain curves.

Moreover, the stress-strain curve will yield additional data, such as the maximum tensile strength and elongation at break, both of which serve as vital indicators of the material's mechanical properties. The maximum tensile strength represents the highest point on the curve, signifying the material's capacity to withstand stretching forces before failure occurs. On the other hand, elongation reflects the extent to which the material can deform before reaching its breaking point.

Through an examination of these parameters, a comprehensive understanding of the mechanical properties of the printed samples can be attained. By comparing these material properties, valuable insights can be drawn to assess the impact of various factors, such as graphene concentration, exposure time, and printing orientation, on the final performance and structural integrity of the 3D printed carbon-based composites. Such comparative analyses play an essential role in guiding material selection and optimizing the fabrication process to achieve desired properties and performance in practical applications.

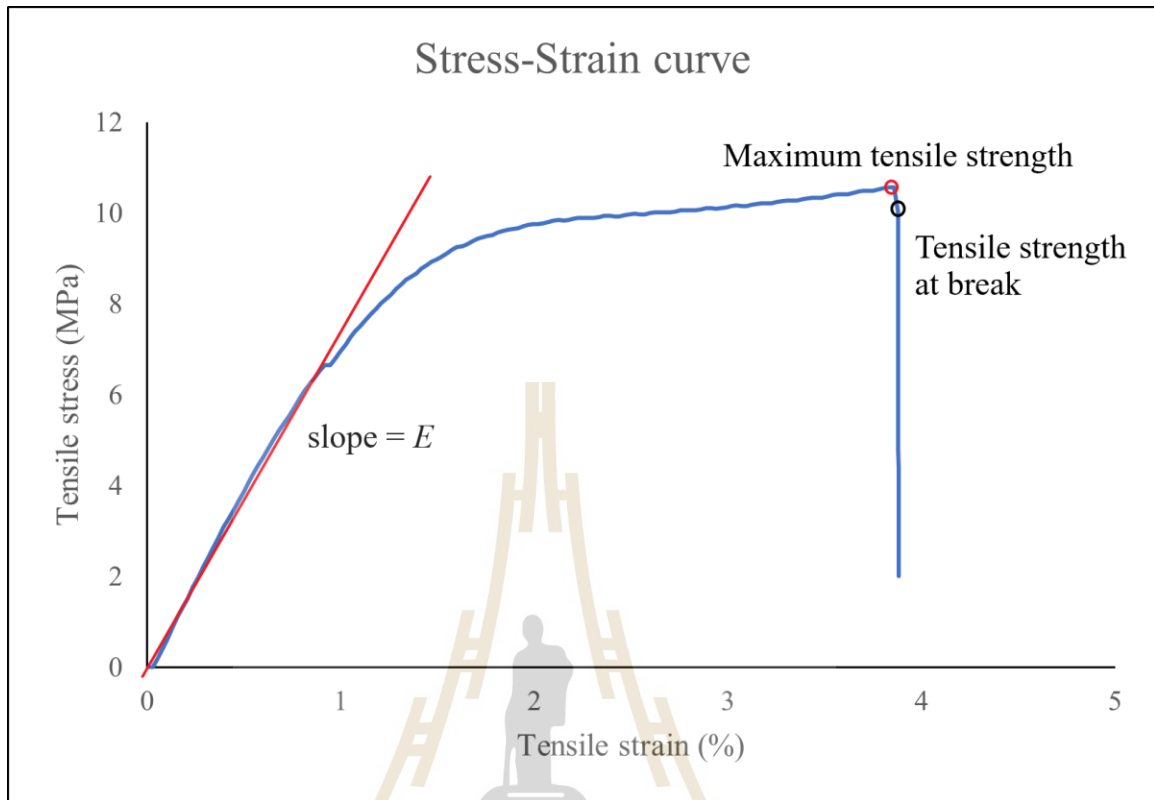


Figure 3.5 During the analysis of the stress-strain curve, the calculation of Young's modulus involves determining the slope of the linear elastic region. Additionally, valuable data concerning the elongation at break can be obtained by evaluating the tensile stress percentages from the curve.

CHAPTER IV

RESULT AND DISSCUSSION

4.1 Material characterization and analysis

4.1.1 Reduced graphene oxide (rGO)

The SEM images of the reduced graphene oxide (rGO), as shown in Figure 4.1, reveal a clumped structure instead of the expected flat sheet morphology. This aggregation may arise from strong van der Waals forces and π - π stacking interactions between the graphene sheets, which cause them to stick together during the reduction process. The removal of functional groups during reduction increases the hydrophobicity of the sheets, further promoting aggregation.

Incomplete exfoliation of the starting graphite oxide material may also contribute to this clumped morphology. If the exfoliation step is not thorough, the sheets may remain partially stacked, leading to aggregation after reduction. Additionally, the absence of dispersing agents, such as surfactants or polymers, could exacerbate the tendency of the sheets to clump together.

It is important to note that this rGO sample was supplied by an industrial source, and the preparation techniques were not disclosed. Specific manufacturing parameters, such as the reduction method and post-processing conditions, could also influence the observed morphology.

This clumped morphology could significantly affect the mechanical properties of rGO when used in composite materials. The reduced effective surface area and poor dispersion can limit the formation of strong interfacial bonds between the rGO and the matrix material. As a result, the material's ability to enhance mechanical strength, stiffness, and toughness in composites may be diminished. To improve the mechanical performance of rGO in applications, efforts should focus on preventing aggregation during the

preparation process. This could include optimizing exfoliation techniques, using stabilizing agents, or modifying reduction methods to achieve a more uniform and sheet-like morphology. Achieving better dispersion of rGO sheets in composite systems could enhance load transfer and improve the overall mechanical properties of the final material.

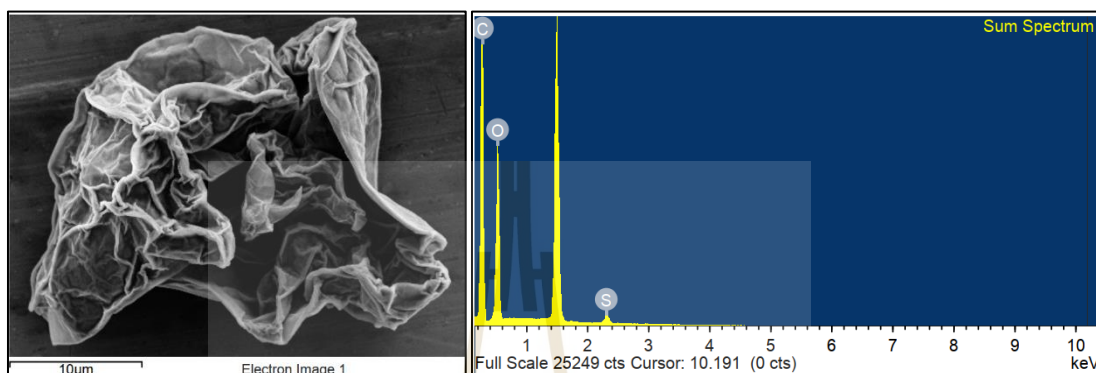


Figure 4.1 The SEM image of rGO, captured at an EHT of 3 kV with a magnification of 1000x, reveals a clumped structure rather than the expected flat sheet morphology (left). The EDS spectrum of rGO indicates an elemental composition of 5.39 wt% carbon, 40.15 wt% oxygen, and 6.46 wt% sulfur (right).

The elemental composition of reduced graphene oxide (rGO), determined through Energy Dispersive X-ray Spectroscopy (EDS), reveals 5.39 wt% carbon, 40.15 wt% oxygen, and 6.46 wt% sulfur. These results provide insights into the material's properties and its influence on the performance of composite 3D resin. The high oxygen content indicates incomplete reduction of graphene oxide, leaving functional groups such as hydroxyl, carboxyl, and epoxy on the surface. These residual functional groups can improve compatibility with the resin matrix by enhancing chemical bonding at the interface, leading to better stress transfer and improved mechanical strength and stiffness. However, the high oxygen content can also reduce the electrical conductivity and thermal stability of the composite, potentially limiting its use in applications requiring these properties.

The presence of sulfur, which likely originates from the synthesis or reduction process, contributes to the chemical functionality of rGO. Sulfur may exist as sulfonic acid groups or other sulfur-containing functionalities. These groups can improve crosslinking or chemical interactions with the resin, enhancing adhesion and mechanical properties.

However, the sulfur content may also introduce structural defects or impurities, which could reduce the overall reinforcement efficiency of the rGO in the composite.

The relatively low carbon content suggests that the graphene-like structure of rGO has not been fully restored, indicating a lack of sufficient sp^2 carbon domains. This limitation affects its mechanical and electrical properties. The reduced carbon content weakens rGO's ability to transfer stress effectively, leading to a less significant improvement in the mechanical properties of the composite. Furthermore, the low carbon content diminishes the potential for rGO to enhance the composite's electrical conductivity.

The clumped morphology of rGO, coupled with the high oxygen and sulfur content, may influence its dispersion within the resin matrix. On one hand, the oxygen and sulfur groups improve dispersibility, preventing aggregation and ensuring a more uniform distribution of rGO within the resin. On the other hand, the incomplete reduction process and potential defects limit the material's ability to act as a reinforcing agent effectively. These functional groups, however, can be leveraged to tailor the composite for specific applications, such as improving adhesion or chemical functionality, although this may compromise its electrical and thermal performance.

4.1.2 Multi-walled carbon nanotubes (MWCNT)

The SEM and EDS analysis of the multi-walled carbon nanotubes (MWCNTs), as shown in figure 4.2, provides key insights into their structure and composition. The SEM images reveal that the MWCNTs do not exist as isolated single tubes but instead form groups of thread-like bundles. This bundling behavior is a common characteristic of MWCNTs due to their strong van der Waals forces and π - π stacking interactions, which promote aggregation. The EDS analysis further shows that the MWCNTs consist of 98.6 wt% carbon and 1.4 wt% oxygen. The high carbon content confirms the purity of the material, while the small amount of oxygen suggests the presence of minimal functional groups or residual oxidation byproducts.

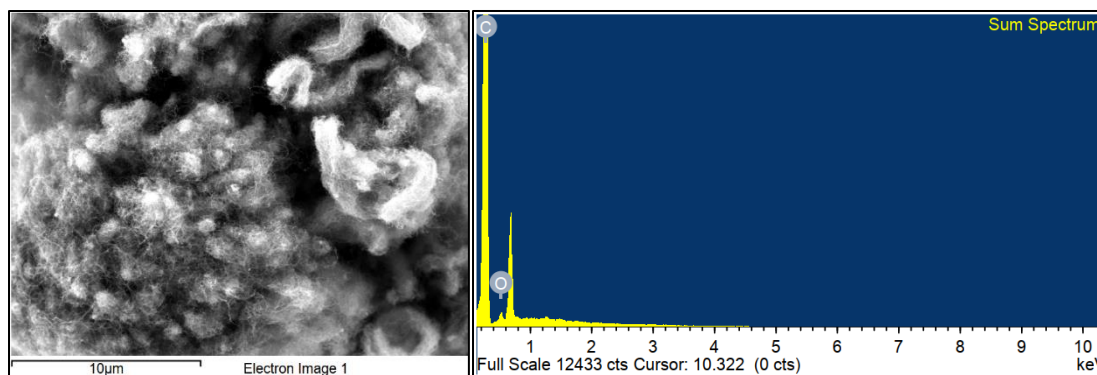


Figure 4.2 The SEM image of MWCNT, captured at an EHT of 3 kV with a magnification of 5000x, show that the MWCNTs are not present as isolated single tubes but instead form grouped, thread-like bundles (left). The EDS analysis indicates that the MWCNTs are composed of 98.6 wt% carbon and 1.4 wt% oxygen (right).

The grouped structure of the MWCNTs, while advantageous for maintaining high tensile strength, could affect their performance in the composite 3D resin. The bundled configuration might limit the effective surface area available for interaction with the resin matrix, reducing the efficiency of stress transfer between the nanotubes and the resin. However, the thread-like structure can still contribute significantly to reinforcing the composite by acting as a framework that distributes mechanical loads more evenly. This is especially beneficial for enhancing the tensile strength and stiffness of the resin.

The small oxygen content plays a dual role in the composite. On the one hand, the presence of oxygen-containing functional groups can improve the compatibility of the MWCNTs with the resin matrix, promoting better interfacial bonding and thereby enhancing the overall mechanical properties. On the other hand, the low level of oxygen indicates that the MWCNTs retain their intrinsic electrical conductivity and thermal stability, which can be advantageous for applications requiring high conductivity or heat dissipation in the composite material.

4.2 Preliminary experiments

This section encompasses the preliminary version of the experiments, which serves as a steppingstone to the subsequent experiment. Following the preliminary experiment

and tensile testing, an issue was observed where the samples would typically break outside the gauge length, resulting in failed results as in Figure 4.3. To delve into this matter, we made various parameter and testing method adjustments. Eventually, we identified the root cause was the inappropriate grip.



Figure 4.3 The preceding samples encountered issues with shear forces and fracture occurred around the grip area rather than at the neck region.

The old grip had a slippery contact surface, leading to shear forces between the grip and the samples. To address this concern, we replaced the grip with a new one featuring a contact surface equipped with miniature spikes (Figure 4.4). These spikes aided in stabilizing the samples during tensile testing, preventing any slippage and ensuring the samples remained securely in place. As a result, this modification successfully resolved the problem, allowing for more reliable and consistent results in subsequent tensile tests.

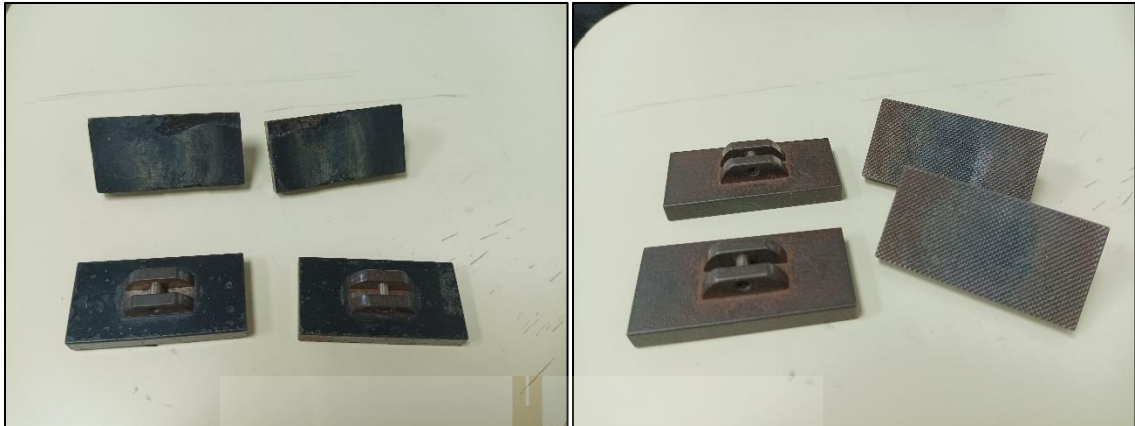


Figure 4.4 The previous grip (left) had a smooth surface contact in contrast to the current grip (right), which features a rough texture.

4.3 Printed samples characteristics

After the grip was changed, the issue of the samples breaking outside the gauge length was successfully resolved. As depicted in Figure 4.5, the samples exhibited consistent behavior, with fracture occurring solely around the neck area for all tested samples.

However, another issue arose during the printing process, specifically concerning the samples in the y direction. It is essential to note that in 3D printing, the initial layer, often referred to as the bottom layer, plays a critical role in preventing the printed layers from detaching from the printing plate. This bottom layer needs to exhibit higher adhesion compared to subsequent layers. Typically, SLA and LCD 3D printing involve around 5 bottom layers. To ensure the bottom layer's effectiveness, it is crucial for it to be adequately exposed to UV light, typically ranging from 20 to 60 seconds, depending on the resin type and light source power. However, a problem emerged with the bottom layers due to excessive exposure to UV light. When the resin is overly exposed, the light can unintentionally affect regions outside the intended selected area, causing the hardening region to spread. This effect is known as the “overexposure” or “overshoot” effect.

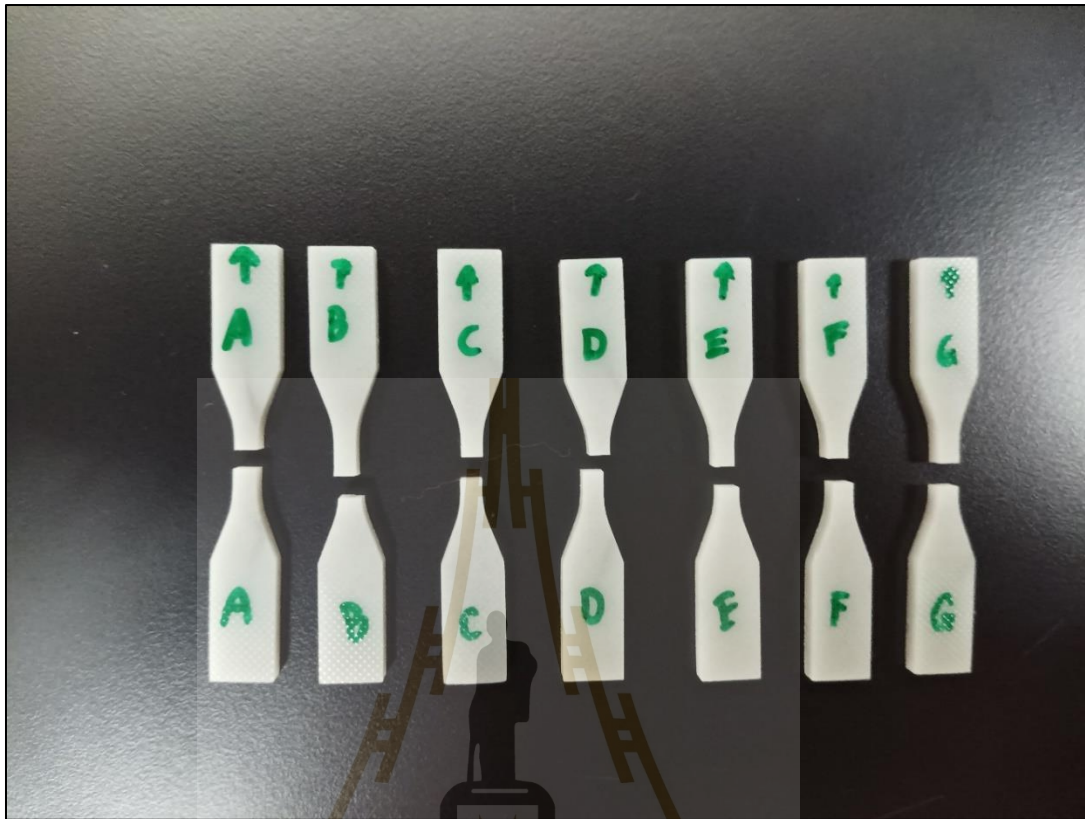


Figure 4.5 After the grip change, the samples demonstrated a consistent pattern, with fracture occurring exclusively around the neck region in all the tested samples. The Figure provided illustrates the 8s neat resin samples after undergoing tensile testing.

The overexposure effect, which is distinctly noticeable in the y orientation samples, can be attributed to the arrangement of the printing samples. The bottom layers of the samples coincide with the initial region of the neck area. Consequently, when overexposure occurs, it affects this region as well, leading to the observed results in Figure 4.6, particularly for the 12s, 16s, and 20s samples. However, the effect is minimal for the 4s and 8s samples, making it negligible.

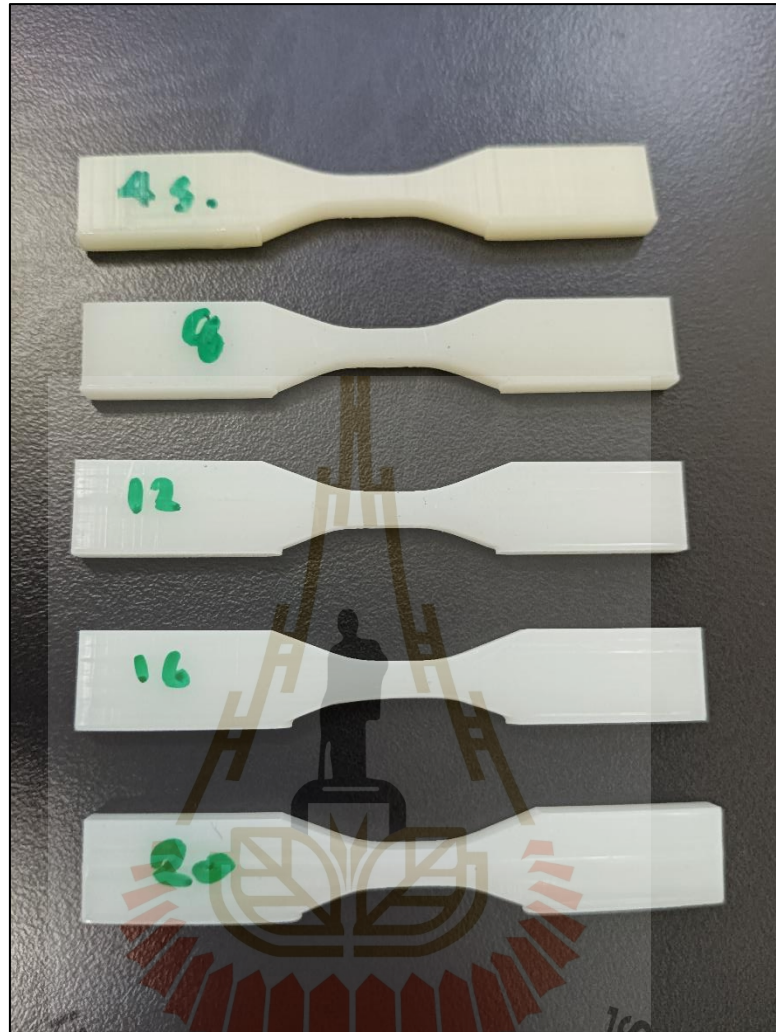


Figure 4.6 The overshoot effect is evident in the y orientation samples from 4s to 20s exposure time. Although the 4s and 8s samples presented minor issues, the 12s, 16s, and 20s samples exhibited more prominent overshooting, even after recalibrating the 3D printer using three layers of A4 paper.

In an attempt to address this issue, we endeavored to re-calibrate the 3D printer. During the calibration process, we employed an A4 paper to cover the screen and then gradually lowered the building plate by loosening the screws. Subsequently, the printing plate was aligned smoothly in parallel with the screen, and the screws around the printing head were tightened. Initially, we hypothesized that the building plate might have been too close to the screen, causing incorrect gap layers. However, after re-calibrating using

three layers of A4 paper (Figure 4.7), we observed improvements in the 4s and 8s samples, with the overshooting area slightly reduced. Nevertheless, for the 12s and longer exposure time samples, the overshoot effect remained unchanged. This observation led us to conclude that the overshoot effect becomes more pronounced after an 8s exposure time. Despite the observed overshoot effect, we proceeded with the process to further investigate its potential impact on the mechanical properties of the samples.



Figure 4.7 The calibration process of the Elegoo Mars 3 3D printer can be demonstrated effectively by employing three pieces of A4 papers.

4.4 Mechanical properties

This section presents the data obtained from the experiment. Our expectations were that longer exposure times would result in higher strength and toughness of the products, as indicated by increased values in both maximum tensile strength (MTS) and Young's modulus. Additionally, we anticipated that the printing orientation would

influence the mechanical properties. This is because the 3D printing process involves constructing the object layer-by-layer, and the adherence between adjacent layers may be affected by the different orientations, subsequently impacting the mechanical properties. Therefore, this section aims to provide a comprehensive overview of the data, covering all the aspects mentioned above, including the effects of exposure time and printing orientation on the mechanical properties of the samples.

4.4.1 Mechanical properties of normal resin

Based on the stress-strain curve analysis, we have obtained the results for both neat or normal resin and carbon-based composite resin samples. As shown in Figure 4.8, the maximum tensile strength of neat resin is presented in units of MPa, corresponding to the exposure time for each of the x, y, and z orientations. From the plot, we observe that the maximum value is 18.84 ± 0.58 MPa for the y-20s sample, while the minimum value recorded was 9.35 ± 0.8 MPa. Based on the plot, a general trend can be observed for both y and z orientations, indicating that the strength of the samples increases with longer exposure times. However, for the x orientation samples, the maximum tensile strength did not exhibit such a distinct pattern, as the x-12s sample displayed a higher MTS compared to the x-16s and x-20s samples. Regarding the influence of orientation, it is evident that, at 12s, 16s, and 20s, the samples in the y direction tend to outperform those in other conditions. However, for the 4s and 8s samples, notable differences are not observed among the orientations.

Figure 4.9 displays the Young's modulus of the neat resin, and we can observe that it follows a similar trend to the maximum tensile strength discussed earlier. Among the x direction samples, the 12s sample stands out as having the highest Young's modulus, deviating from the expected pattern. On the other hand, the z orientation samples seem to adhere more closely to the expected behavior in this plot. Notably, the 12s, 16s, and 20s samples cluster around 1.2 GPa, a particularly intriguing observation. At this stage, we do not have a definitive explanation for this behavior, so we plan to investigate further and consider additional results to shed light on this interesting phenomenon.

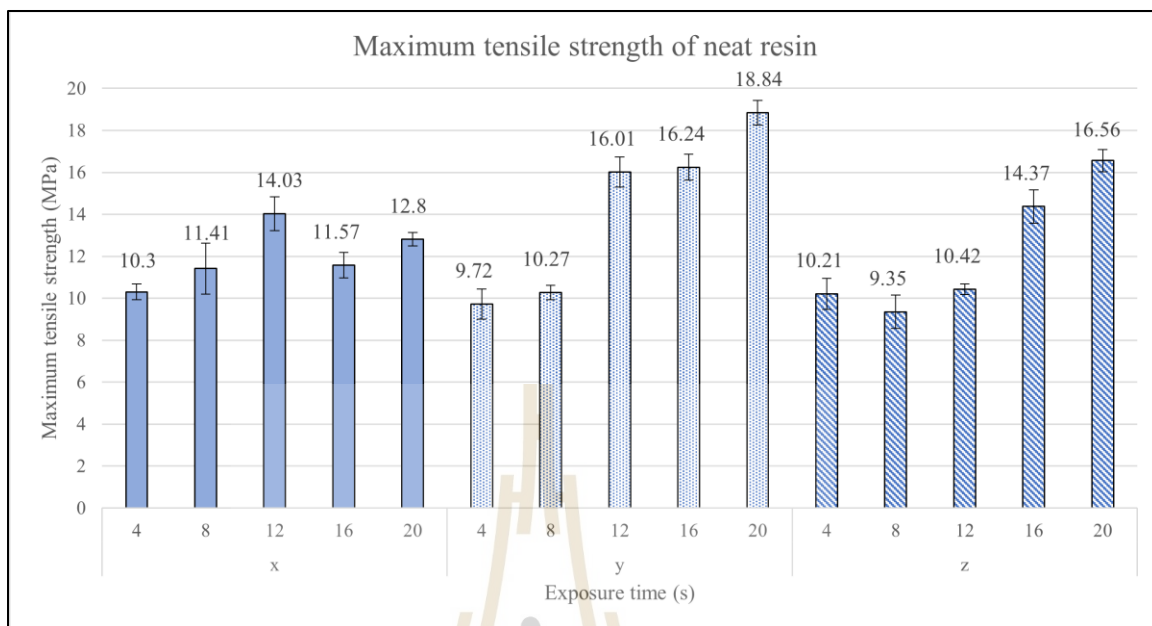


Figure 4.8 The maximum tensile strength of the neat resin is displayed in MPa units, corresponding to the exposure time for the x, y, and z orientations.

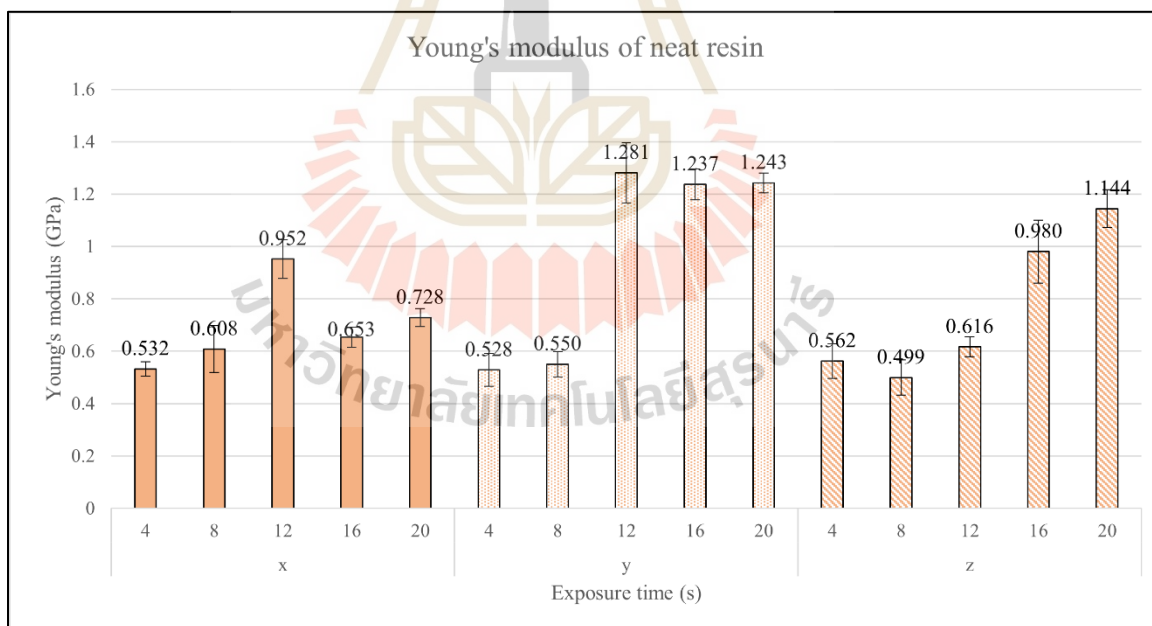


Figure 4.9 The Young's modulus of the neat resin is displayed in GPa units, corresponding to the exposure time for the x, y, and z orientations.

4.4.2 Mechanical properties of 0.1%w rGO composite resin

Concerning the addition of rGO, our expectations were that both Young's modulus and maximum tensile strength (MTS) would be higher than those of the normal resin. As such, we can now compare the mechanical properties between the normal printed product and the reinforced product, considering the enhancements attributed to the incorporation of rGO. This comparison will provide valuable insights into the benefits and improvements brought about by the addition of rGO in terms of the mechanical performance of the printed products.

Upon analyzing the plot of the maximum tensile strength for the 0.1% w/w rGO composite resin at various exposure times and orientations, the overall results appear promising, except for the x direction (Figure 4.10). The MTS value for the 12s sample in the x direction was notably lower, and there was little distinction between the 16s and 20s samples compared to the 8s samples. Conversely, the y and z orientations align more closely with the expected outcomes, with the z-20s sample being very similar to the 16s sample, although the difference is acceptable given the values obtained. Further investigations are warranted to understand the specific factors contributing to the observed discrepancies in the x direction.

Regarding the Young's modulus shown in Figure 4.11, it exhibits a similar trend to the previous result for the neat resin. Notably, the highest Young's modulus was achieved in the y-20s sample. When comparing samples in the same direction, the difference between the y-20s and y-4s samples is not substantial, as is the case with the z orientation samples. However, the x orientation samples present a distinct pattern, with the x-12s sample displaying a significantly lower Young's modulus compared to the others. Conversely, the x-4s, x-8s, x-16s, and x-20s samples are closely grouped together. Further analysis is required to understand the specific factors contributing to the observed variations in Young's modulus among the different exposure times and orientations.

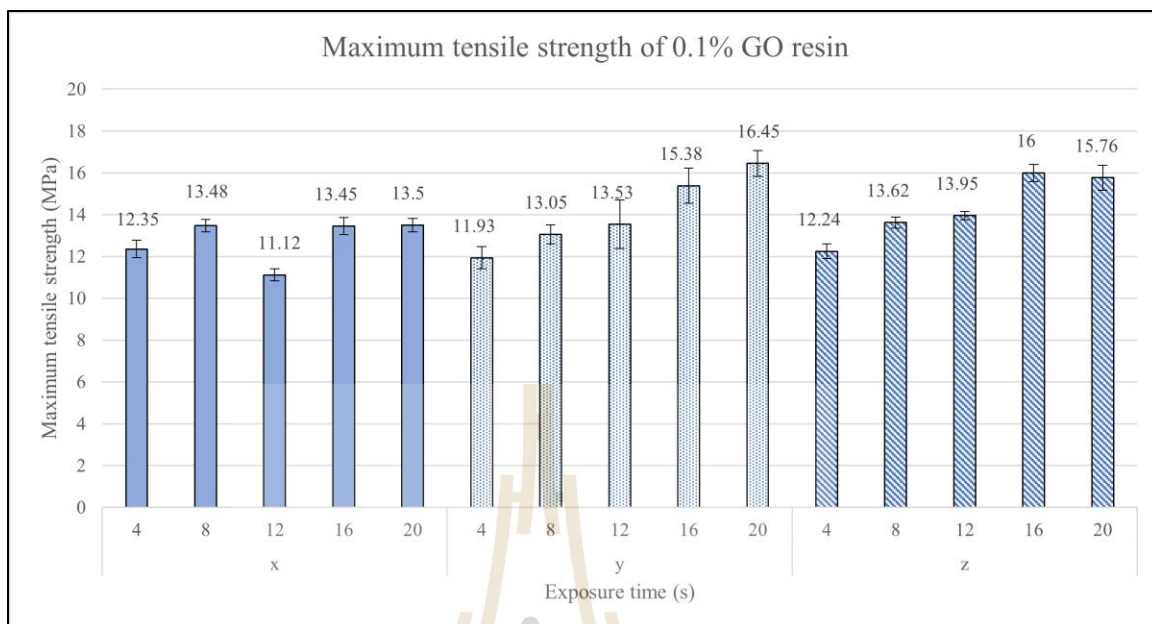


Figure 4.10 The maximum tensile strength of the 0.1% w/w rGO composite resin is displayed in MPa units, corresponding to the exposure time for the x, y, and z orientations.

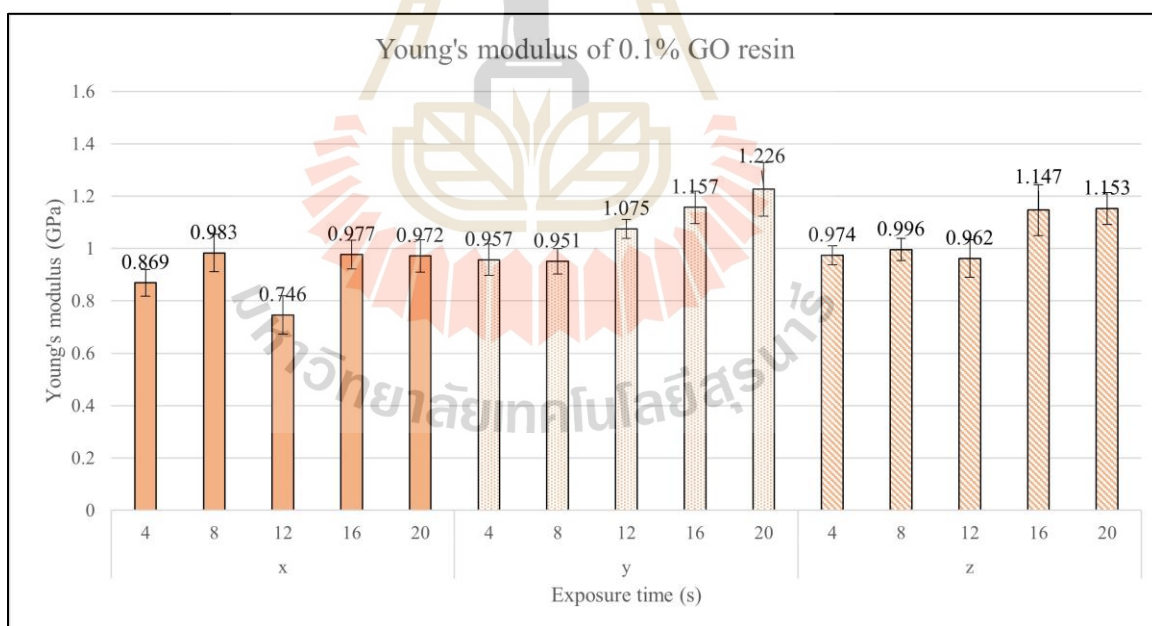


Figure 4.11 The Young's modulus of the 0.1% w/w rGO composite resin is displayed in GPa units, corresponding to the exposure time for the x, y, and z orientations.

4.4.3 Mechanical properties of 0.1%w MWCNT composite resin

We are now able to conduct a comprehensive comparison of the mechanical properties among the three types of resin. Based on the data presented in Figure 4.12, the results for the maximum tensile strength align with our expectations, showing that MTS increases with longer exposure times. It is worth noting that the y-4s sample yielded a comparatively lower MTS of 8.35 ± 0.44 MPa when compared to the other samples. On the other hand, the x-16s and x-20s samples displayed MTS values of 15.2 ± 0.89 MPa and 14.78 ± 0.43 MPa, respectively, indicating a minor difference between them.

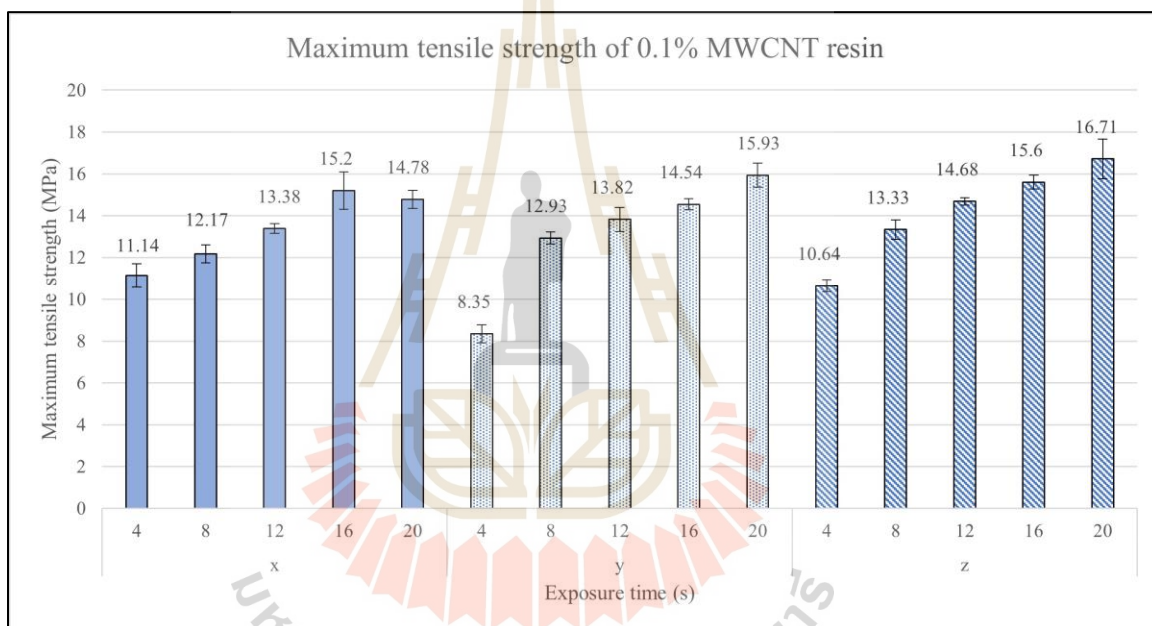


Figure 4.12 The maximum tensile strength of the 0.1% w/w MWCNT composite resin is presented in units of MPa, corresponding to the exposure time for each of the x, y, and z orientations.

The plot of Young's modulus for the 0.1% w/w MWCNT samples also follows the trend observed for MTS, similar to other conditions. In Figure 4.13, the y-4s sample yields the lowest modulus, measuring only 0.483 ± 0.031 GPa, while the highest and averaged Young's modulus was found in the z-20s sample, measuring 1.367 ± 0.070 GPa. Additionally, the x-20s sample exhibits a slightly lower Young's modulus of 1.008 ± 0.090 GPa compared to the x-16s sample, which yields 1.113 ± 0.091 GPa. Overall, the results seem to align

with the expected trend, demonstrating that Young's modulus is influenced by exposure time and orientation, similar to the observations made for MTS.

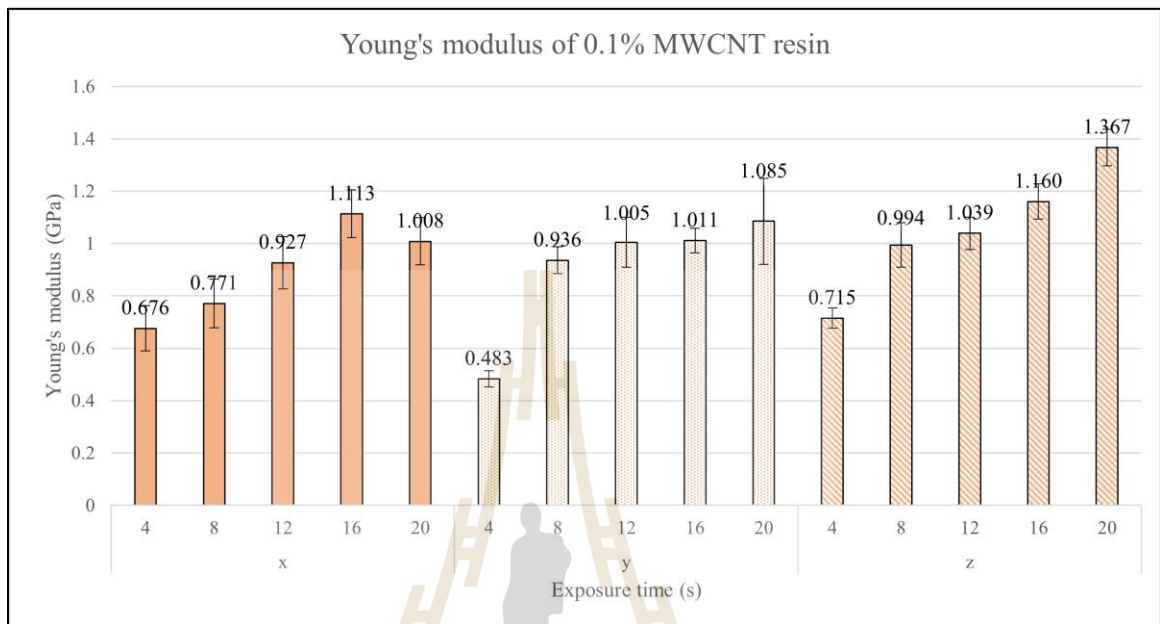


Figure 4.13 The Young's modulus of the 0.1% w/w MWCNT composite resin is presented in units of GPa, corresponding to the exposure time for each of the x, y, and z orientations.

4.4.4 Elongation at break

In this section, our focus is on examining the impact of printing conditions on the elongation at break of the subject material. Elongation at break is a crucial parameter that reflects the material's ability to withstand deformation under stress. It quantifies the efficiency of the material in tolerating deformation, expressed as a percentage change in stress relative to the applied force. By investigating the elongation at break under different printing conditions, we aim to gain insights into how variations in the printing process can influence the material's ability to withstand stretching forces and adapt to deformation. Understanding this relationship is vital for optimizing the mechanical performance of 3D-printed products, as elongation at break provides valuable information on a material's ductility, resilience, and overall mechanical reliability.

According to Figure 4.14, the maximum percent elongation observed was $4.28 \pm 0.73\%$, while the minimum was $2.15 \pm 0.31\%$. The relatively low percentage of elongation

suggests that this resin may not be a ductile material, as it exhibits limited ability to deform under stress.

Moving on to Figure 4.15, which represents the rGO mixed samples, the minimum and maximum elongation values were $1.97 \pm 0.12\%$ and $3.32 \pm 0.31\%$, respectively. Additionally, Figure 4.16, which depicts the MWCNT mixed samples, showed minimum and maximum elongation values of $1.67 \pm 0.19\%$ and $2.97 \pm 0.41\%$, respectively.

Based on these results, it can be inferred that the reinforced resin specimens may not be as flexible as the normal resin, given their lower elongation values. However, it is crucial to note that despite the reduced flexibility, the reinforced resin samples exhibited higher strength, as evident from the results of maximum tensile strength (MTS) and Young's modulus, indicating that the trade-off between flexibility and strength was balanced in favor of enhanced mechanical properties.

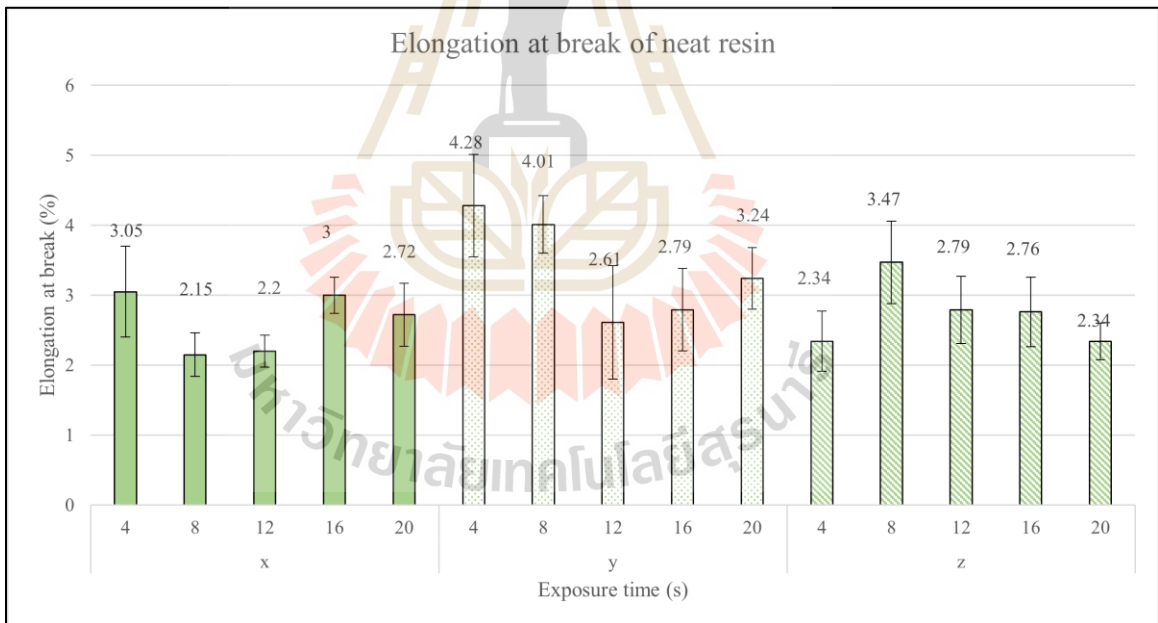


Figure 4.14 The plot represents the elongation at break corresponding to the exposure time for each orientation of the neat resin samples. The data reveals that the maximum percent elongation observed was $4.28 \pm 0.73\%$, while the minimum was $2.15 \pm 0.31\%$.

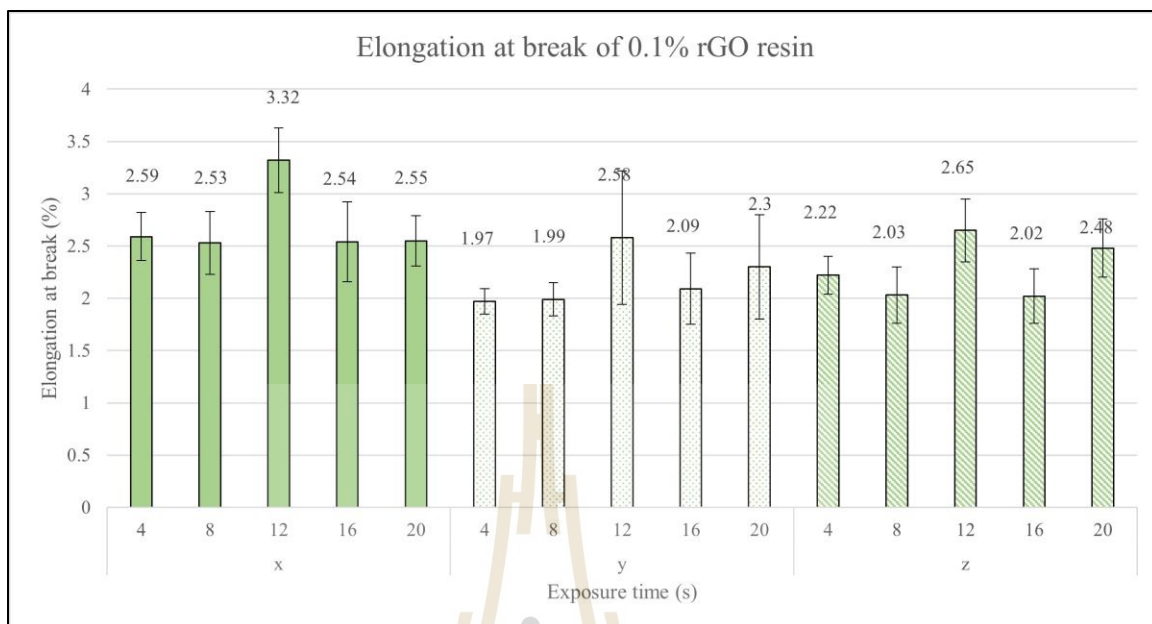


Figure 4.15 The plot represents the elongation at break corresponding to the exposure time for each orientation of the 0.1% added rGO resin samples.

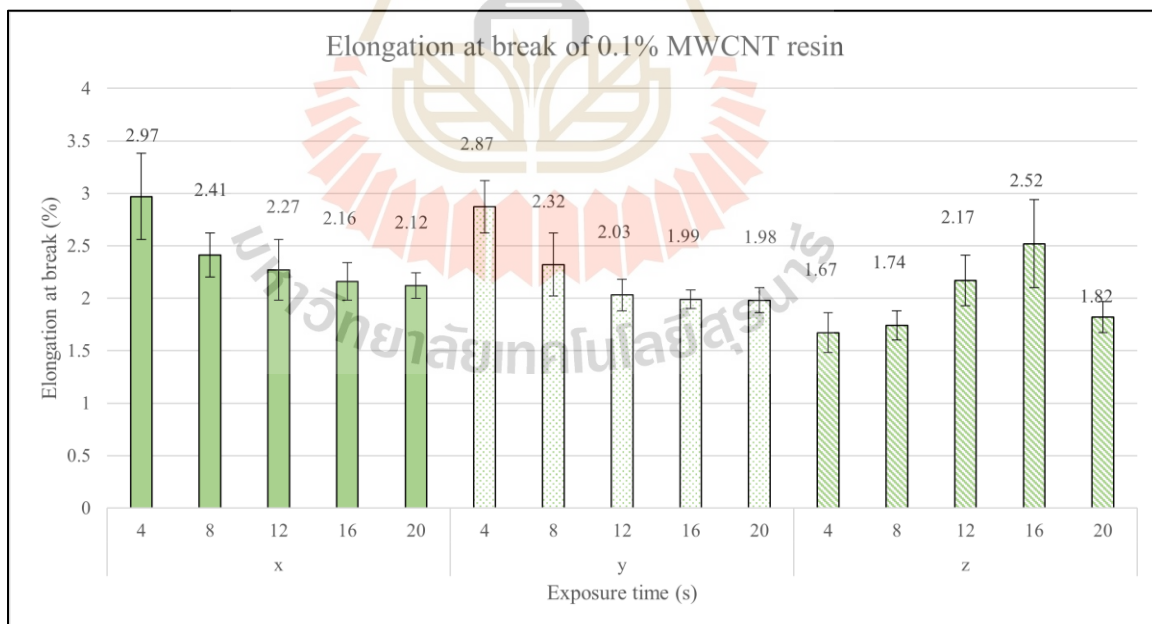
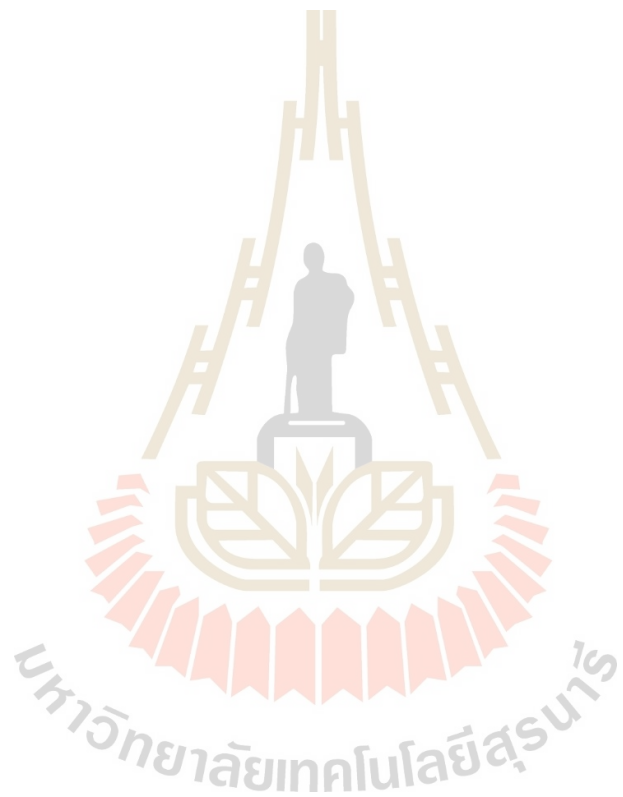


Figure 4.16 The plot illustrates the elongation at break for the 0.1% added MWCNT resin samples, corresponding to the exposure time for each orientation.

Furthermore, based on the results, we can conclude that the printing orientation does not significantly affect the elongation at break. Although there is a slight indication that the normal resin may exhibit slightly more elongation compared to the reinforced resin, there is no discernible pattern to confirm a significant influence of the printing orientation on this matter.



CHAPTER V

CONCLUSION

In this experiment, we delved into the mechanical properties and performance of 3D-printed samples using different resin compositions, exposure times, and printing orientations. The goal was to analyze the effects of these parameters on the tensile strength, Young's modulus, and elongation at break of the printed specimens. The comprehensive exploration covered three types of resin: neat resin, resin with 0.1% w/w reduced graphene oxide (rGO), and resin with 0.1% w/w multi-wall carbon nanotube (MWCNT).

The EDS analysis highlights the challenges and opportunities in utilizing rGO for composite 3D resin applications. While the oxygen and sulfur content offer benefits for bonding and dispersion, the low carbon content and incomplete reduction may limit the material's full potential. Optimizing the reduction process or modifying the rGO structure can address these limitations and enhance its performance in resin composites. The SEM and EDS results suggest that the MWCNTs, despite their bundled morphology, have the potential to significantly enhance the mechanical properties of the composite 3D resin. Their high carbon content ensures strong structural integrity, while the minimal oxygen presence provides a balance between resin compatibility and retained intrinsic properties. This makes MWCNTs a promising reinforcement material for composite applications.

Through all experimentation and analysis, we observed various intriguing findings and trends in the mechanical behavior of the printed samples. The tensile strength, a crucial indicator of material strength and ability to withstand stretching forces, demonstrated a consistent trend across all orientations and exposure times. Generally, higher exposure times were associated with increased tensile strength, indicating improved

material performance with longer printing periods. However, some exceptions were noted in specific orientations, where certain exposure times exhibited unexpected behavior.

Similarly, Young's modulus, which indicates the material's stiffness and elasticity, displayed consistent trends with respect to exposure times and orientations. We observed that Young's modulus tended to increase with longer exposure times, suggesting a direct relationship between exposure duration and the material's stiffness. Again, exceptions were found in specific orientations, highlighting the significance of considering printing orientation in optimizing material properties.

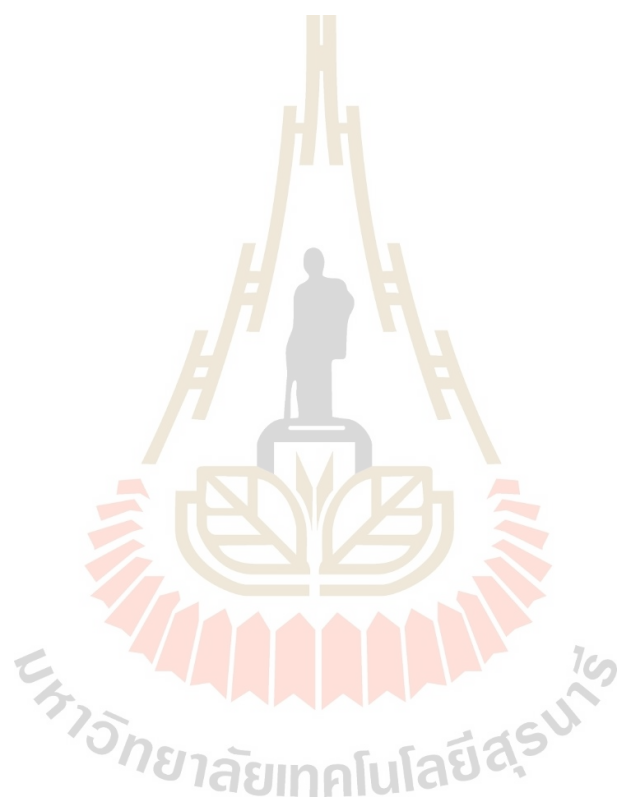
Elongation at break, a critical parameter reflecting the material's flexibility and tolerance to deformation, provided valuable insights into the materials' ductility. Interestingly, we noticed that the normal resin samples generally exhibited higher elongation at break compared to the reinforced resin samples containing rGO and MWCNT. However, we found no conclusive patterns confirming a significant influence of the printing orientation on elongation at break.

Comparing the reinforced resin samples with the normal resin, we observed that while the reinforced samples displayed reduced elongation, they exhibited improved tensile strength and Young's modulus. This suggests a trade-off between flexibility and mechanical strength, where the addition of rGO and MWCNT enhanced the material's mechanical properties at the expense of some flexibility.

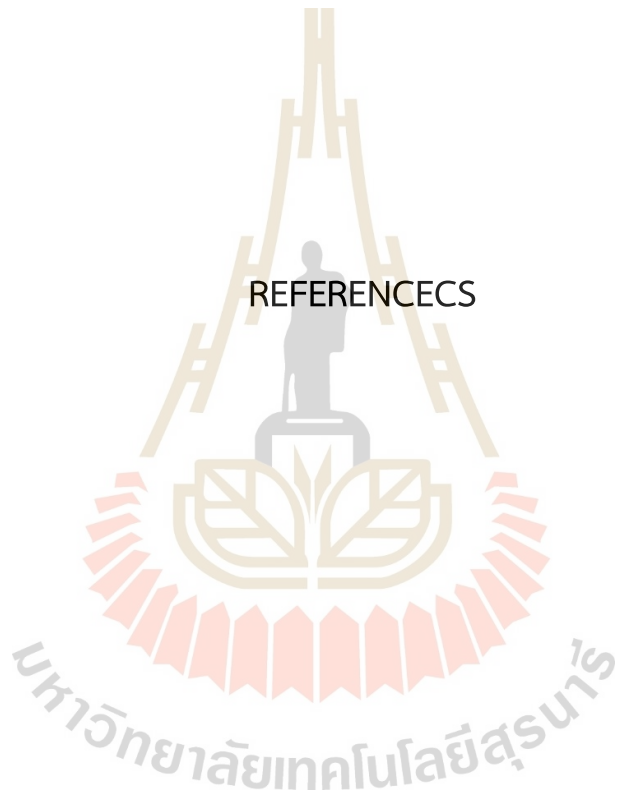
In summary, this study has shed light on the intricate relationships between exposure times, printing orientations, and the mechanical properties of 3D-printed samples. The findings have practical implications for optimizing the design and fabrication of 3D-printed products, as they highlight the importance of selecting appropriate exposure times and understanding the influence of printing orientation on mechanical performance. Further investigations and refinement in resin compositions and printing parameters are warranted to fully unlock the potential of 3D printing in various engineering and scientific applications.

Overall, this comprehensive exploration contributes valuable knowledge to the field of 3D printing and materials science, opening new avenues for advancing additive

manufacturing technologies and expanding the horizons of innovative product development.



REFERENCES

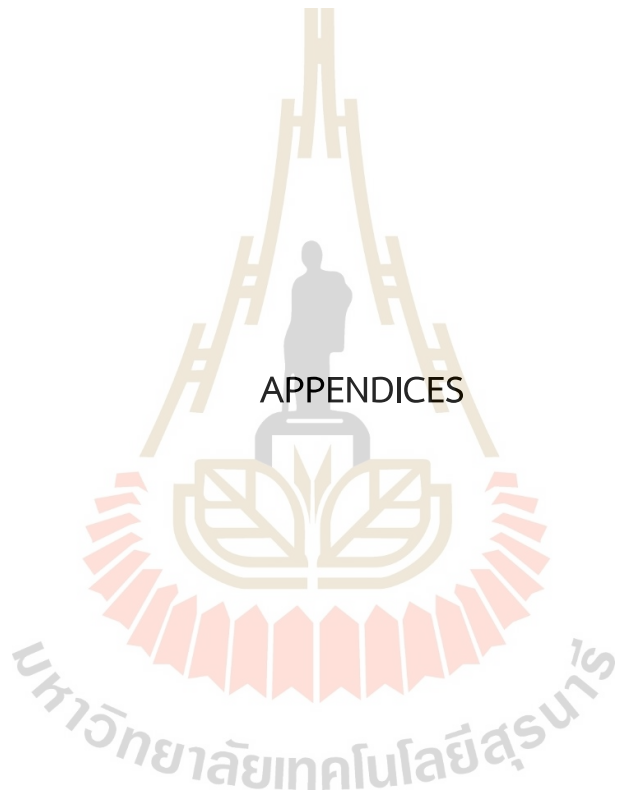


REFERENCES

- Abdollahi, S., Davis, A., Miller, J. H. and Feinberg, A. W. (2018). Expert-guided optimization for 3D printing of soft and liquid materials. *PLoS ONE*, 13(4), e0194890. doi:10.1371/journal.pone.0194890.
- Ahn, D., Stevens, L. M., Zhou, K. and Page, Z. A. (2020). Rapid High-Resolution Visible Light 3D Printing. *ACS Central Science*, 6(9), 1555-1563. doi:10.1021/acscentsci.0c00929
- Andrews, R. and Weisenberger, M.C. (2004). Carbon nanotube polymer composites. *Current Opinion in Solid State and Materials Science*, 8(1), 31-37. doi:10.1016/j.cossms.2003.10.006.
- Borodulina, S., Kulachenko, A., Galland, S., Nygards, M. (2012). Stress-strain curve of paper revisited. *Nordic Pulp and Paper Research Journal*, 27(2), 318. doi:10.3183/NPPRJ-2012-27-02-p318-328
- Coiffic, J. C., Fayolle, M., Maitrejean, S., Foa Torres, L. E. F., Le Poche, H. (2007). Conduction regime in innovative carbon nanotube via interconnect architectures. *Applied Physics Letters*, 91(25), 252107. doi:10.1063/1.2826274
- Feng, Z., Li, Y., Xin, C., Tang, D., Xiong, W. and Zhang, H. (2019) Fabrication of Graphene-Reinforced Nanocomposites with Improved Fracture Toughness in Net Shape for Complex 3D Structures via Digital Light Processing. *C*, 5(2), 25. doi:10.3390/c5020025.
- Hanon, M., Ghaly, A., Zsidai, L., Szakál, Z., Szabó, I. and Kátai, L. (2021). Investigations of the Mechanical Properties of DLP 3D Printed Graphene/Resin Composites. *Acta Polytechnica Hungarica*, 18, 143-161. doi:10.12700/APH.18.8.2021.8.8.
- Harding, J. and Welsh, L.M. (1983). A tensile testing technique for fibre-reinforced composites at impact rates of strain. *Journal of Materials Science*, 18, 1810–1826. doi:10.1007/BF00542078.
- Harris, P.J.F. (2004). Carbon nanotube composites. *International Materials Reviews*,

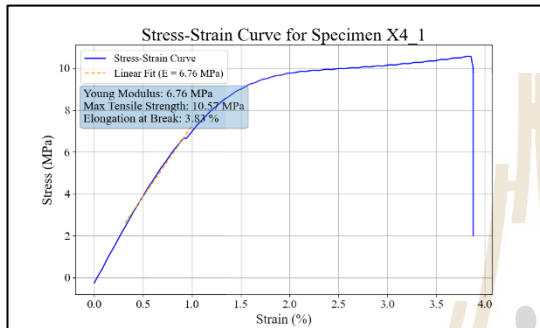
49(1), 31-43, doi:10.1179/095066004225010505.

- Lee, C. S., Kim, S. G., Kim, H. J. and Ahn, S. H. (2007). Measurement of anisotropic compressive strength of rapid prototyping parts. *Journal of Materials Processing Technology*, 187–188, 627–630. Doi:0.1016/j.jmatprotec.2006.11.095
- Lee, J. Y., An, J., Chua, C. K. (2017). Fundamentals and applications of 3D printing for novel materials. *Applied Materials Today*, 7, 120-133. doi:10.1016/j.apmt.2017.02.004.
- Lim, S. M., Shin, B. S. and Kim, K. (2017). Characterization of Products Using Additive Manufacturing with Graphene/Photopolymer-Resin Nano-Fluid. *Journal of Nanoscience and Nanotechnology*, 1, 5492–5495. doi:10.1166/jnn.2017.14159.
- Malas, A., Isakov, D., Couling, K. and Gibbons, G. J. (2019). Fabrication of High Permittivity Resin Composite for Vat Photopolymerization 3D Printing: Morphology, Thermal, Dynamic Mechanical and Dielectric Properties. *Materials*, 12(23), 3818. doi:10.3390/ma12233818.
- Markandan, K. and Lai, C. Q., (2020). Enhanced mechanical properties of 3D printed graphene-polymer composite lattices at very low graphene concentrations, *Composites Part A: Applied Science and Manufacturing*, 129, 105726. doi:10.1016/j.compositesa.2019.105726.
- Mohamed, M. G. A., Kumar, H., Wang, Z., Martin, N., Mills, B. and Kim, K. (2019). Rapid and inexpensive fabrication of multi-depth microfluidic device using high-resolution LCD stereolithographic 3D printing. *Journal of Manufacturing and Materials Processing*, 3, 26. doi:10.3390/jmmp3010026
- Shahrubudin, N., Lee, T. C. and Ramlan, R. (2019). An Overview on 3D Printing Technology: Technological, Materials, and Applications. *Procedia Manufacturing*, 35, 1286-1296. doi:10.1016/j.promfg.2019.06.089.
- Sharon, M. and Sharon, M. (2010). *Carbon Nanoforms and Applications*. New York: McGraw-Hill.

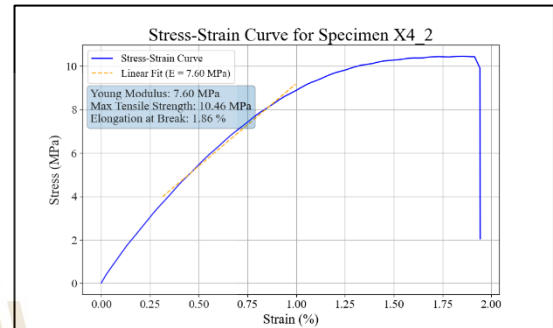


APPENDIX A

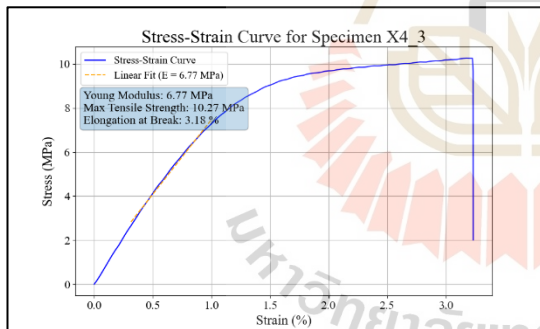
THE STRESS-STRAIN CURVE OF EACH CONDITION



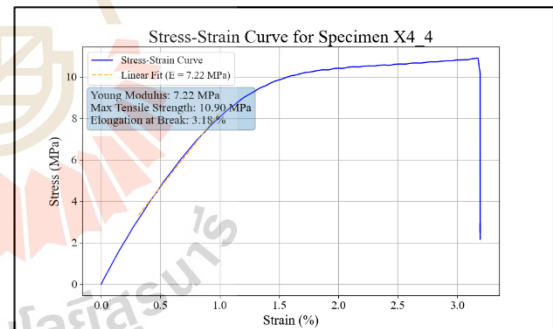
neat resin, x-orientation, 4s exposure time,
sample No.1



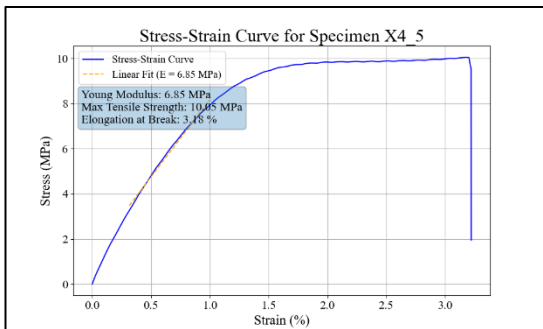
neat resin, x-orientation, 4s exposure time,
sample No.2



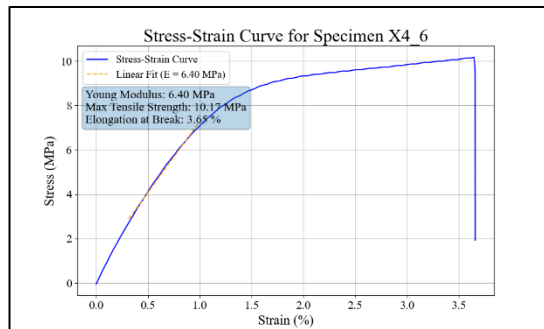
neat resin, x-orientation, 4s exposure time,
sample No.3



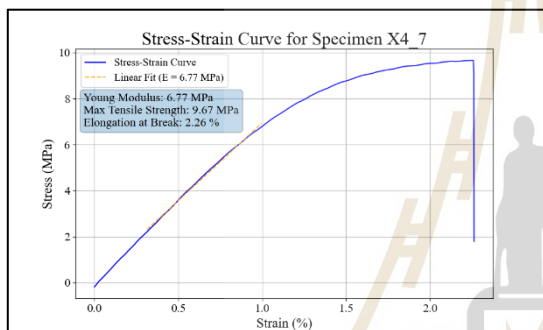
neat resin, x-orientation, 4s exposure time,
sample No.4



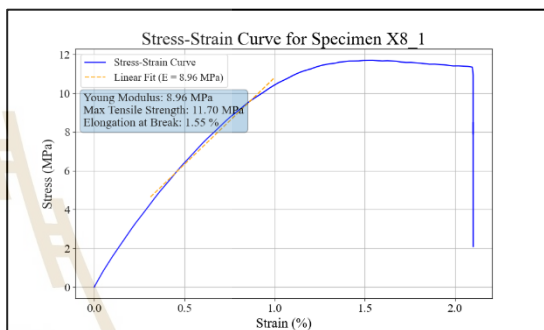
neat resin, x-orientation, 4s exposure time, sample No.5



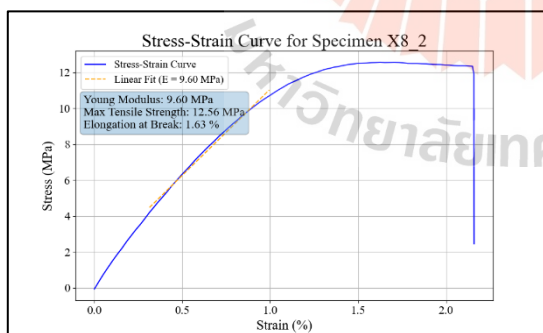
neat resin, x-orientation, 4s exposure time, sample No.6



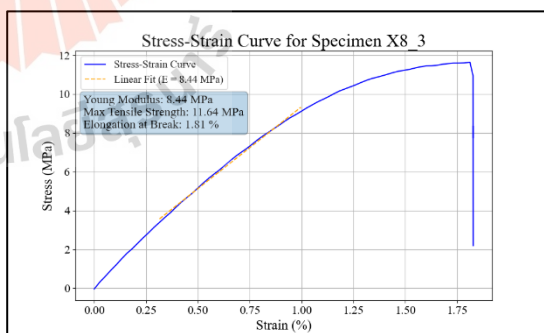
neat resin, x-orientation, 4s exposure time, sample No.7



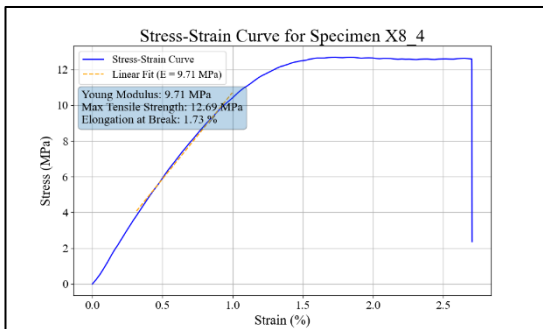
neat resin, x-orientation, 8s exposure time, sample No.1



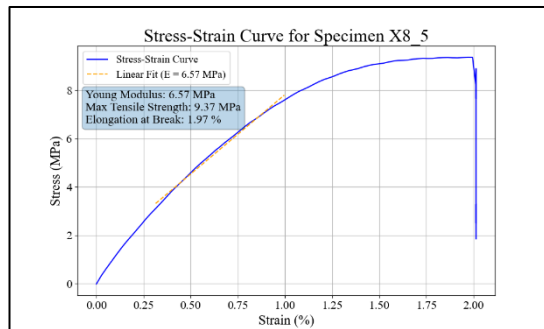
neat resin, x-orientation, 8s exposure time, sample No.2



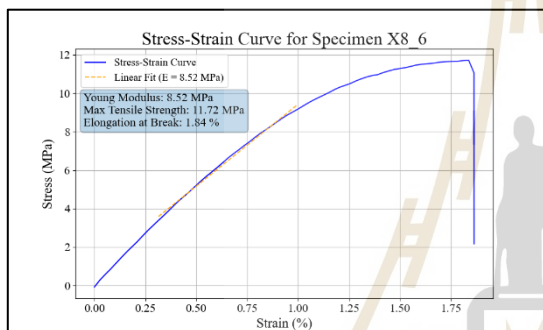
neat resin, x-orientation, 8s exposure time, sample No.3



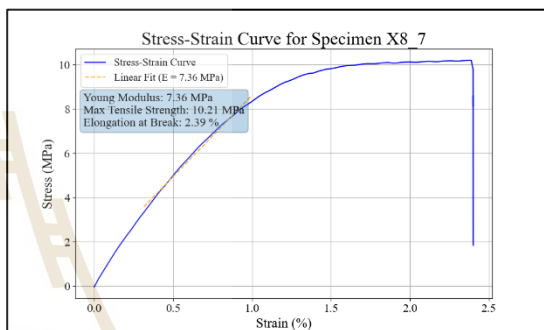
neat resin, x-orientation, 8s exposure time, sample No.4



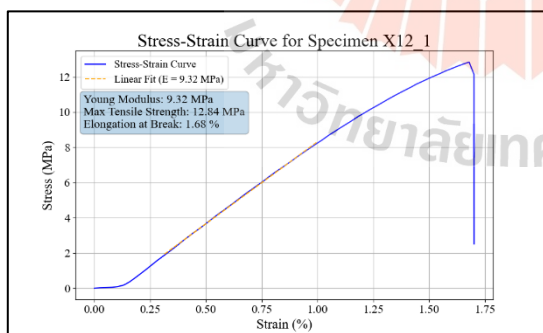
neat resin, x-orientation, 8s exposure time, sample No.5



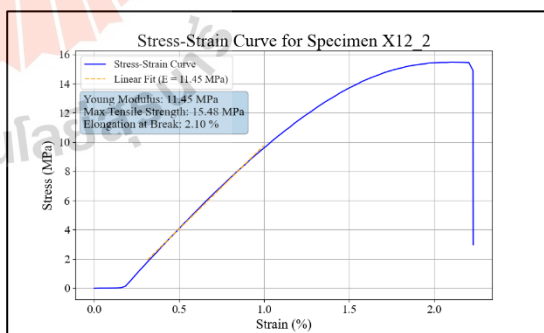
neat resin, x-orientation, 8s exposure time, sample No.6



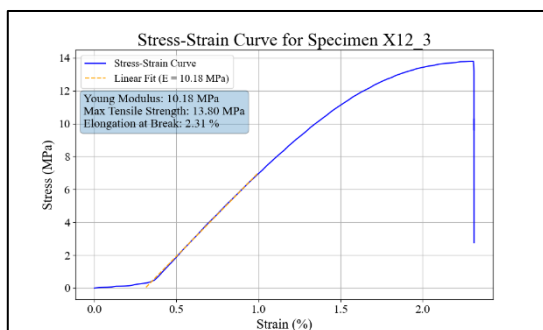
neat resin, x-orientation, 8s exposure time, sample No.7



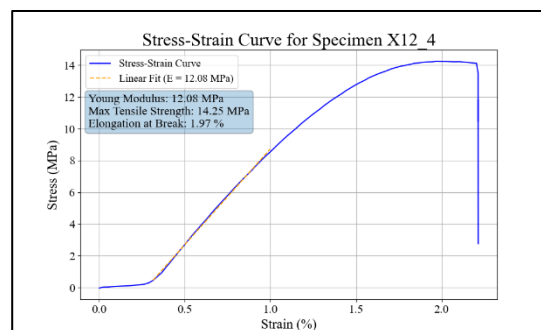
neat resin, x-orientation, 12s exposure time, sample No.1



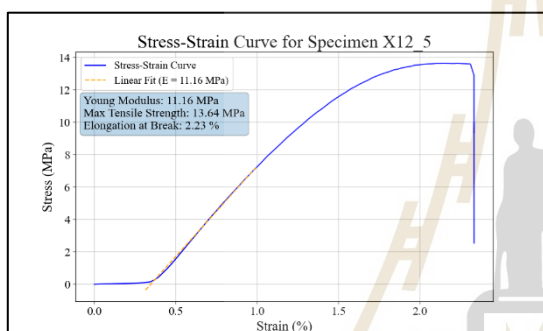
neat resin, x-orientation, 12s exposure time, sample No.2



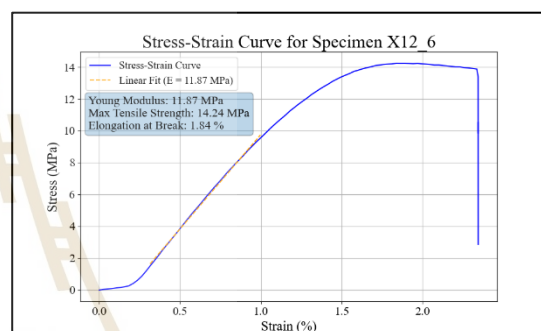
neat resin, x-orientation, 12s exposure time,
sample No.3



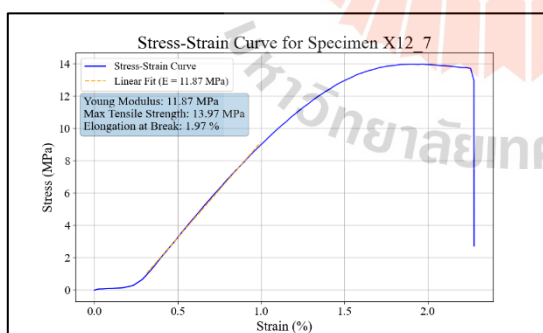
neat resin, x-orientation, 12s exposure time,
sample No.4



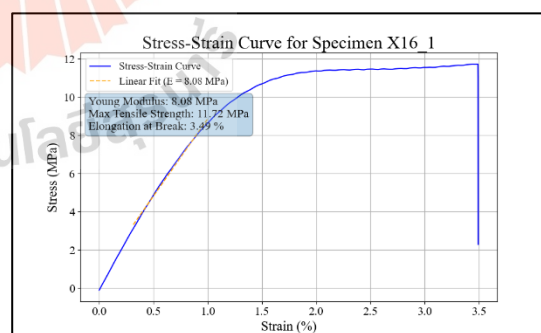
neat resin, x-orientation, 12s exposure time,
sample No.5



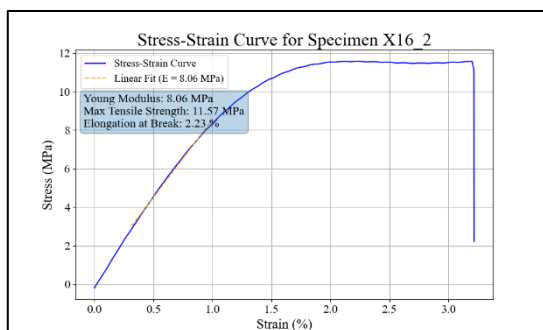
neat resin, x-orientation, 12s exposure time,
sample No.6



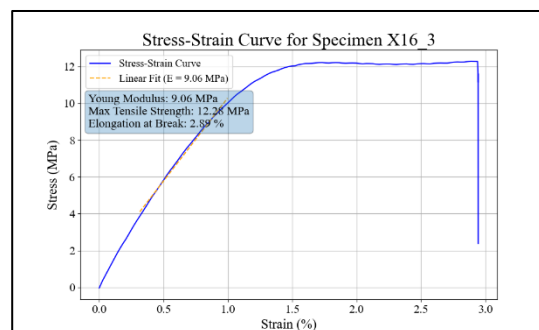
neat resin, x-orientation, 12s exposure time,
sample No.7



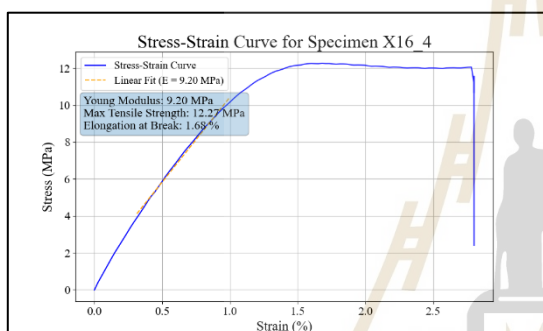
neat resin, x-orientation, 16s exposure time,
sample No.1



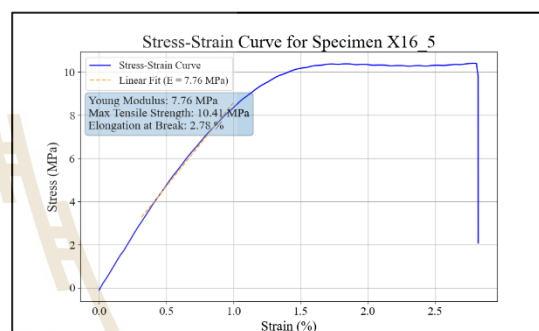
neat resin, x-orientation, 16s exposure time,
sample No.2



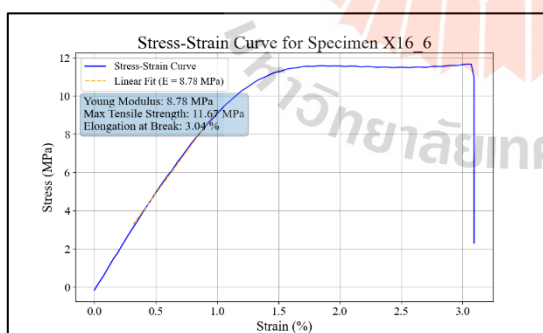
neat resin, x-orientation, 16s exposure time,
sample No.3



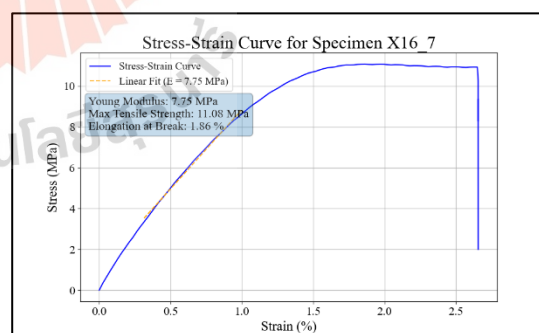
neat resin, x-orientation, 16s exposure time,
sample No.4



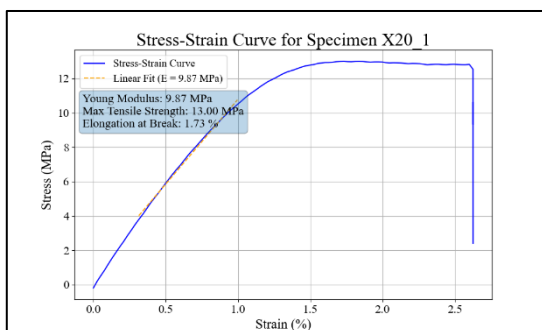
neat resin, x-orientation, 16s exposure time,
sample No.5



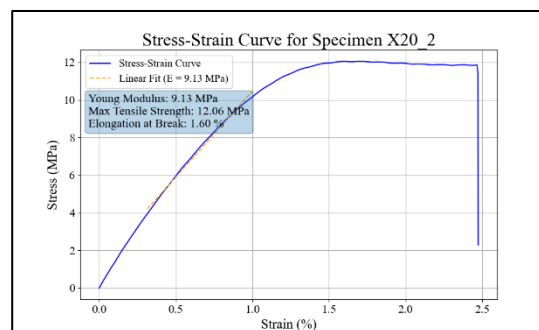
neat resin, x-orientation, 16s exposure time,
sample No.6



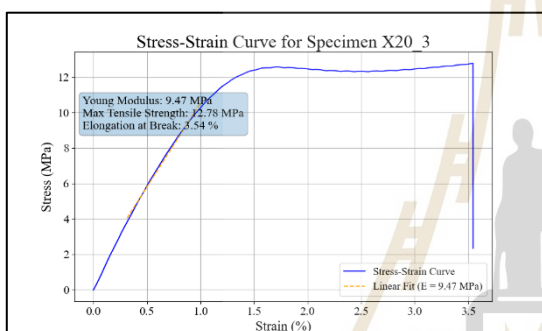
neat resin, x-orientation, 16s exposure time,
sample No.7



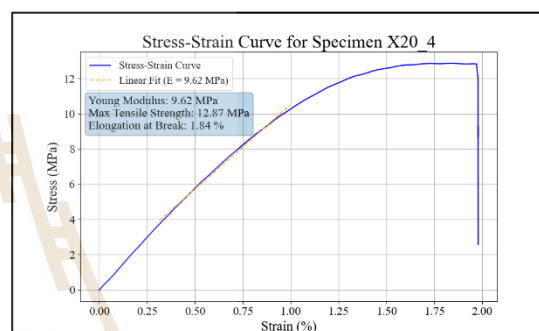
neat resin, x-orientation, 20s exposure time,
sample No.1



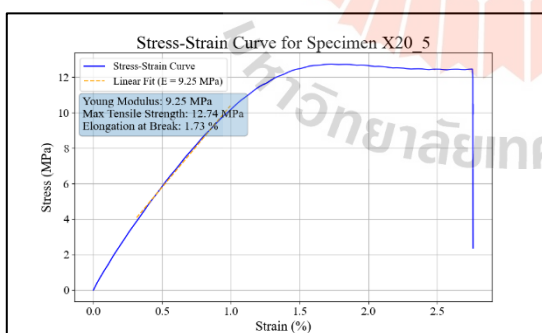
neat resin, x-orientation, 20s exposure time,
sample No.2



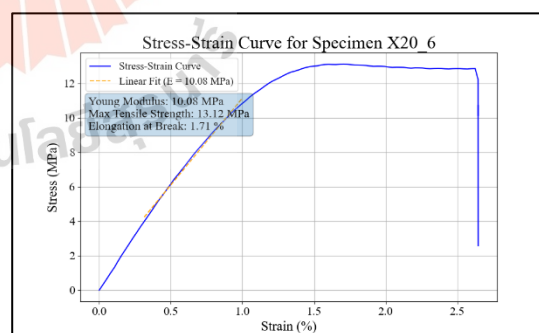
neat resin, x-orientation, 20s exposure time,
sample No.3



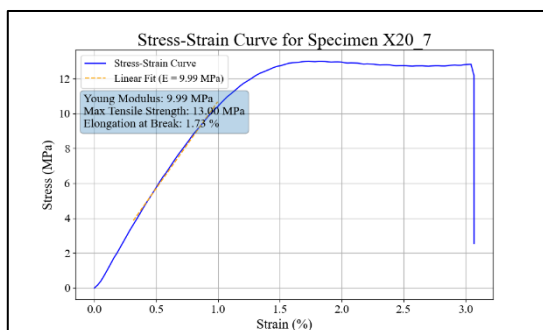
neat resin, x-orientation, 20s exposure time,
sample No.4



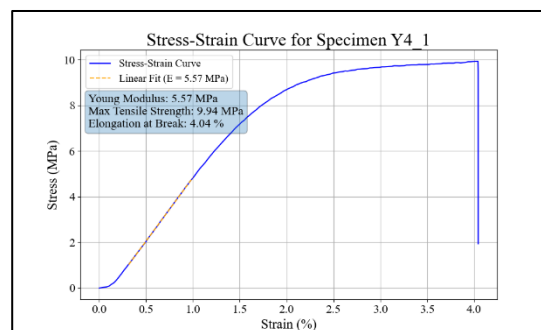
neat resin, x-orientation, 20s exposure time,
sample No.5



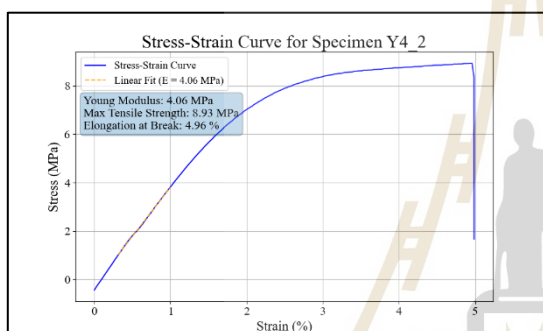
neat resin, x-orientation, 20s exposure time,
sample No.6



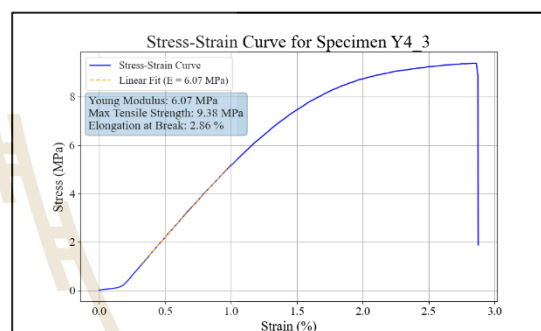
neat resin, x-orientation, 20s exposure time,
sample No.7



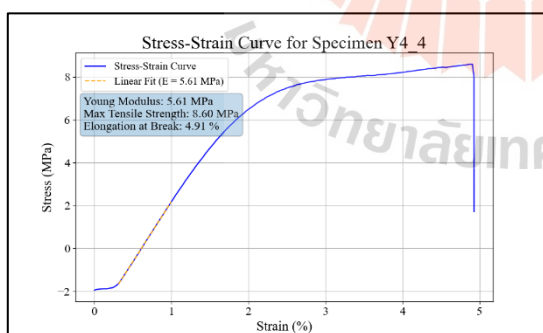
neat resin, y-orientation, 4s exposure time,
sample No.1



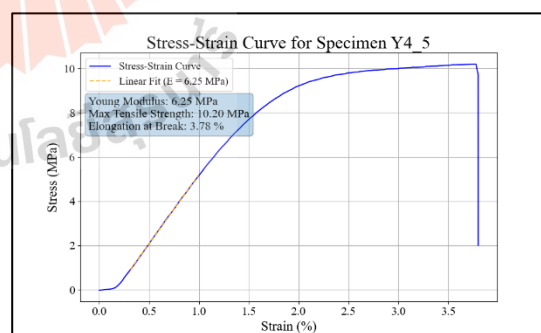
neat resin, y-orientation, 4s exposure time,
sample No.2



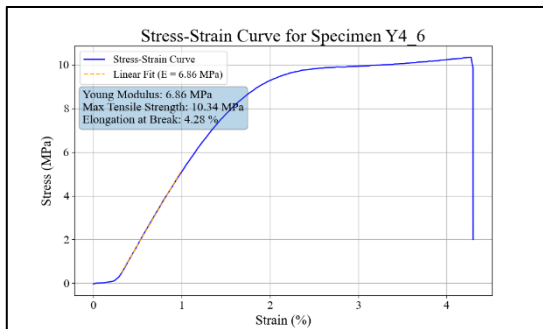
neat resin, y-orientation, 4s exposure time,
sample No.3



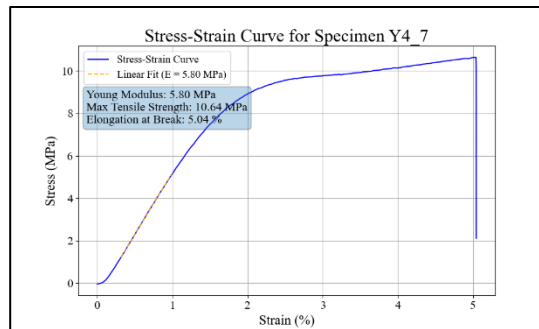
neat resin, y-orientation, 4s exposure time,
sample No.4



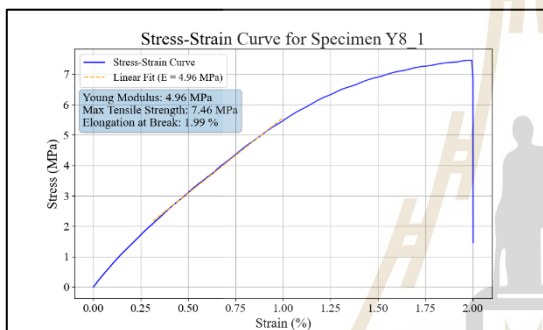
neat resin, y-orientation, 4s exposure time,
sample No.5



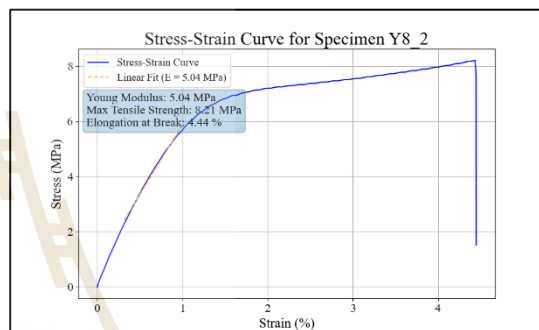
neat resin, y-orientation, 4s exposure time, sample No.6



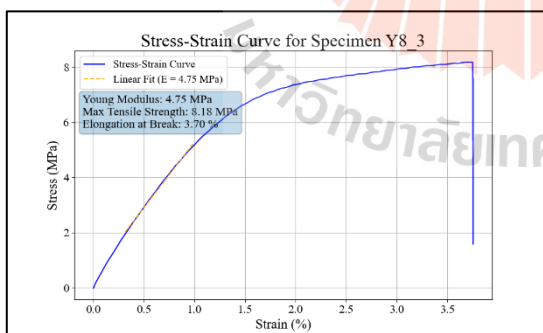
neat resin, y-orientation, 4s exposure time, sample No.7



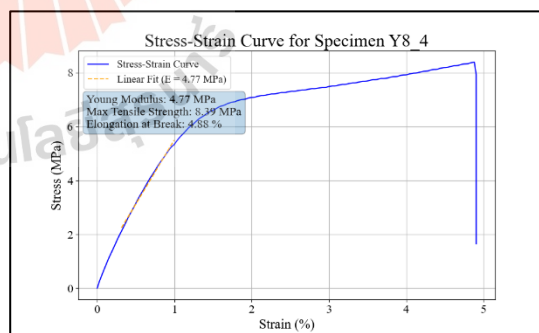
neat resin, y-orientation, 8s exposure time, sample No.1



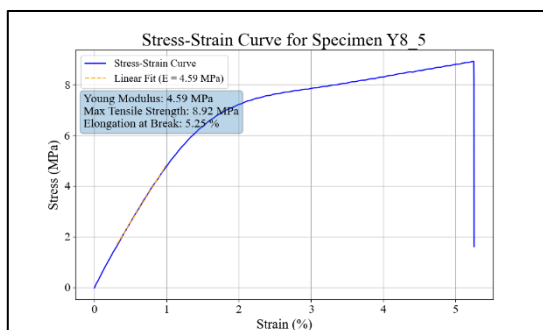
neat resin, y-orientation, 8s exposure time, sample No.2



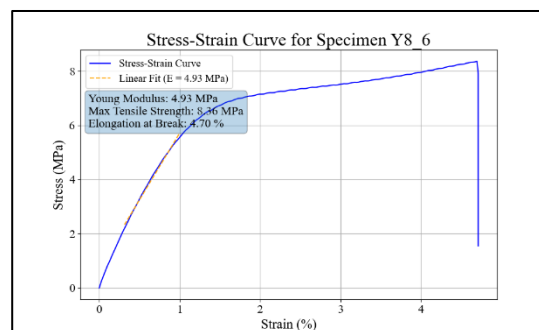
neat resin, y-orientation, 8s exposure time, sample No.3



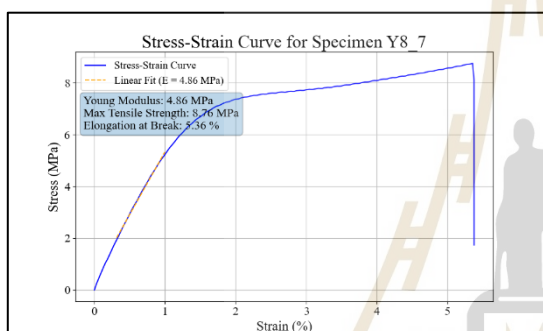
neat resin, y-orientation, 8s exposure time, sample No.4



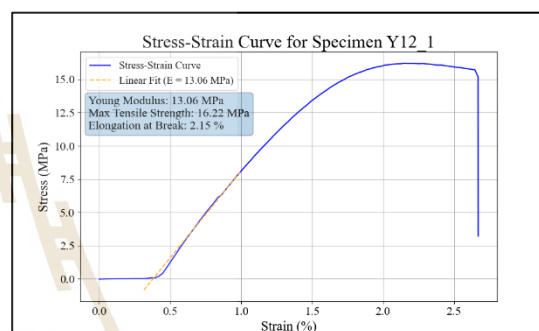
neat resin, y-orientation, 8s exposure time,
sample No.5



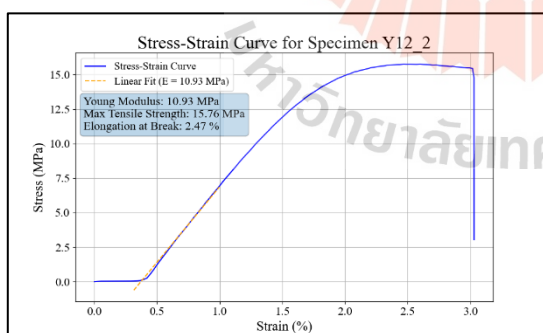
neat resin, y-orientation, 8s exposure time,
sample No.6



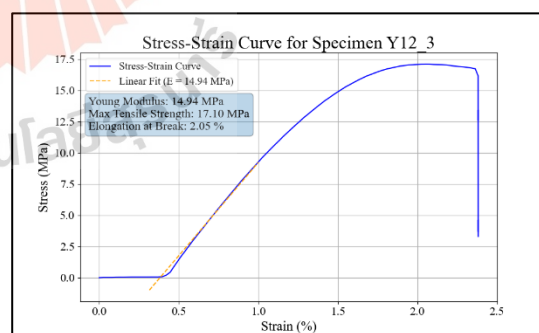
neat resin, y-orientation, 8s exposure time,
sample No.7



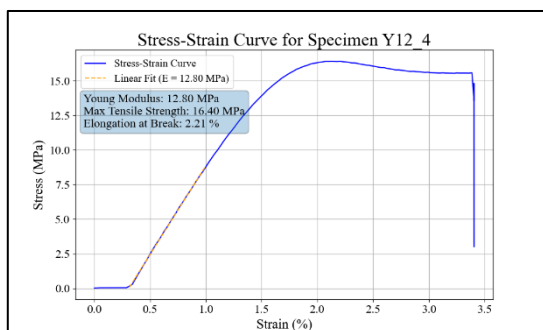
neat resin, y-orientation, 12s exposure time,
sample No.1



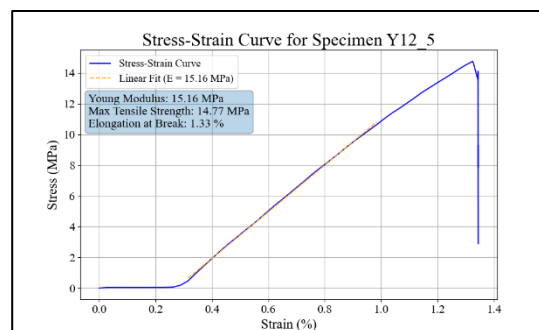
neat resin, y-orientation, 12s exposure time,
sample No.2



neat resin, y-orientation, 12s exposure time,
sample No.3



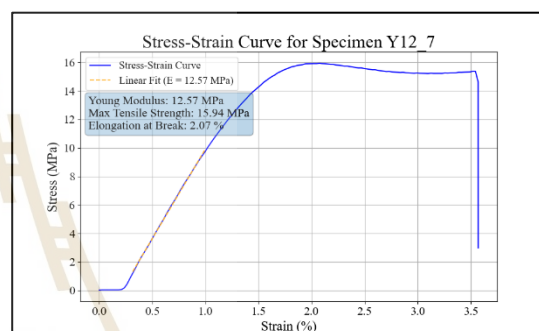
neat resin, y-orientation, 12s exposure time,
sample No.4



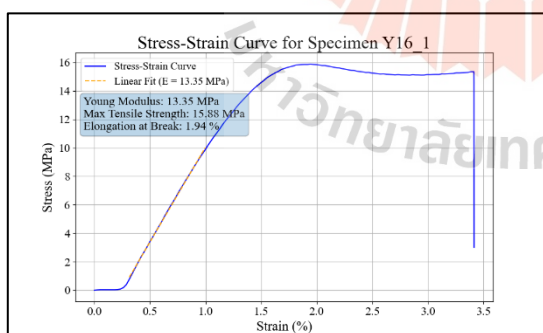
neat resin, y-orientation, 12s exposure time,
sample No.5



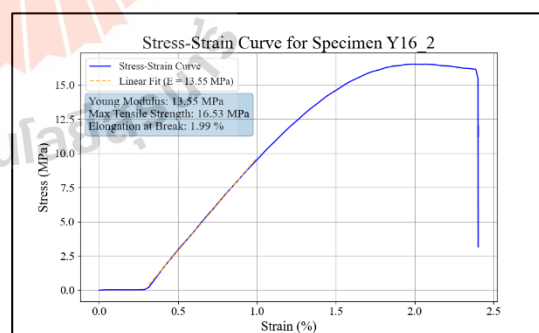
neat resin, y-orientation, 12s exposure time,
sample No.6



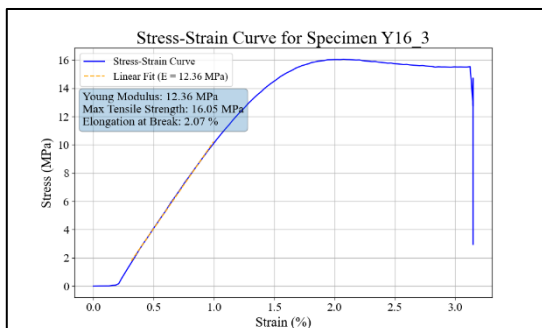
neat resin, y-orientation, 12s exposure time,
sample No.7



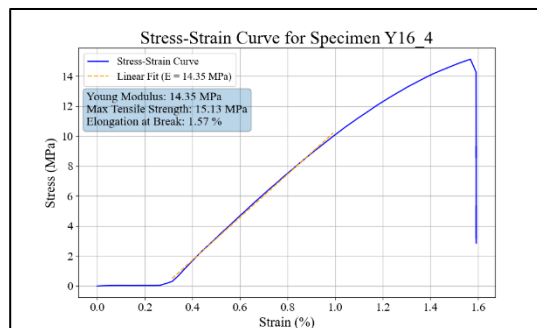
neat resin, y-orientation, 16s exposure time,
sample No.1



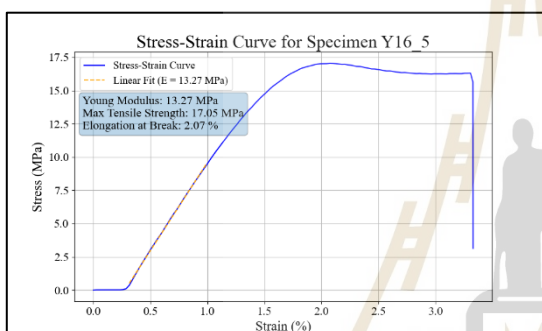
neat resin, y-orientation, 16s exposure time,
sample No.2



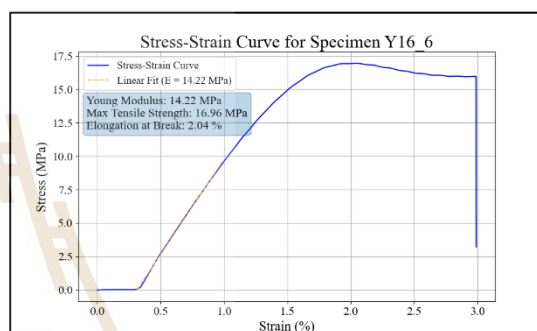
neat resin, y-orientation, 16s exposure time,
sample No.3



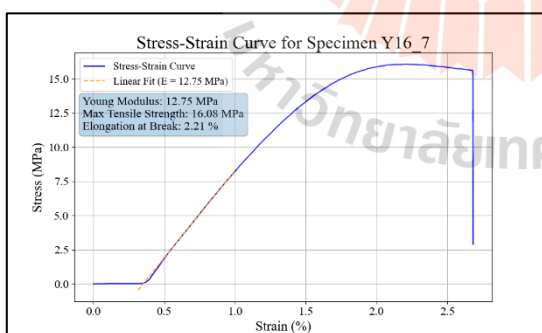
neat resin, y-orientation, 16s exposure time,
sample No.4



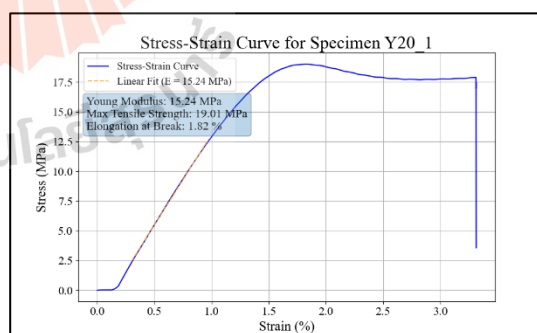
neat resin, y-orientation, 16s exposure time,
sample No.5



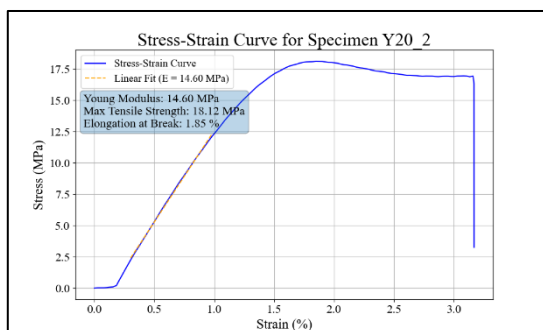
neat resin, y-orientation, 16s exposure time,
sample No.6



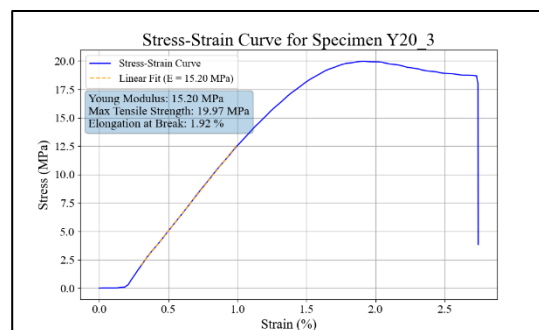
neat resin, y-orientation, 16s exposure time,
sample No.7



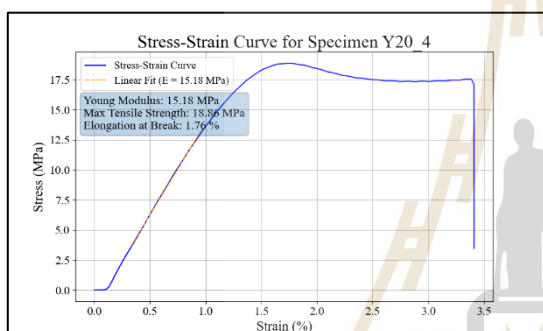
neat resin, y-orientation, 20s exposure time,
sample No.1



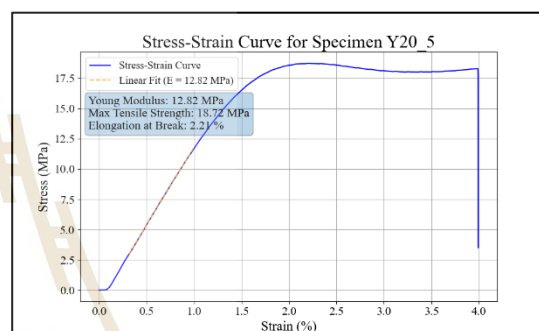
neat resin, y-orientation, 20s exposure time,
sample No.2



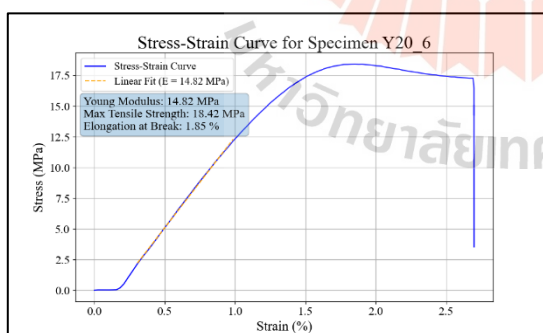
neat resin, y-orientation, 20s exposure time,
sample No.3



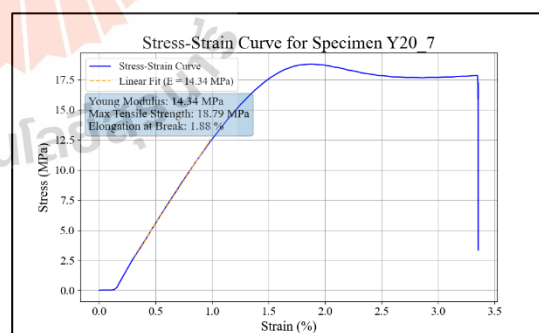
neat resin, y-orientation, 20s exposure time,
sample No.4



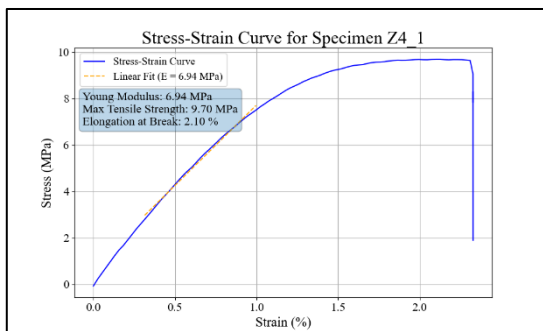
neat resin, y-orientation, 20s exposure time,
sample No.5



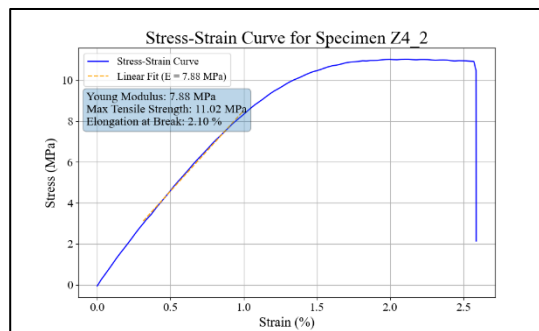
neat resin, y-orientation, 20s exposure time,
sample No.6



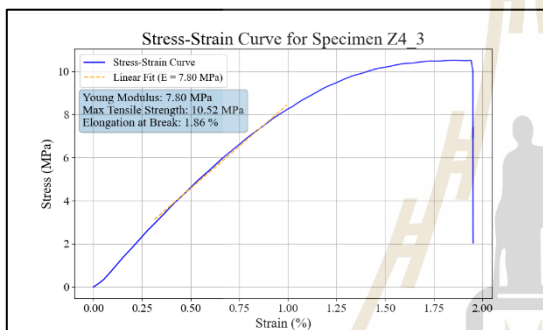
neat resin, y-orientation, 20s exposure time,
sample No.7



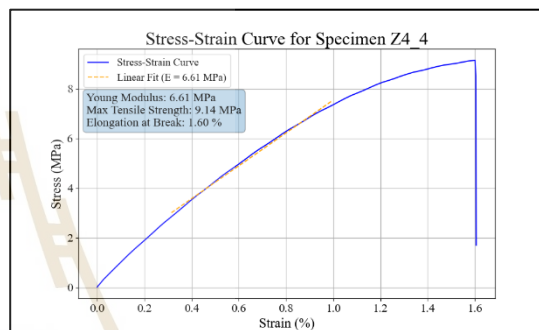
neat resin, z-orientation, 4s exposure time, sample No.1



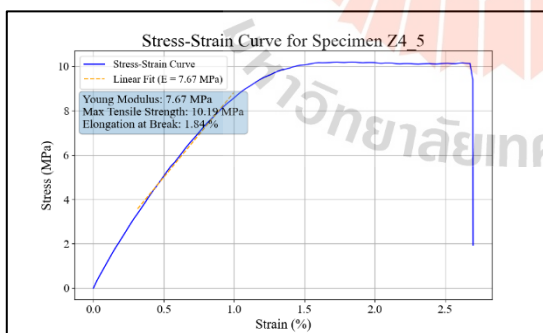
neat resin, z-orientation, 4s exposure time, sample No.2



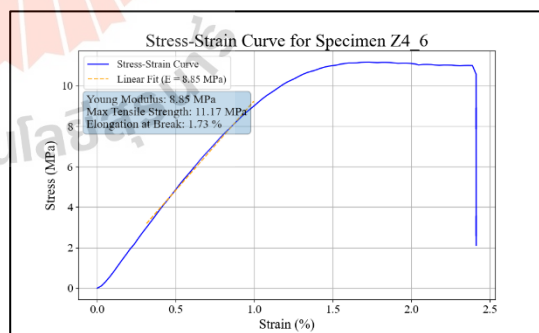
neat resin, z-orientation, 4s exposure time, sample No.3



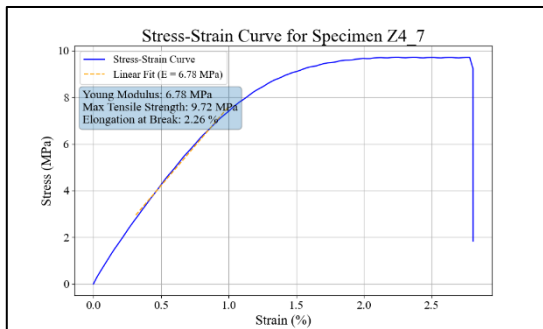
neat resin, z-orientation, 4s exposure time, sample No.4



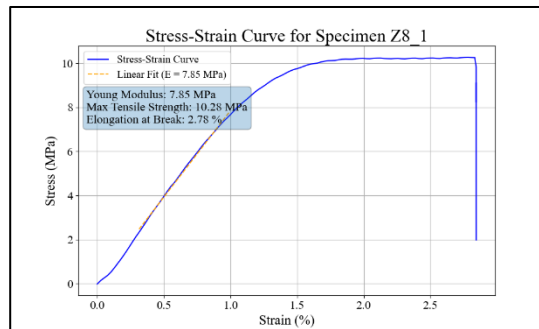
neat resin, z-orientation, 4s exposure time, sample No.5



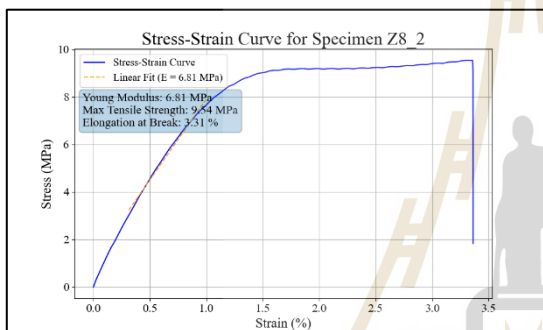
neat resin, z-orientation, 4s exposure time, sample No.6



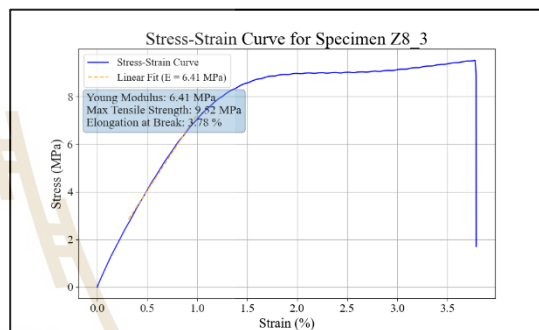
neat resin, z-orientation, 4s exposure time, sample No.7



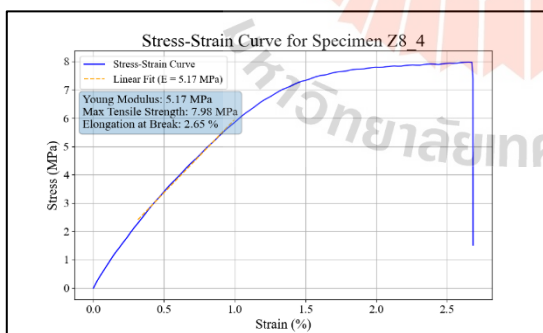
neat resin, z-orientation, 8s exposure time, sample No.1



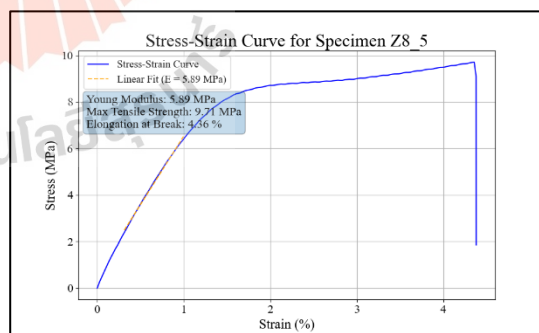
neat resin, z-orientation, 8s exposure time, sample No.2



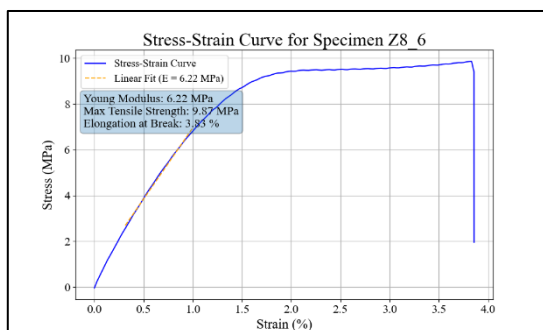
neat resin, z-orientation, 8s exposure time, sample No.3



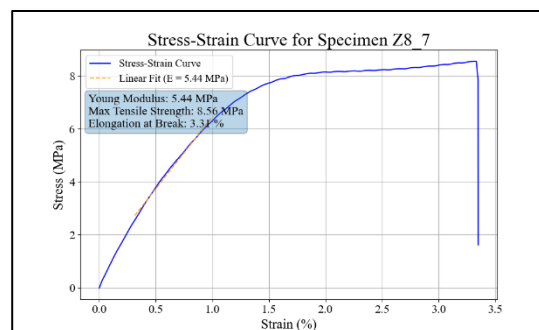
neat resin, z-orientation, 8s exposure time, sample No.4



neat resin, z-orientation, 8s exposure time, sample No.5



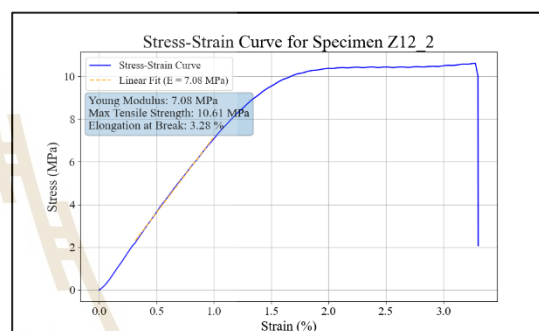
neat resin, z-orientation, 8s exposure time,
sample No.6



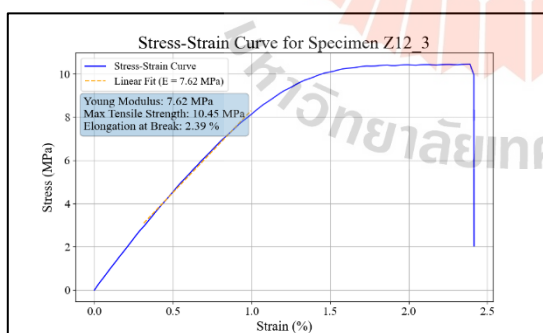
neat resin, z-orientation, 8s exposure time,
sample No.7



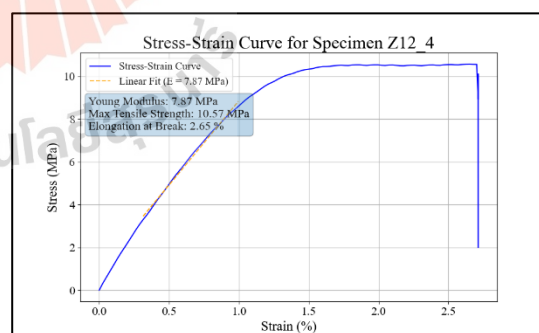
neat resin, z-orientation, 12s exposure time,
sample No.1



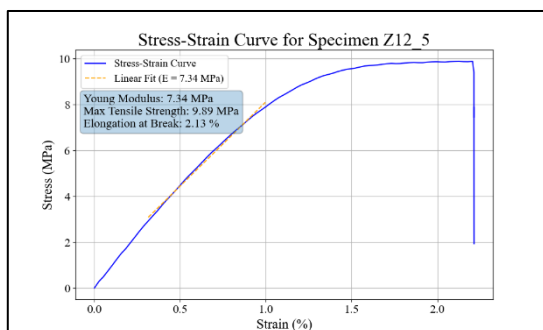
neat resin, z-orientation, 12s exposure time,
sample No.2



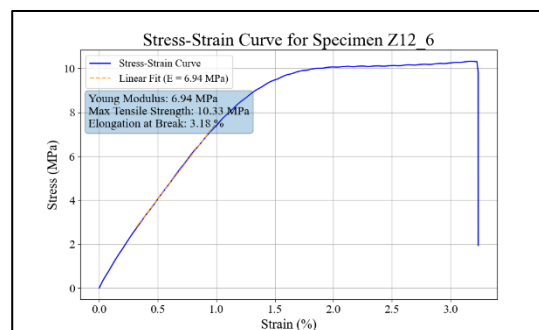
neat resin, z-orientation, 12s exposure time,
sample No.3



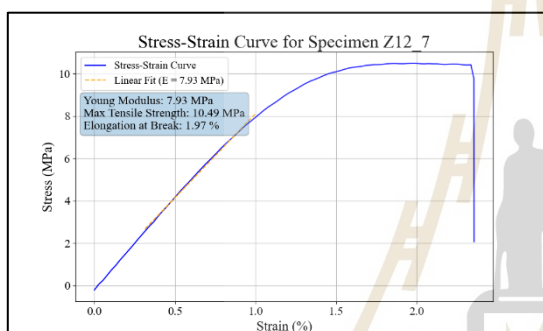
neat resin, z-orientation, 12s exposure time,
sample No.4



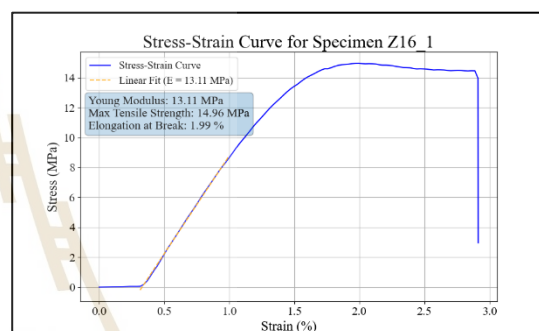
neat resin, z-orientation, 12s exposure time,
sample No.5



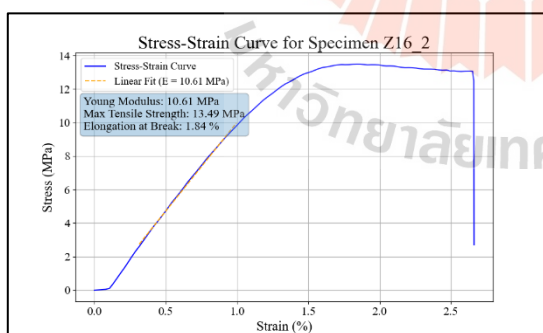
neat resin, z-orientation, 12s exposure time,
sample No.6



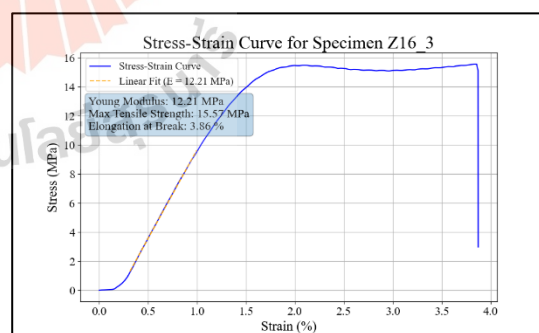
neat resin, z-orientation, 12s exposure time,
sample No.7



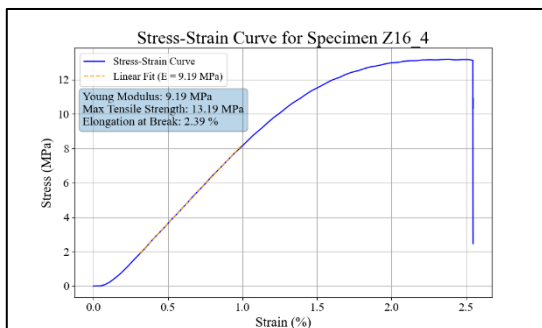
neat resin, z-orientation, 16s exposure time,
sample No.1



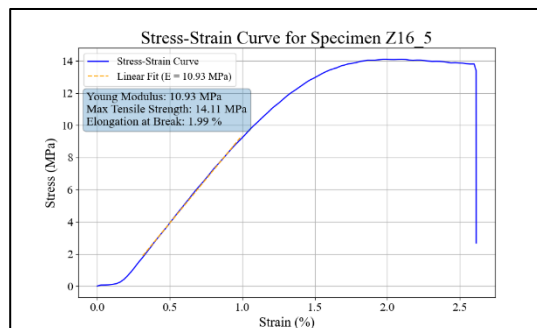
neat resin, z-orientation, 16s exposure time,
sample No.2



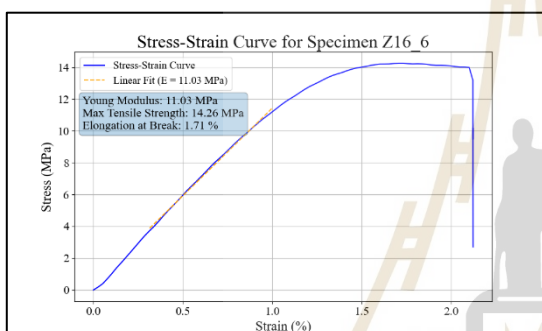
neat resin, z-orientation, 16s exposure time,
sample No.3



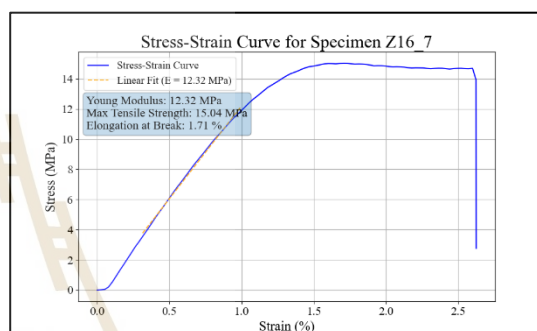
neat resin, z-orientation, 16s exposure time,
sample No.4



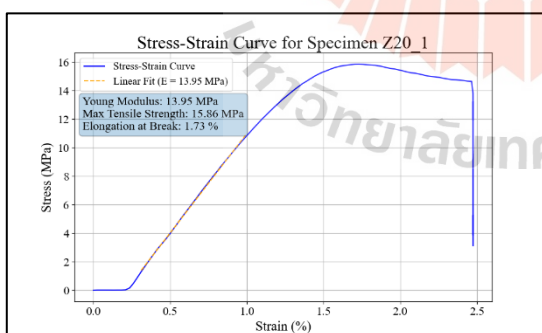
neat resin, z-orientation, 16s exposure time,
sample No.5



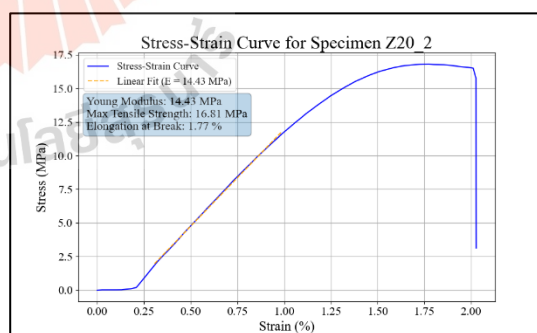
neat resin, z-orientation, 16s exposure time,
sample No.6



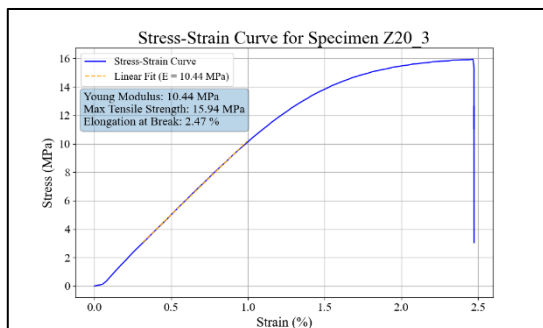
neat resin, z-orientation, 16s exposure time,
sample No.7



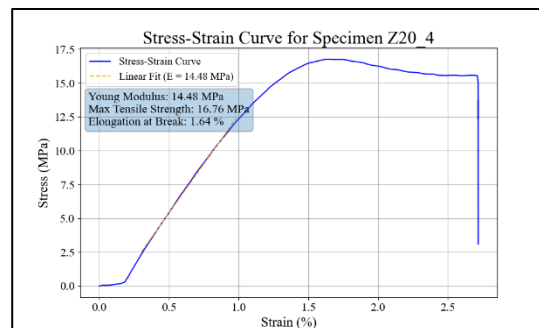
neat resin, z-orientation, 20s exposure time,
sample No.1



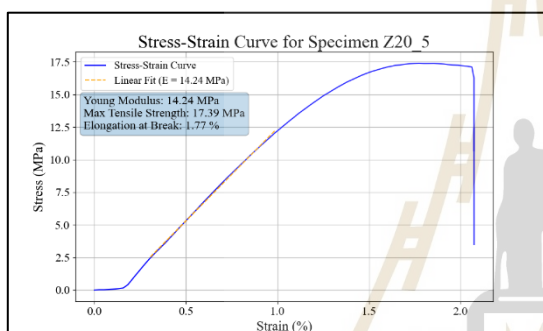
neat resin, z-orientation, 20s exposure time,
sample No.2



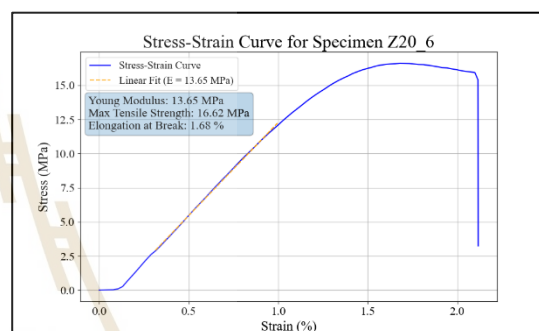
neat resin, z-orientation, 20s exposure time,
sample No.3



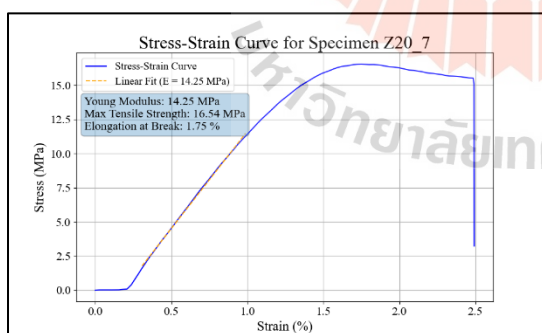
neat resin, z-orientation, 20s exposure time,
sample No.4



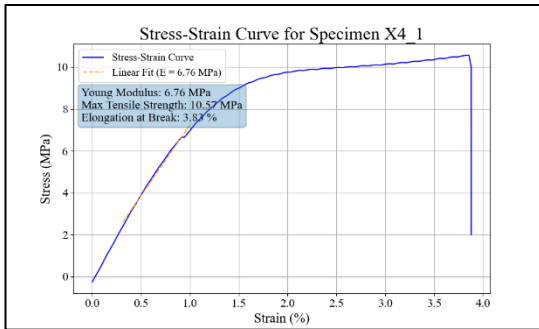
neat resin, z-orientation, 20s exposure time,
sample No.5



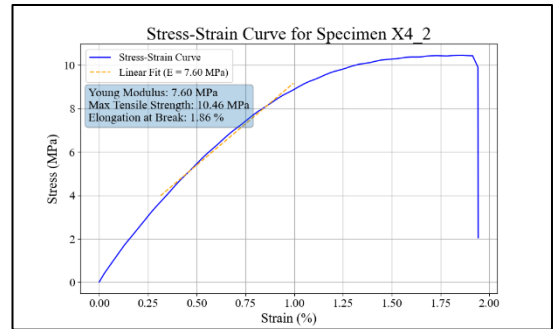
neat resin, z-orientation, 20s exposure time,
sample No.6



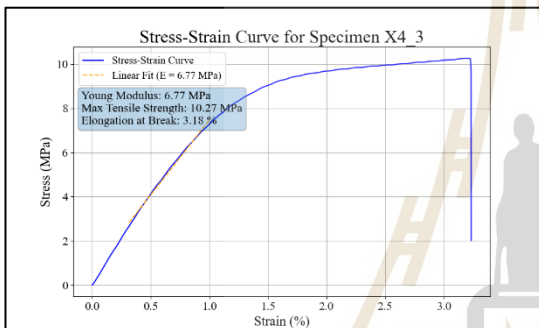
neat resin, z-orientation, 20s exposure time,
sample No.7



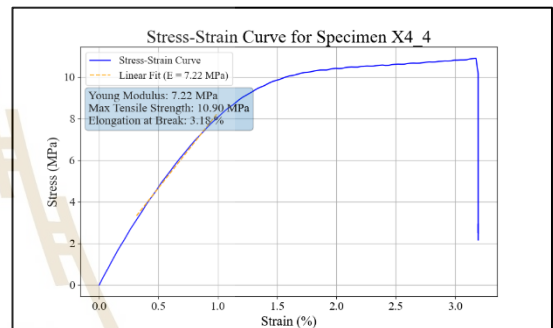
neat resin, x-orientation, 4s exposure time,
sample No.1



neat resin, x-orientation, 4s exposure time,
sample No.2

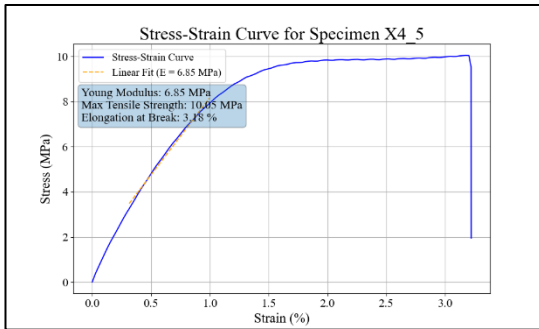


neat resin, x-orientation, 4s exposure time,
sample No.3

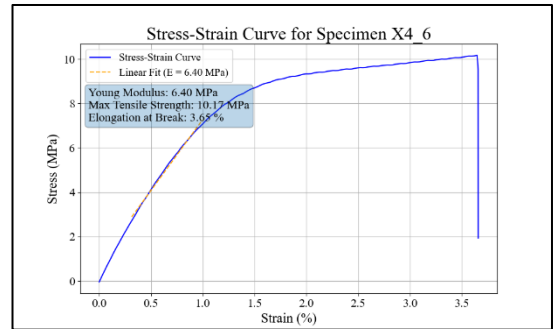


neat resin, x-orientation, 4s exposure time,
sample No.4

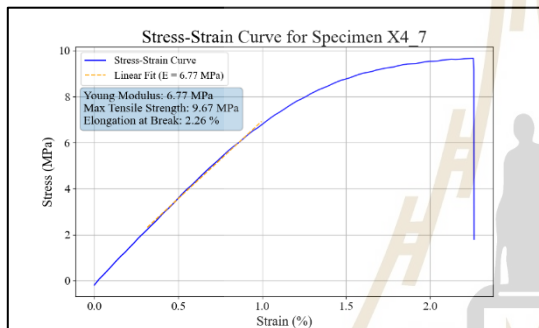




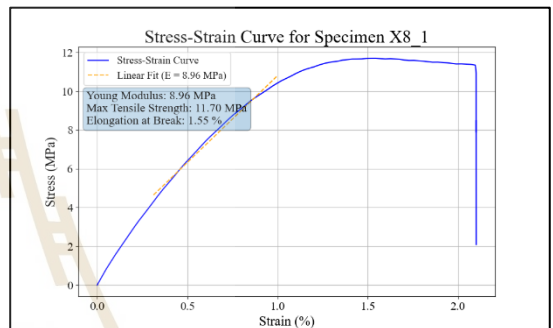
neat resin, x-orientation, 4s exposure time,
sample No.5



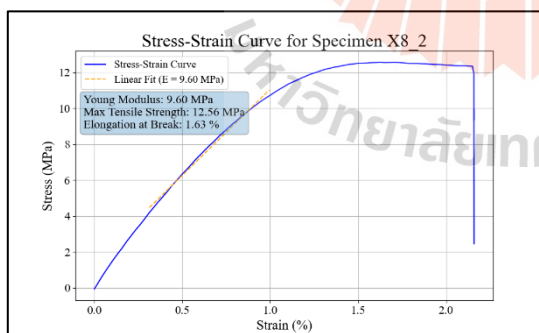
neat resin, x-orientation, 4s exposure time,
sample No.6



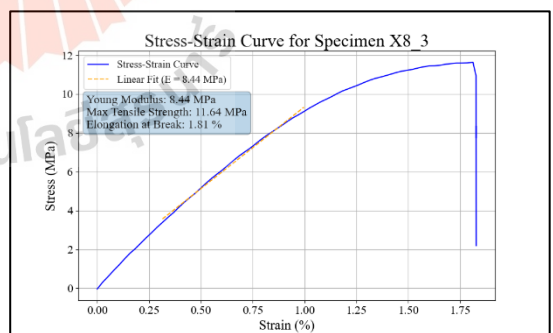
neat resin, x-orientation, 4s exposure time,
sample No.7



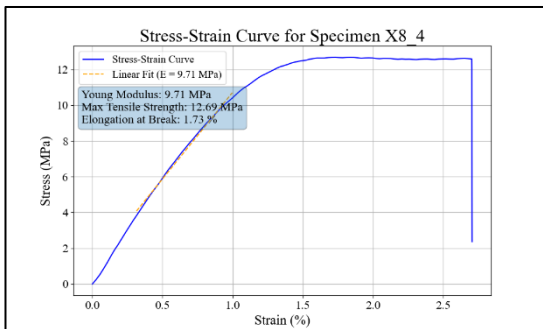
neat resin, x-orientation, 8s exposure time,
sample No.1



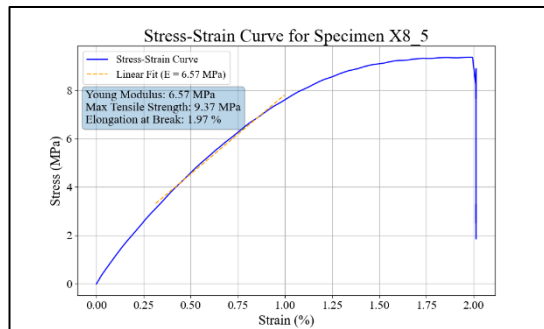
neat resin, x-orientation, 8s exposure time,
sample No.2



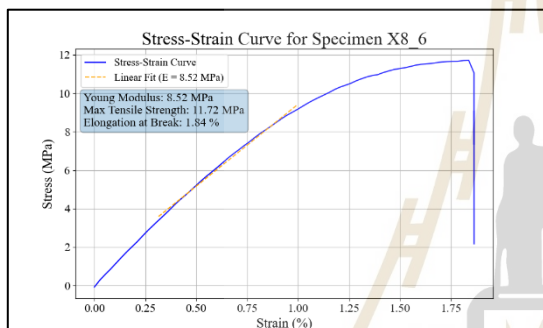
neat resin, x-orientation, 8s exposure time,
sample No.3



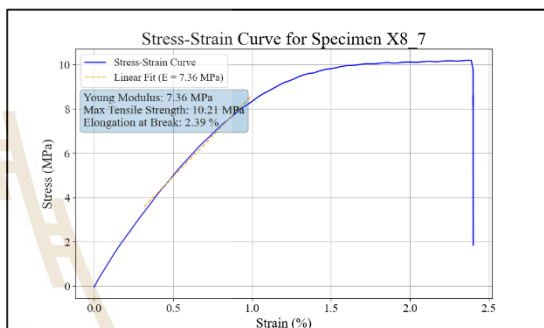
neat resin, x-orientation, 8s exposure time, sample No.4



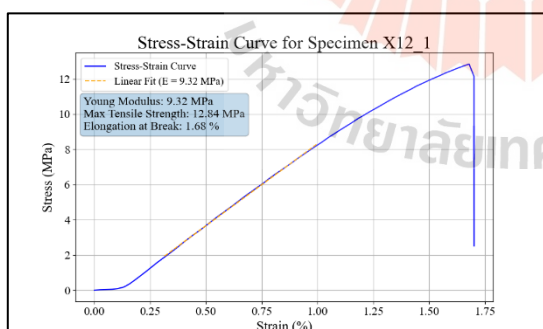
neat resin, x-orientation, 8s exposure time, sample No.5



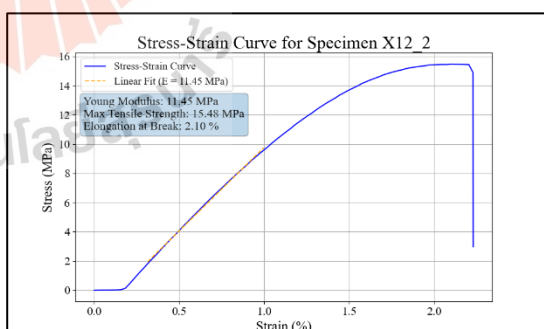
neat resin, x-orientation, 8s exposure time, sample No.6



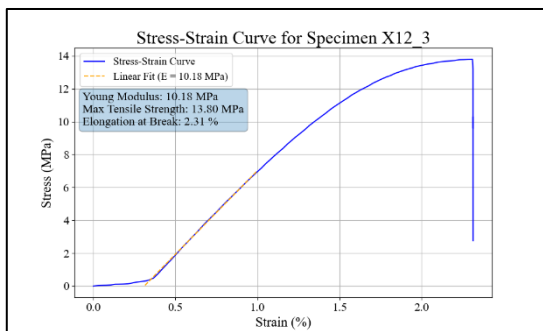
neat resin, x-orientation, 8s exposure time, sample No.7



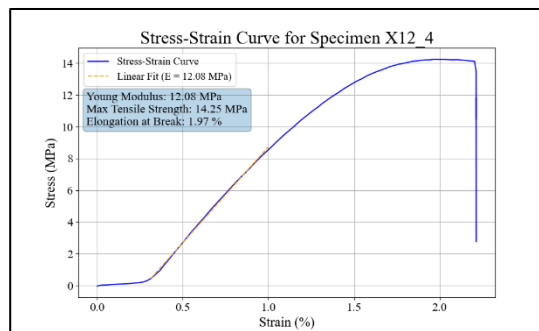
neat resin, x-orientation, 12s exposure time, sample No.1



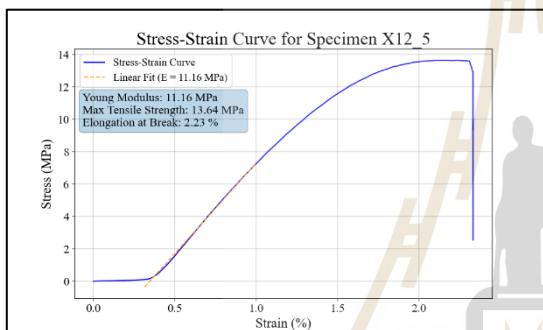
neat resin, x-orientation, 12s exposure time, sample No.2



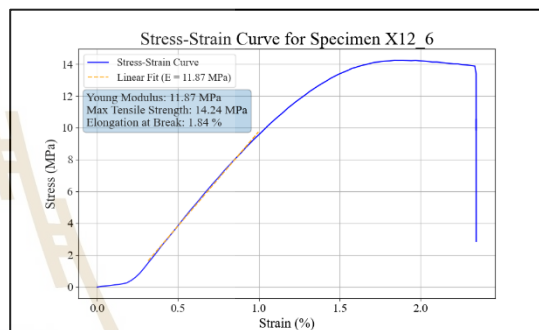
neat resin, x-orientation, 12s exposure time, sample No.3



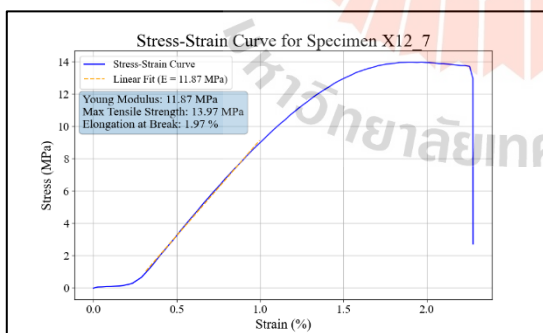
neat resin, x-orientation, 12s exposure time, sample No.4



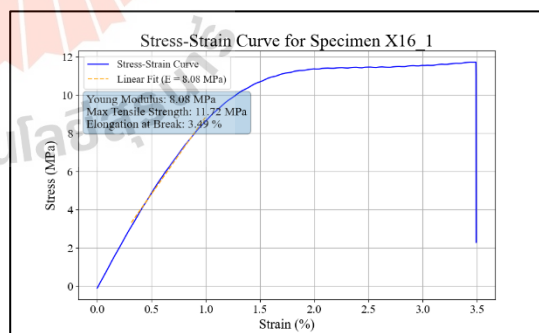
neat resin, x-orientation, 12s exposure time, sample No.5



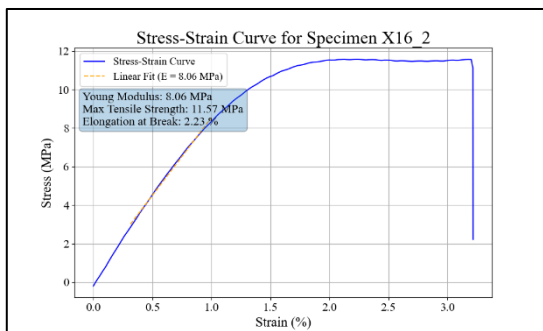
neat resin, x-orientation, 12s exposure time, sample No.6



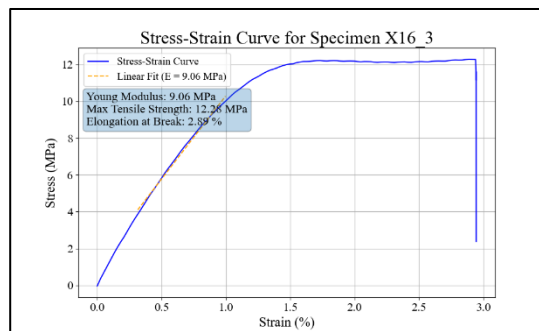
neat resin, x-orientation, 12s exposure time, sample No.7



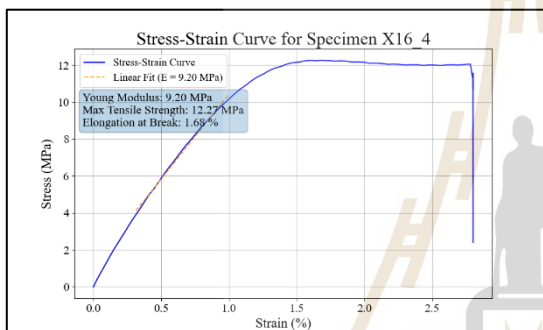
neat resin, x-orientation, 16s exposure time, sample No.1



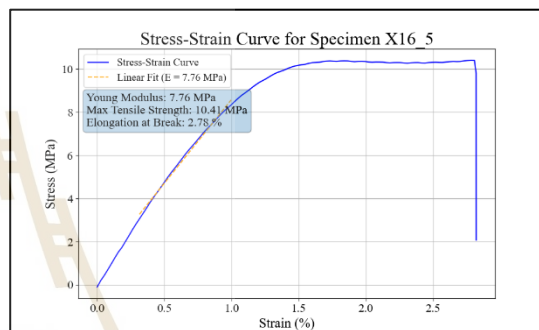
neat resin, x-orientation, 16s exposure time,
sample No.2



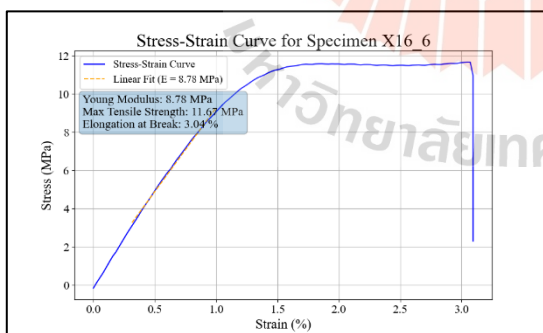
neat resin, x-orientation, 16s exposure time,
sample No.3



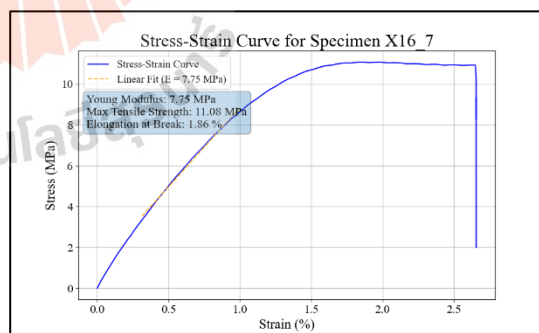
neat resin, x-orientation, 16s exposure time,
sample No.4



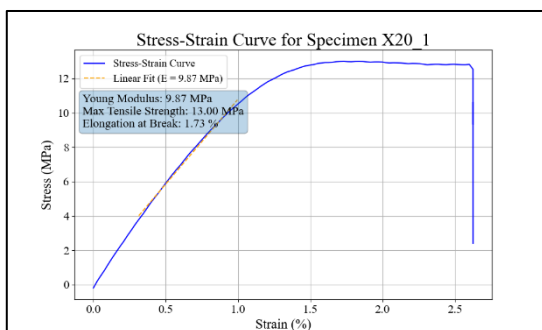
neat resin, x-orientation, 16s exposure time,
sample No.5



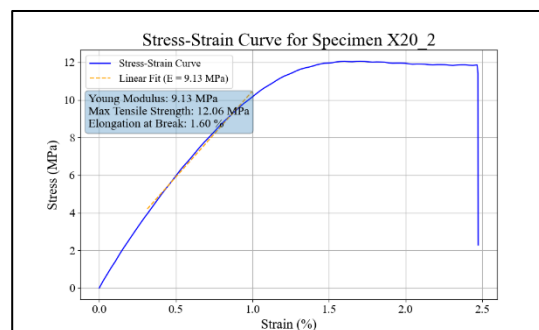
neat resin, x-orientation, 16s exposure time,
sample No.6



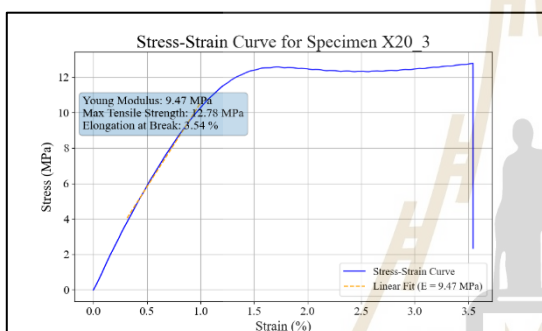
neat resin, x-orientation, 16s exposure time,
sample No.7



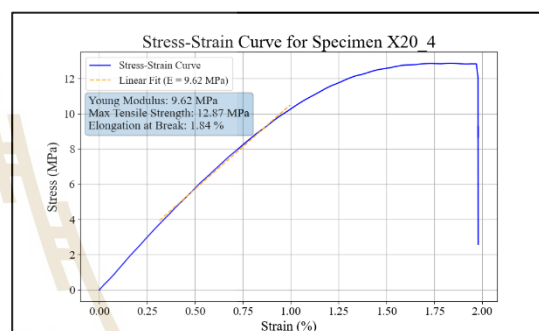
neat resin, x-orientation, 20s exposure time,
sample No.1



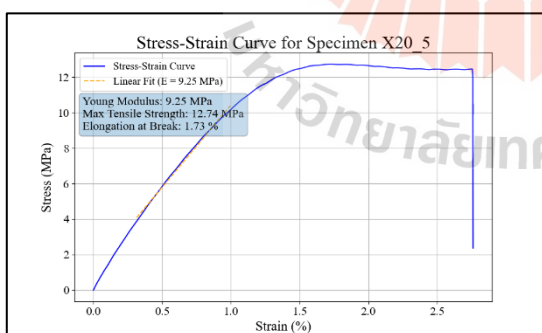
neat resin, x-orientation, 20s exposure time,
sample No.2



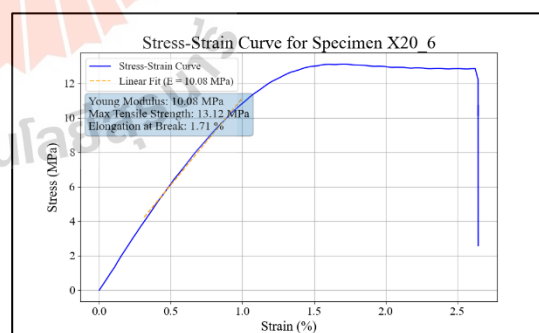
neat resin, x-orientation, 20s exposure time,
sample No.3



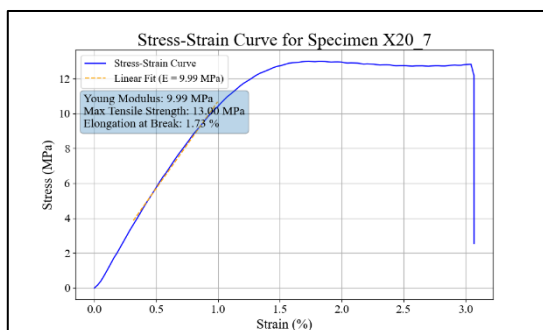
neat resin, x-orientation, 20s exposure time,
sample No.4



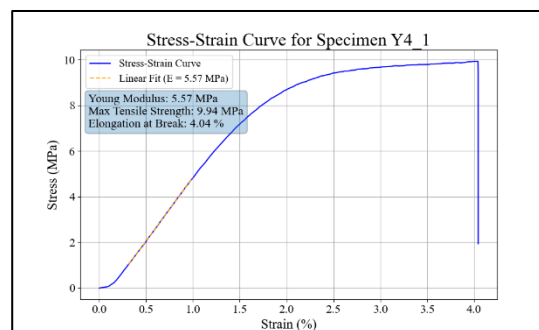
neat resin, x-orientation, 20s exposure time,
sample No.5



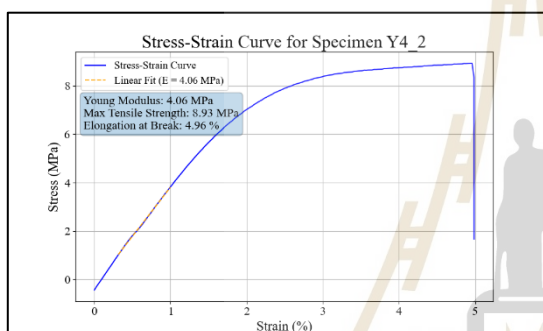
neat resin, x-orientation, 20s exposure time,
sample No.6



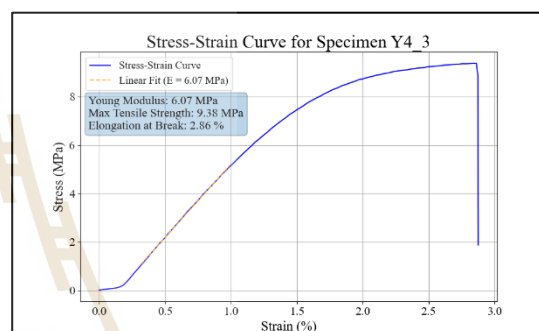
neat resin, x-orientation, 20s exposure time,
sample No.7



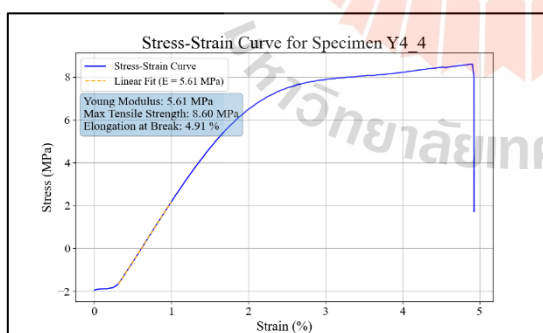
neat resin, y-orientation, 4s exposure time,
sample No.1



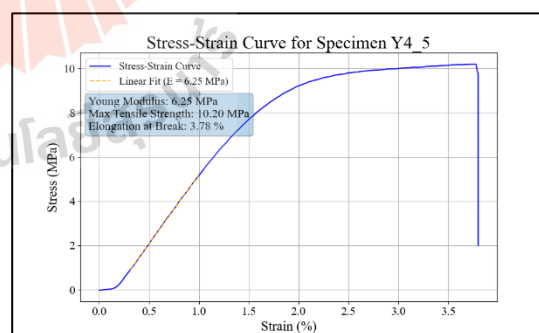
neat resin, y-orientation, 4s exposure time,
sample No.2



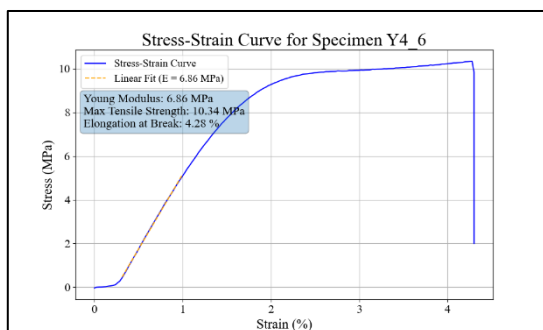
neat resin, y-orientation, 4s exposure time,
sample No.3



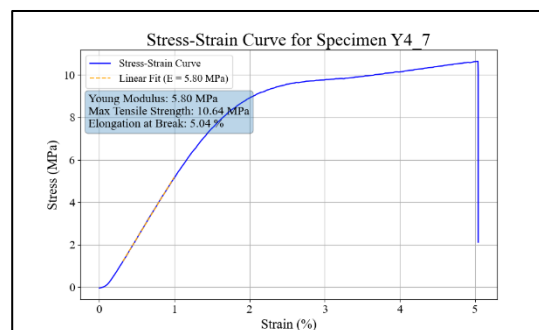
neat resin, y-orientation, 4s exposure time,
sample No.4



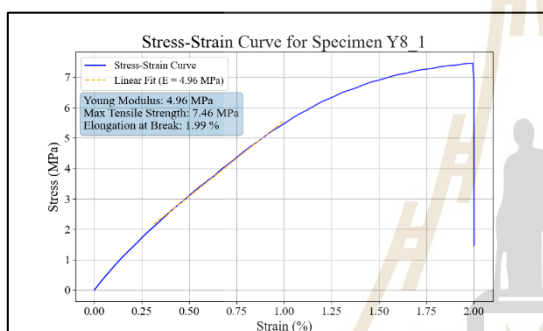
neat resin, y-orientation, 4s exposure time,
sample No.5



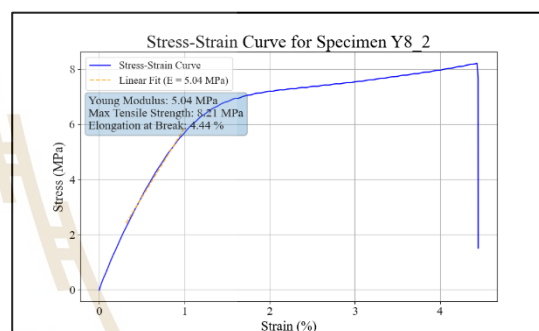
neat resin, y-orientation, 4s exposure time,
sample No.6



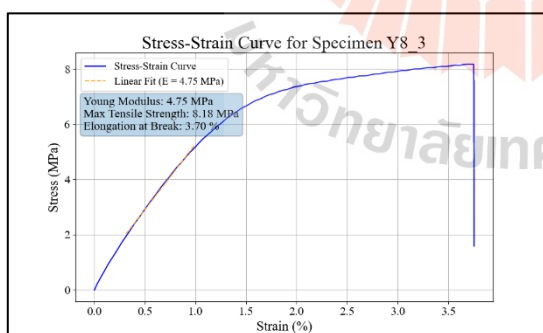
neat resin, y-orientation, 4s exposure time,
sample No.7



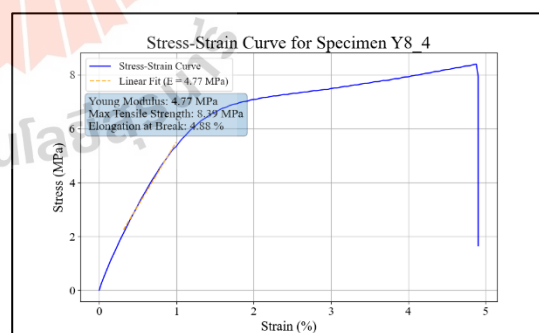
neat resin, y-orientation, 8s exposure time,
sample No.1



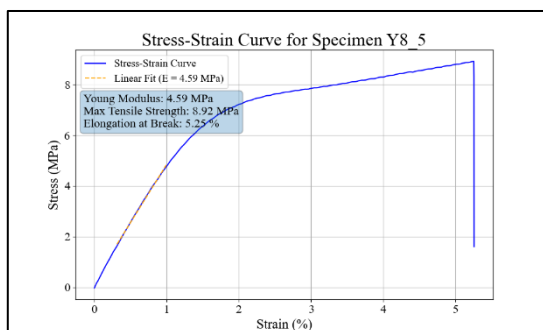
neat resin, y-orientation, 8s exposure time,
sample No.2



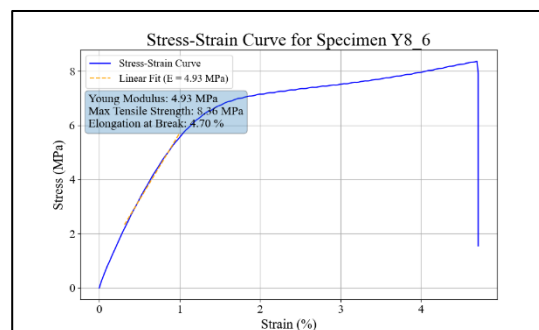
neat resin, y-orientation, 8s exposure time,
sample No.3



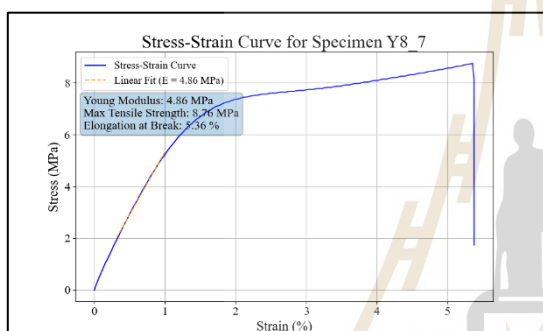
neat resin, y-orientation, 8s exposure time,
sample No.4



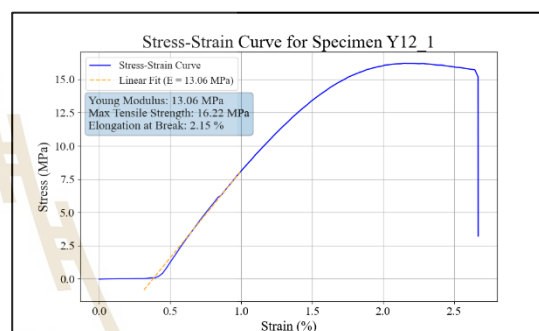
neat resin, y-orientation, 8s exposure time,
sample No.5



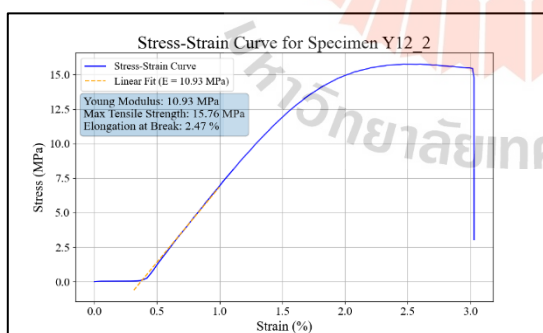
neat resin, y-orientation, 8s exposure time,
sample No.6



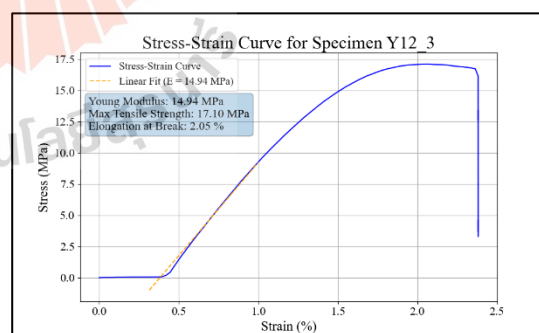
neat resin, y-orientation, 8s exposure time,
sample No.7



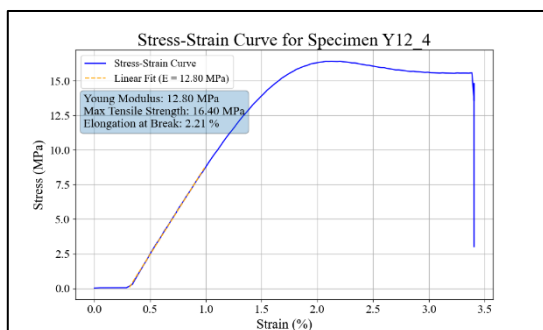
neat resin, y-orientation, 12s exposure time,
sample No.1



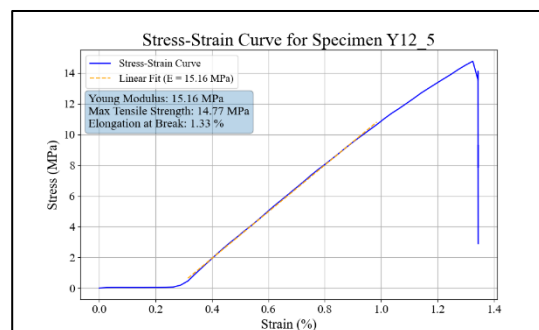
neat resin, y-orientation, 12s exposure time,
sample No.2



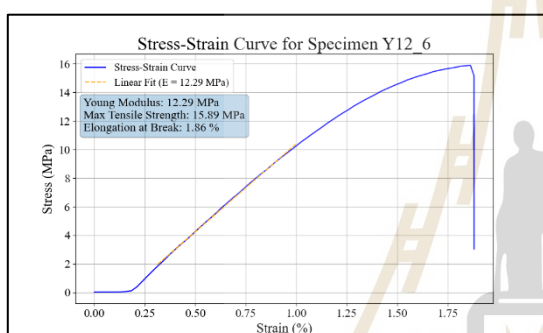
neat resin, y-orientation, 12s exposure time,
sample No.3



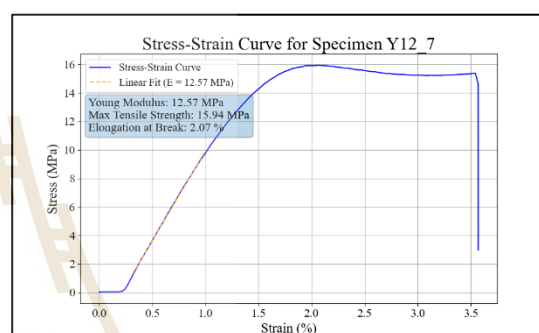
neat resin, y-orientation, 12s exposure time,
sample No.4



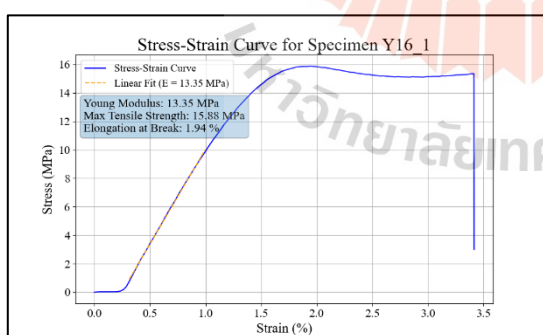
neat resin, y-orientation, 12s exposure time,
sample No.5



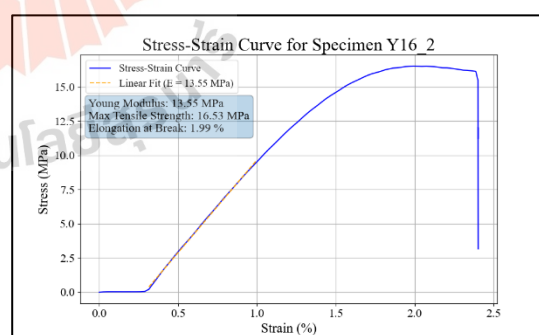
neat resin, y-orientation, 12s exposure time,
sample No.6



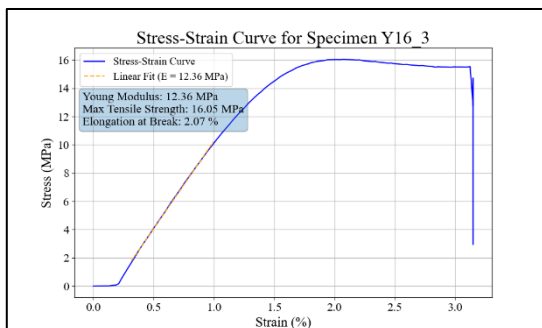
neat resin, y-orientation, 12s exposure time,
sample No.7



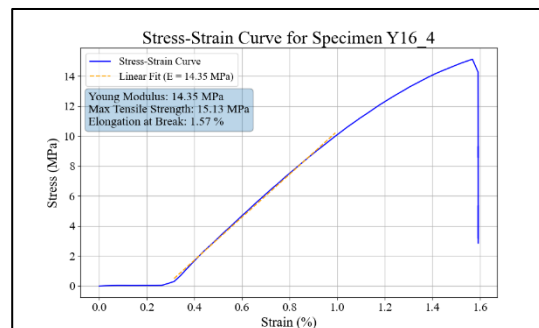
neat resin, y-orientation, 16s exposure time,
sample No.1



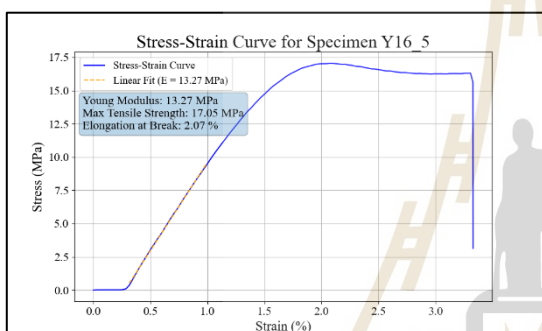
neat resin, y-orientation, 16s exposure time,
sample No.2



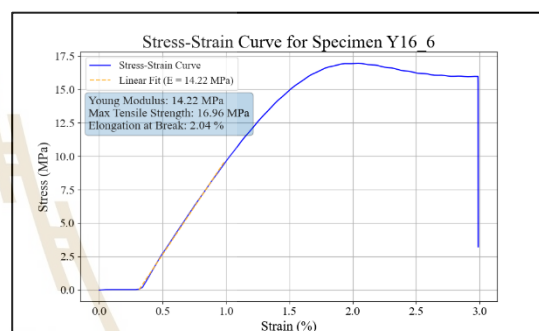
neat resin, y-orientation, 16s exposure time,
sample No.3



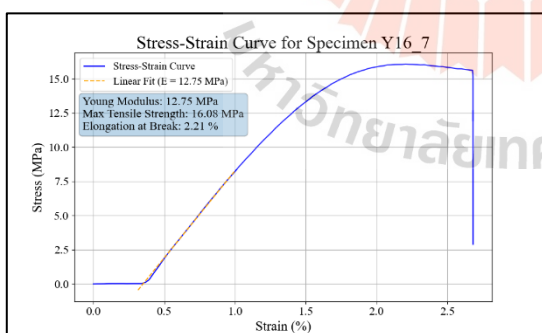
neat resin, y-orientation, 16s exposure time,
sample No.4



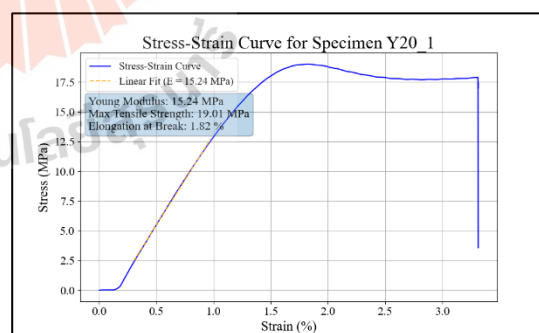
neat resin, y-orientation, 16s exposure time,
sample No.5



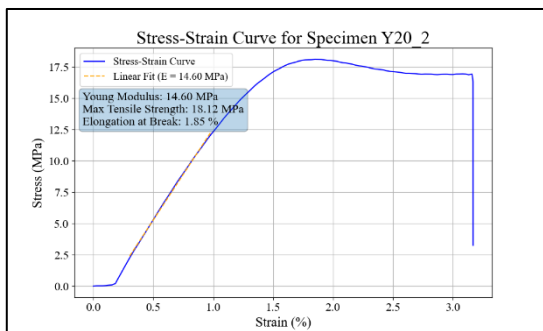
neat resin, y-orientation, 16s exposure time,
sample No.6



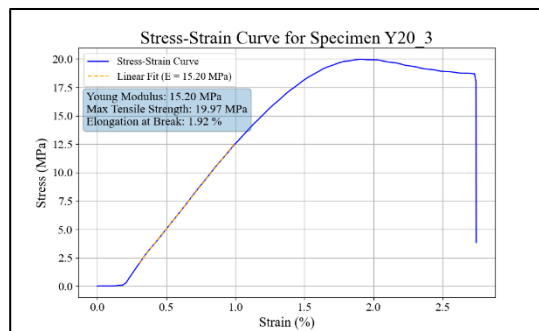
neat resin, y-orientation, 16s exposure time,
sample No.7



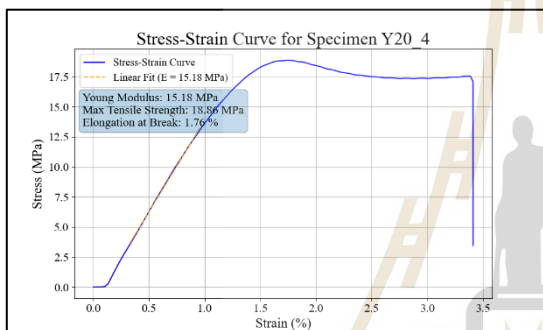
neat resin, y-orientation, 20s exposure time,
sample No.1



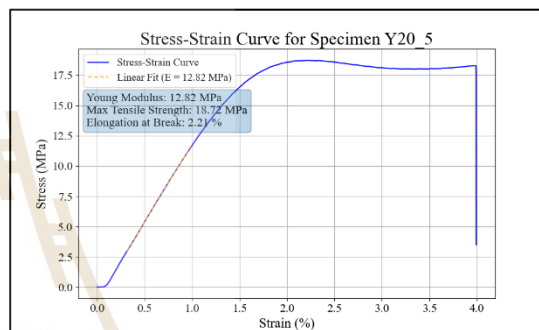
neat resin, y-orientation, 20s exposure time, sample No.2



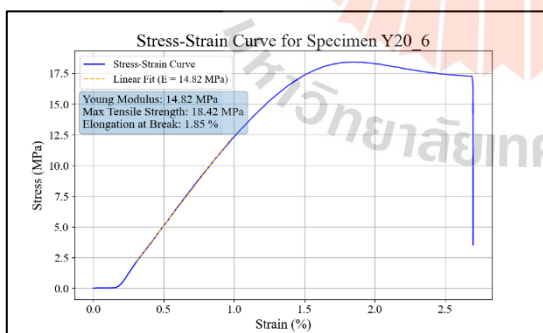
neat resin, y-orientation, 20s exposure time, sample No.3



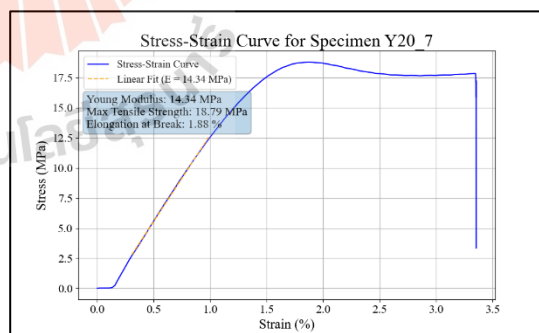
neat resin, y-orientation, 20s exposure time, sample No.4



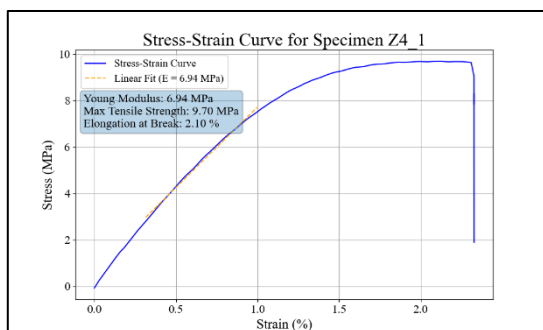
neat resin, y-orientation, 20s exposure time, sample No.5



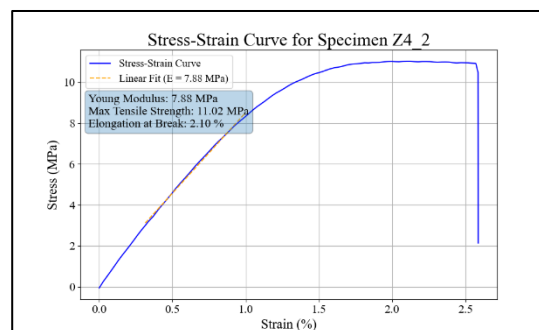
neat resin, y-orientation, 20s exposure time, sample No.6



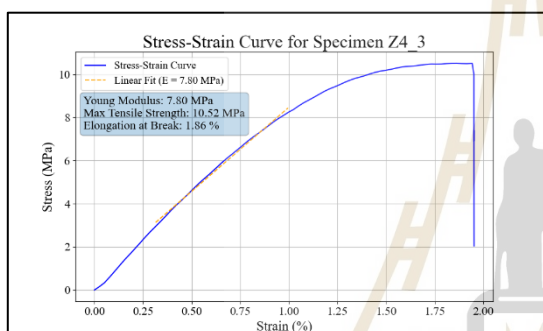
neat resin, y-orientation, 20s exposure time, sample No.7



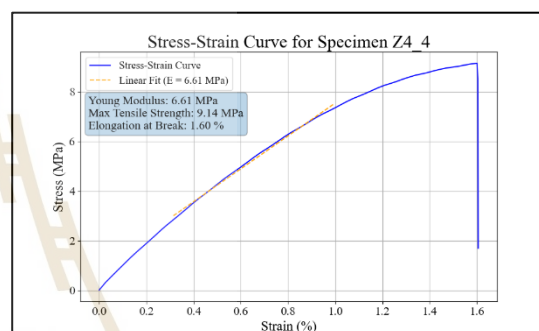
neat resin, z-orientation, 4s exposure time,
sample No.1



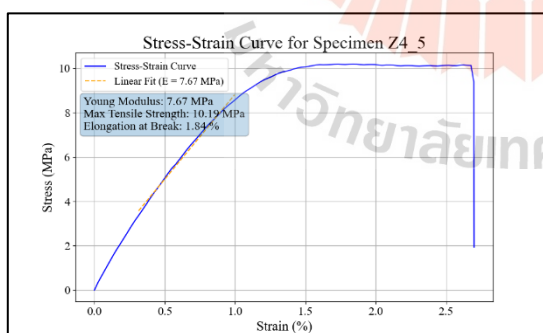
neat resin, z-orientation, 4s exposure time,
sample No.2



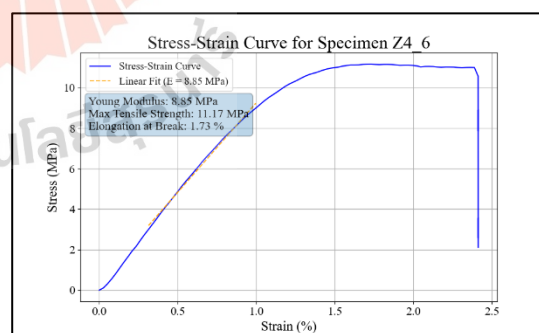
neat resin, z-orientation, 4s exposure time,
sample No.3



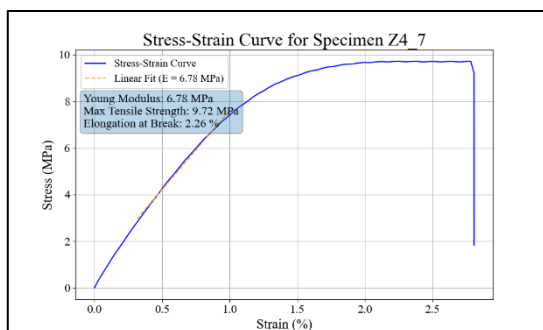
neat resin, z-orientation, 4s exposure time,
sample No.4



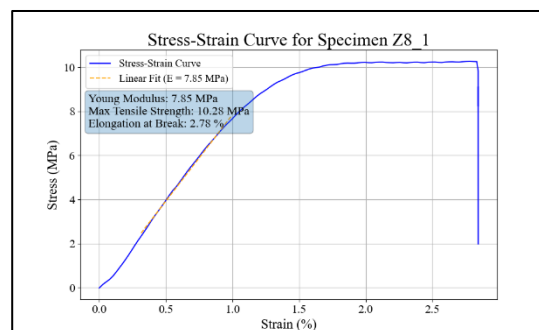
neat resin, z-orientation, 4s exposure time,
sample No.5



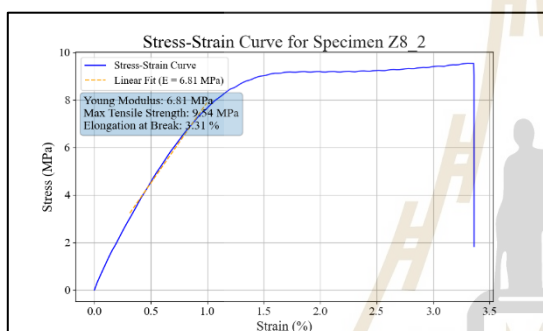
neat resin, z-orientation, 4s exposure time,
sample No.6



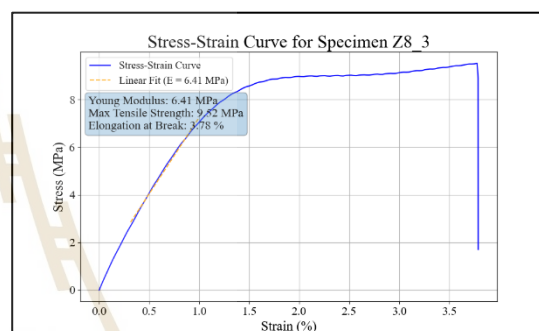
neat resin, z-orientation, 4s exposure time,
sample No.7



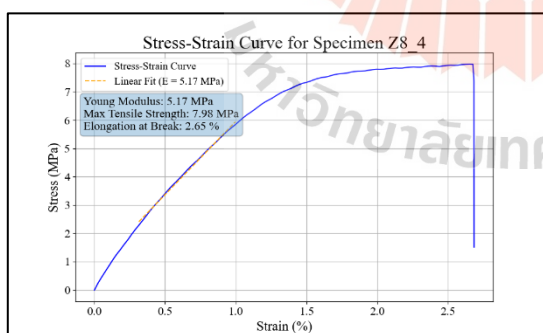
neat resin, z-orientation, 8s exposure time,
sample No.1



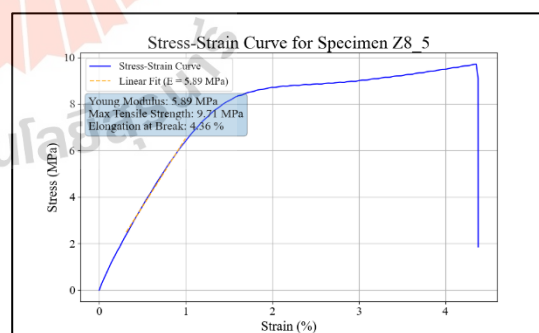
neat resin, z-orientation, 8s exposure time,
sample No.2



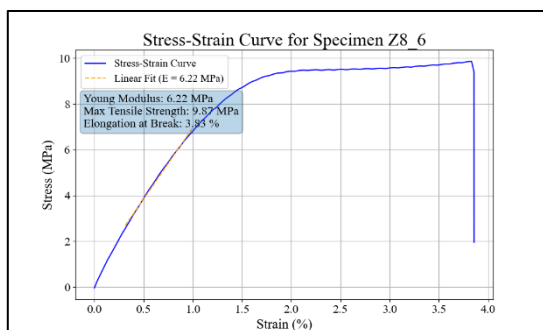
neat resin, z-orientation, 8s exposure time,
sample No.3



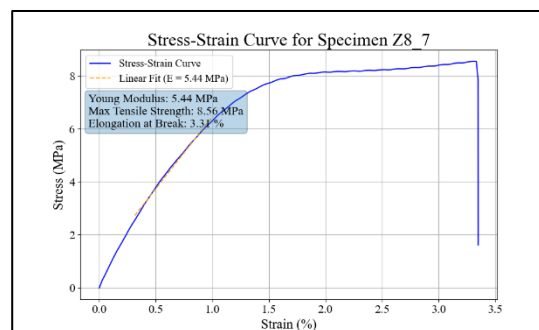
neat resin, z-orientation, 8s exposure time,
sample No.4



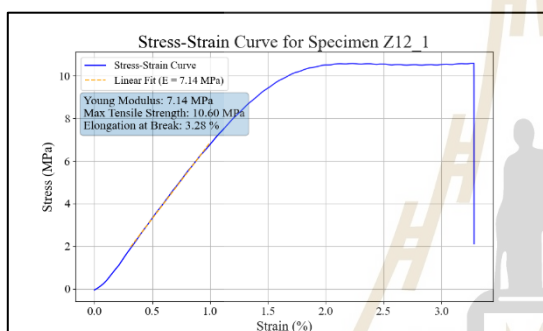
neat resin, z-orientation, 8s exposure time,
sample No.5



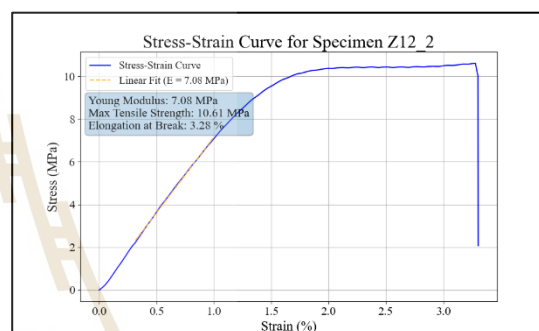
neat resin, z-orientation, 8s exposure time,
sample No.6



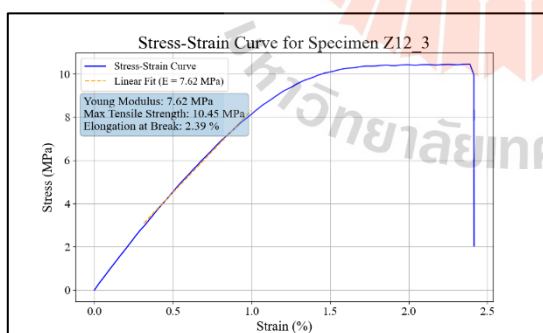
neat resin, z-orientation, 8s exposure time,
sample No.7



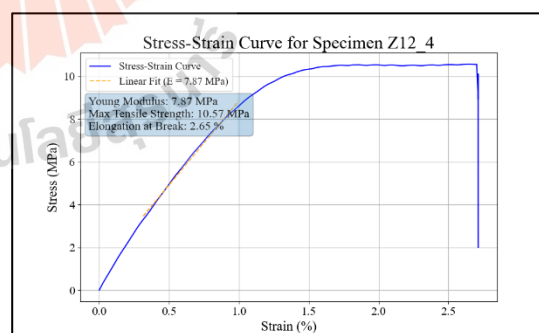
neat resin, z-orientation, 12s exposure time,
sample No.1



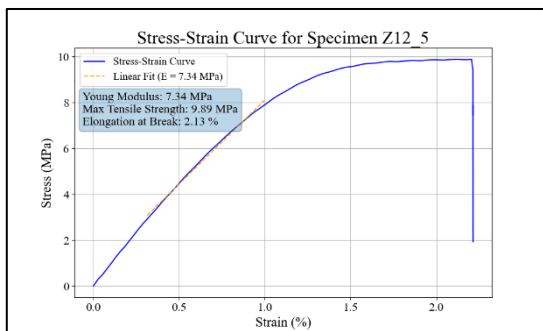
neat resin, z-orientation, 12s exposure time,
sample No.2



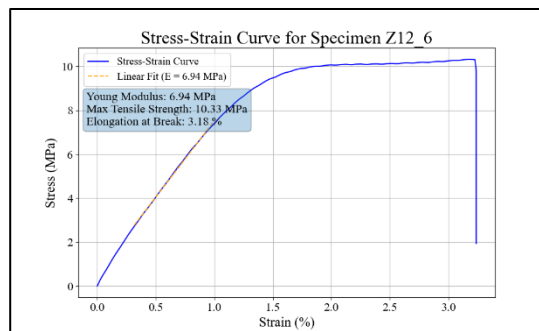
neat resin, z-orientation, 12s exposure time,
sample No.3



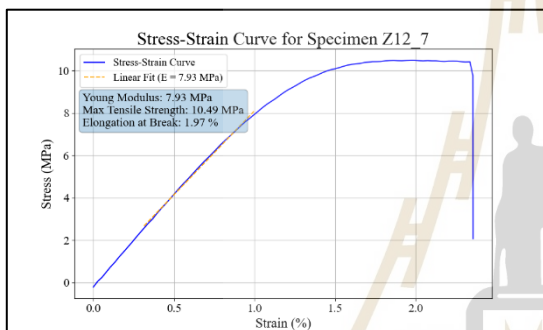
neat resin, z-orientation, 12s exposure time,
sample No.4



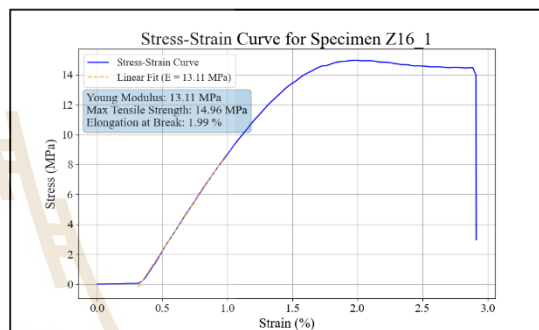
neat resin, z-orientation, 12s exposure time,
sample No.5



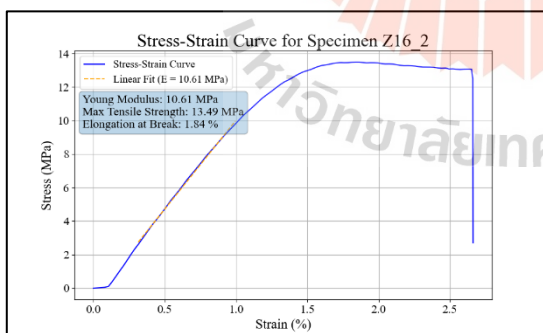
neat resin, z-orientation, 12s exposure time,
sample No.6



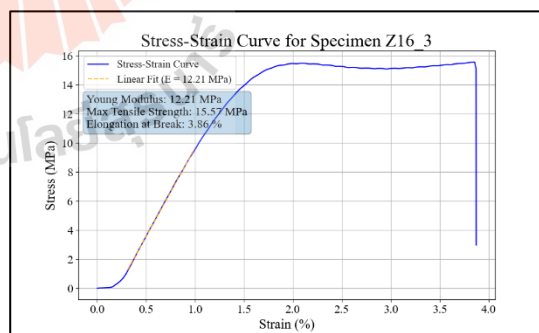
neat resin, z-orientation, 12s exposure time,
sample No.7



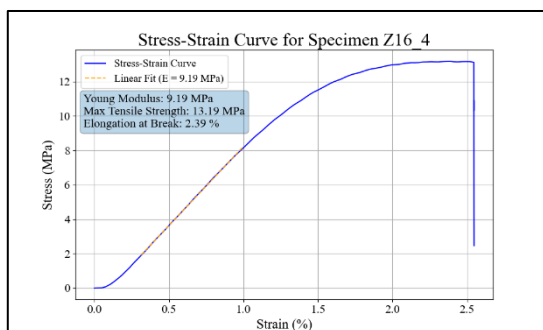
neat resin, z-orientation, 16s exposure time,
sample No.1



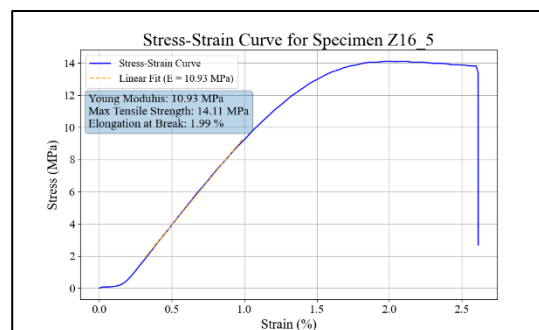
neat resin, z-orientation, 16s exposure time,
sample No.2



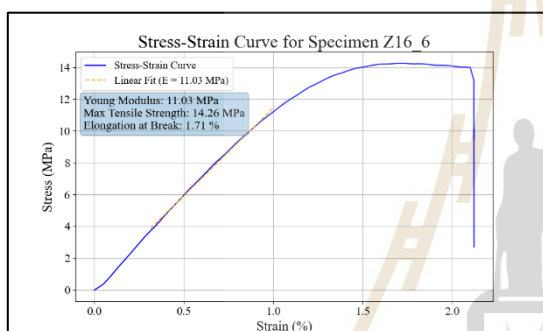
neat resin, z-orientation, 16s exposure time,
sample No.3



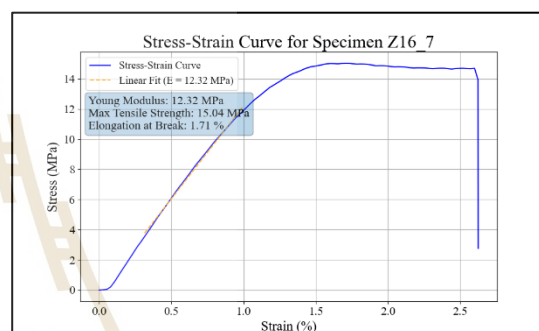
neat resin, z-orientation, 16s exposure time,
sample No.4



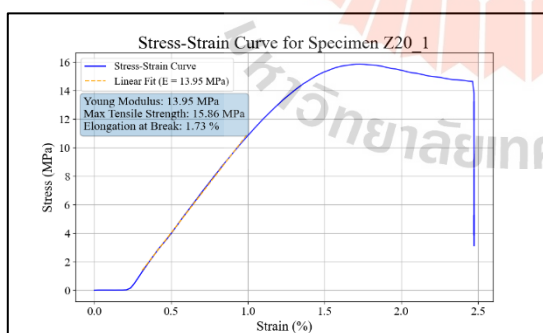
neat resin, z-orientation, 16s exposure time,
sample No.5



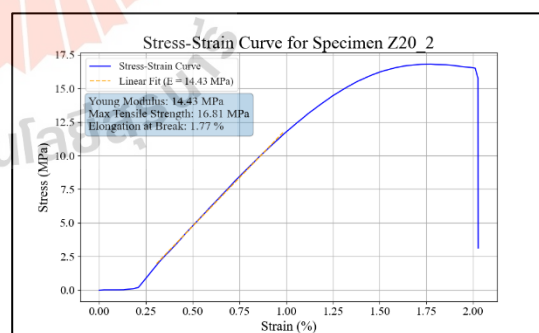
neat resin, z-orientation, 16s exposure time,
sample No.6



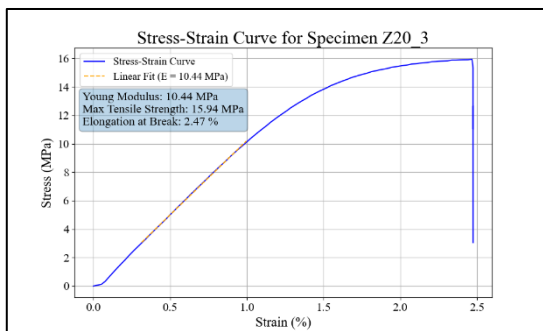
neat resin, z-orientation, 16s exposure time,
sample No.7



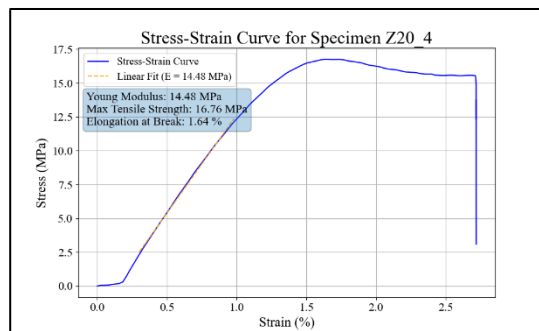
neat resin, z-orientation, 20s exposure time,
sample No.1



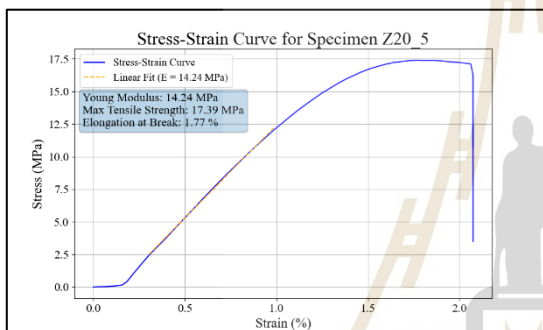
neat resin, z-orientation, 20s exposure time,
sample No.2



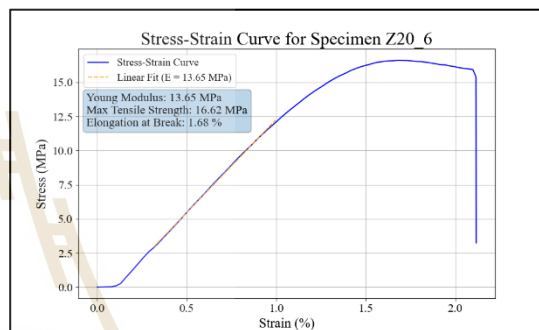
neat resin, z-orientation, 20s exposure time, sample No.3



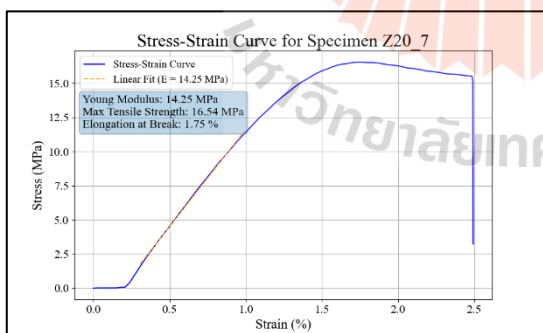
neat resin, z-orientation, 20s exposure time, sample No.4



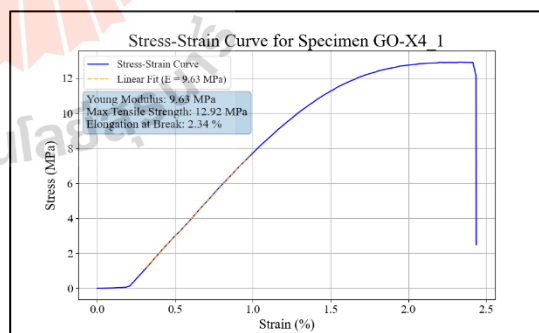
neat resin, z-orientation, 20s exposure time, sample No.5



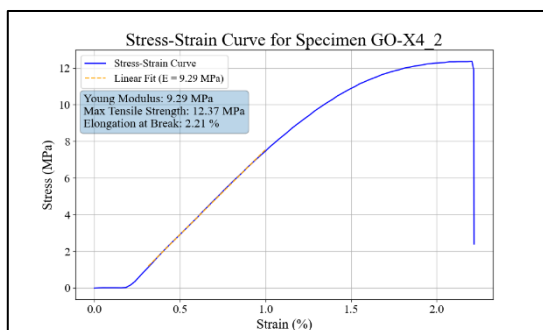
neat resin, z-orientation, 20s exposure time, sample No.6



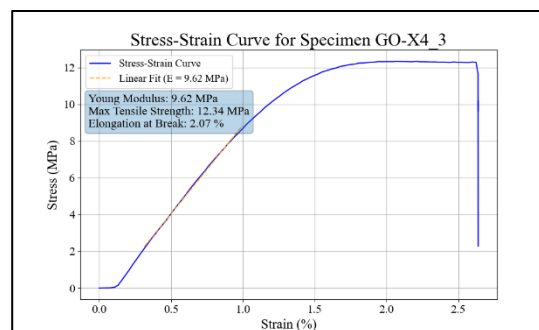
neat resin, z-orientation, 20s exposure time, sample No.7



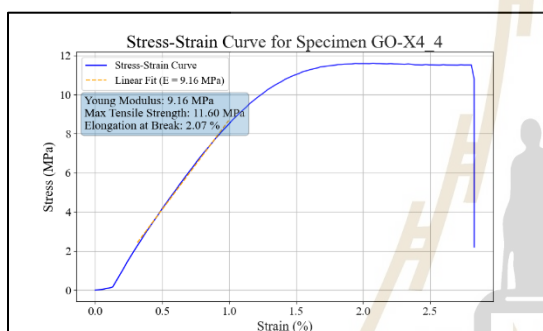
rGO resin, x-orientation, 4s exposure time, sample No.1



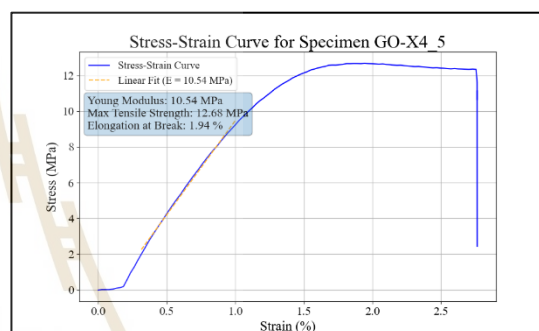
rGO resin, x-orientation, 4s exposure time,
sample No.2



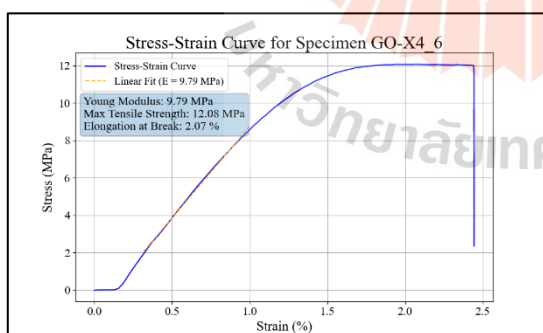
rGO resin, x-orientation, 4s exposure time,
sample No.3



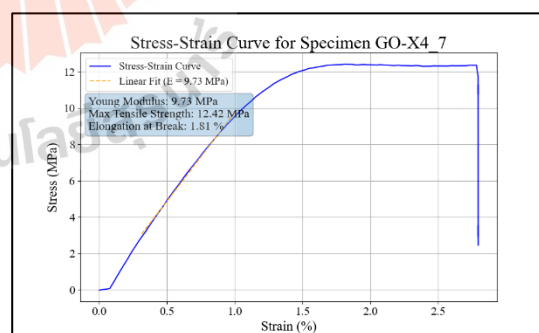
rGO resin, x-orientation, 4s exposure time,
sample No.4



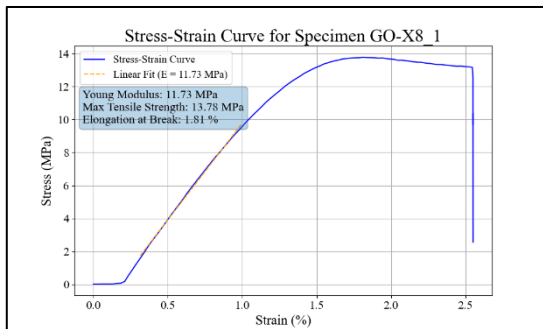
rGO resin, x-orientation, 4s exposure time,
sample No.5



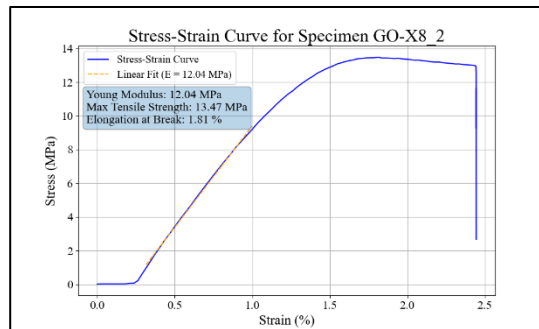
rGO resin, x-orientation, 4s exposure time,
sample No.6



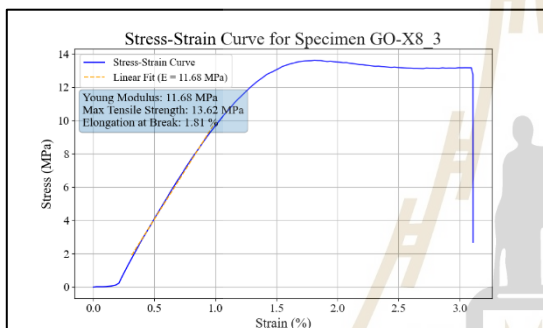
rGO resin, x-orientation, 4s exposure time,
sample No.7



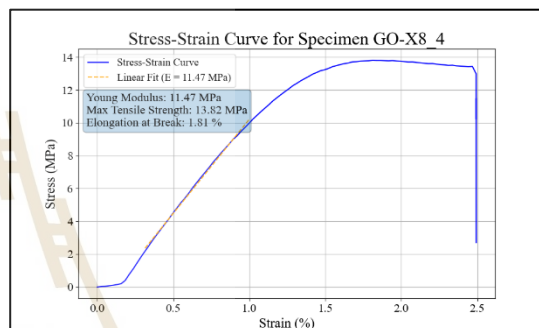
rGO resin, x-orientation, 8s exposure time, sample No.1



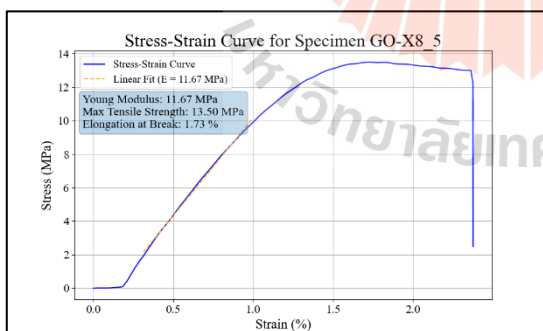
rGO resin, x-orientation, 8s exposure time, sample No.2



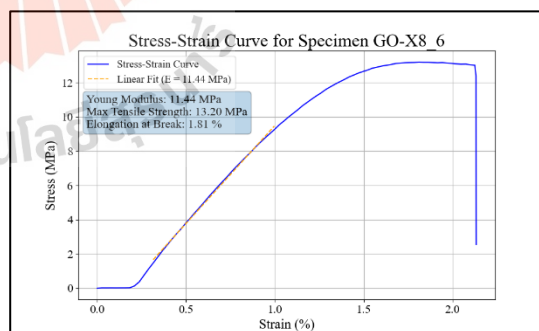
rGO resin, x-orientation, 8s exposure time, sample No.3



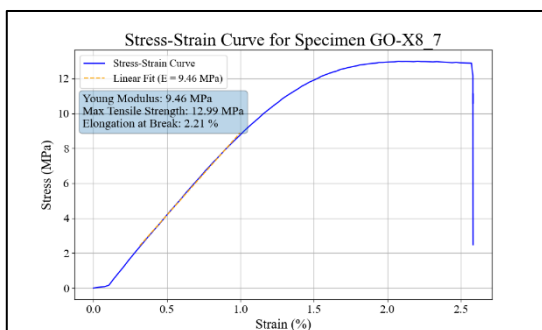
rGO resin, x-orientation, 8s exposure time, sample No.4



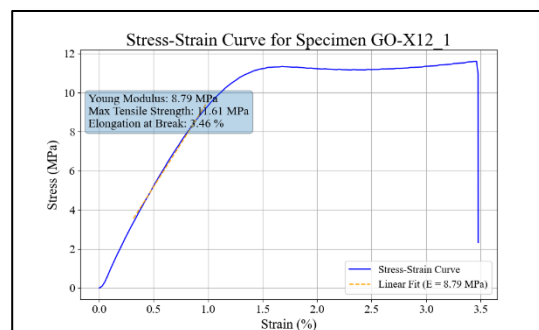
rGO resin, x-orientation, 8s exposure time, sample No.5



rGO resin, x-orientation, 8s exposure time, sample No.6



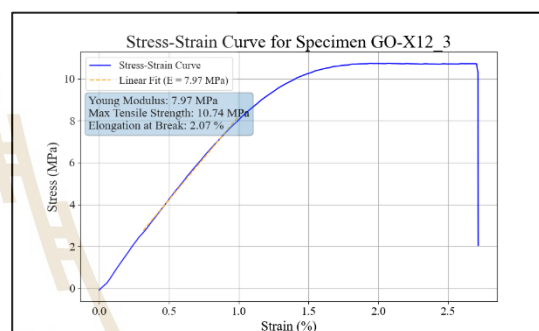
rGO resin, x-orientation, 8s exposure time,
sample No.7



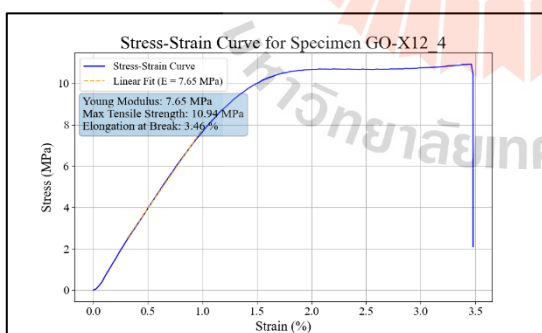
rGO resin, x-orientation, 12s exposure time,
sample No.1



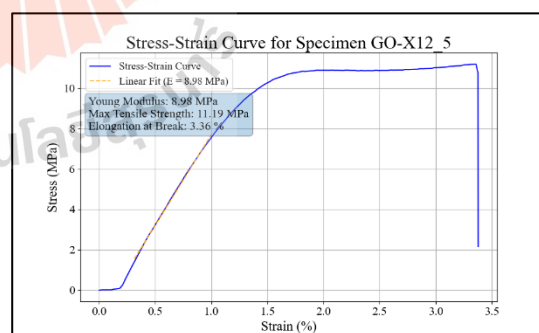
rGO resin, x-orientation, 12s exposure time,
sample No.2



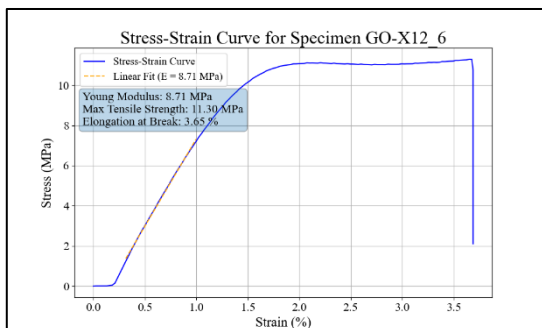
rGO resin, x-orientation, 12s exposure time,
sample No.3



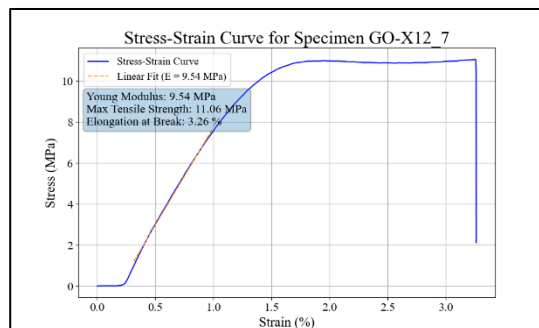
rGO resin, x-orientation, 12s exposure time,
sample No.4



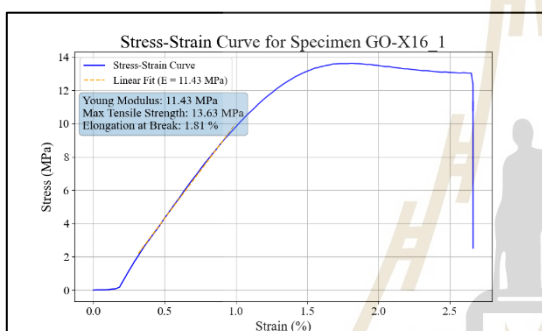
rGO resin, x-orientation, 12s exposure time,
sample No.5



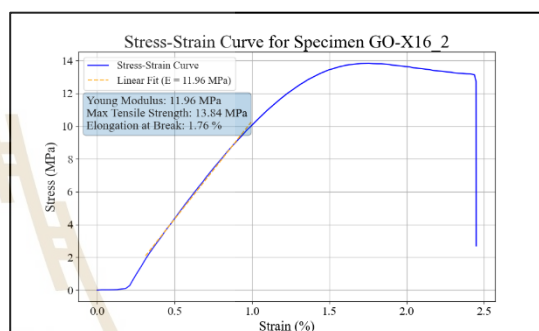
rGO resin, x-orientation, 12s exposure time,
sample No.6



rGO resin, x-orientation, 12s exposure time,
sample No.7



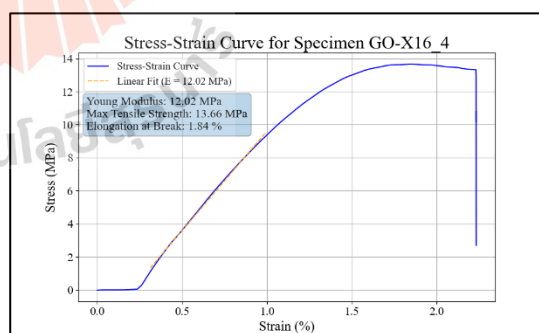
rGO resin, x-orientation, 16s exposure time,
sample No.1



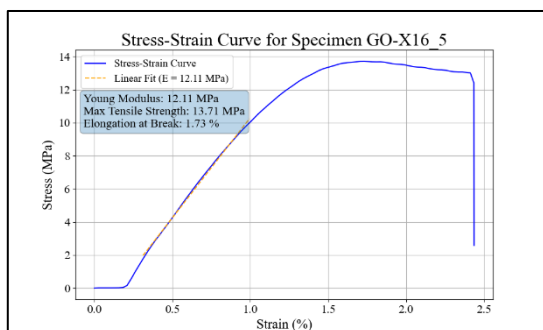
rGO resin, x-orientation, 16s exposure time,
sample No.2



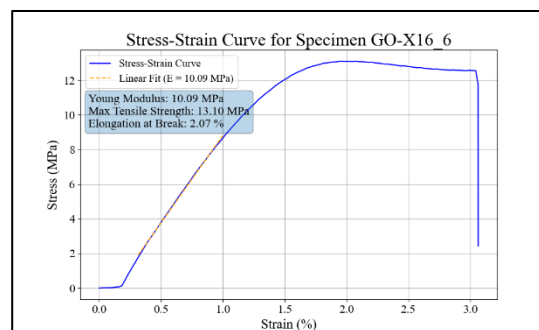
rGO resin, x-orientation, 16s exposure time,
sample No.3



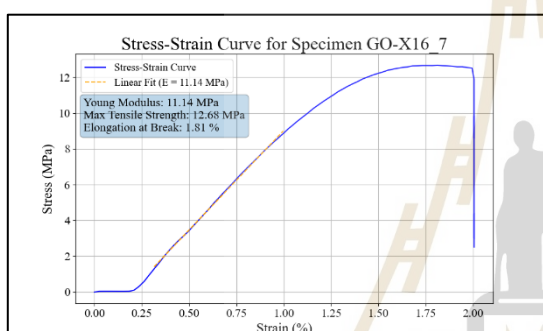
rGO resin, x-orientation, 16s exposure time,
sample No.4



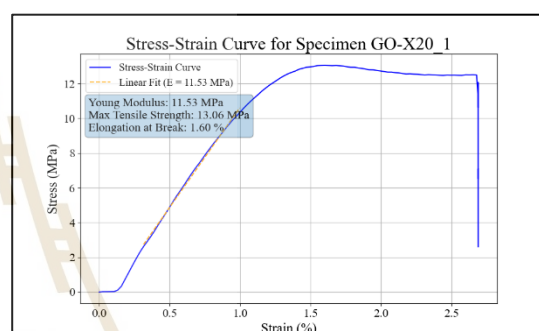
rGO resin, x-orientation, 16s exposure time,
sample No.5



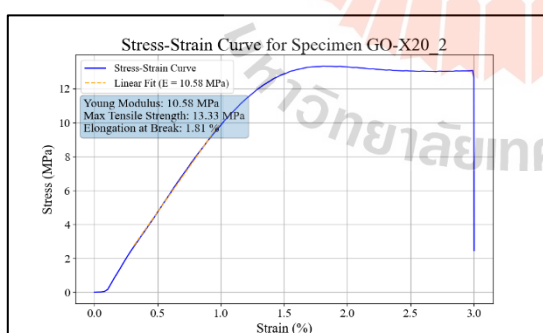
rGO resin, x-orientation, 16s exposure time,
sample No.6



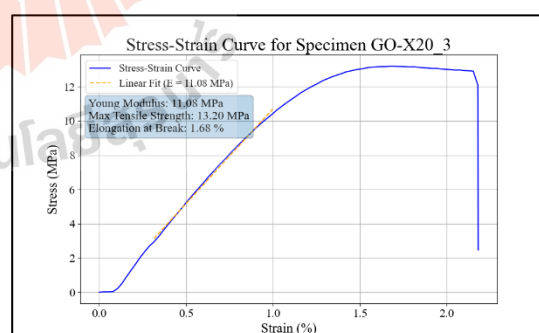
rGO resin, x-orientation, 16s exposure time,
sample No.7



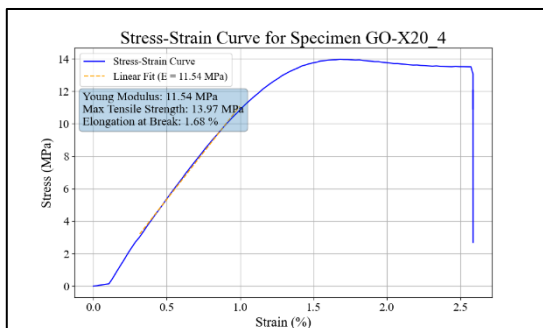
rGO resin, x-orientation, 20s exposure time,
sample No.1



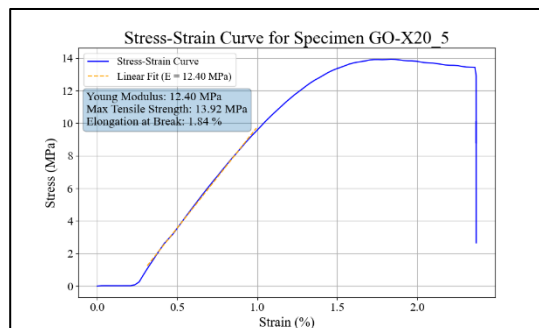
rGO resin, x-orientation, 20s exposure time,
sample No.2



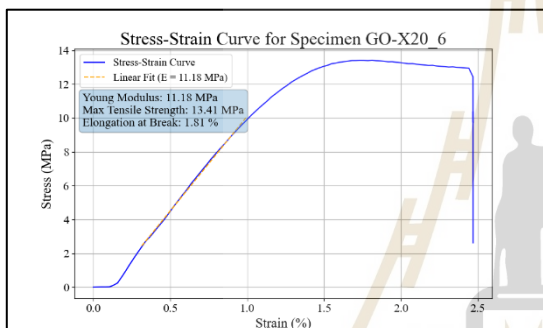
rGO resin, x-orientation, 20s exposure time,
sample No.3



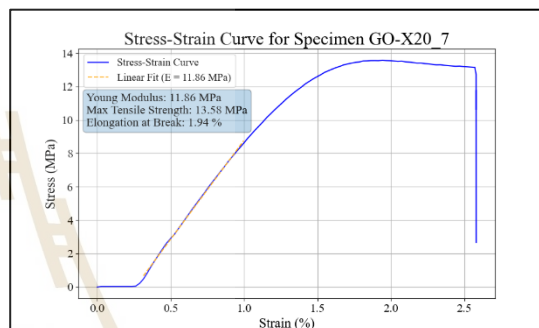
rGO resin, x-orientation, 20s exposure time, sample No.4



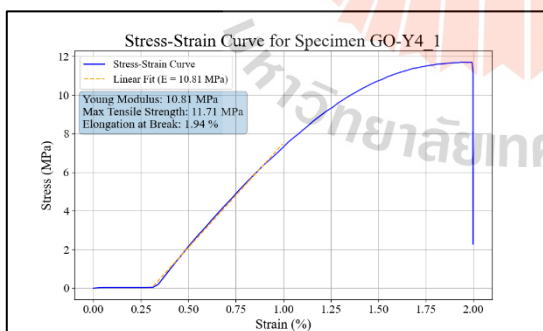
rGO resin, x-orientation, 20s exposure time, sample No.5



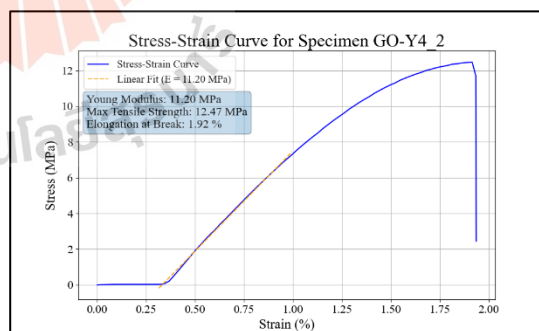
rGO resin, x-orientation, 20s exposure time, sample No.6



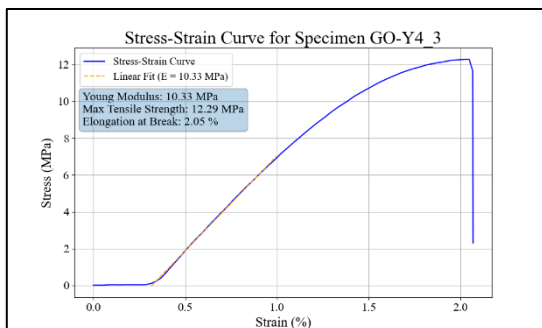
rGO resin, x-orientation, 20s exposure time, sample No.7



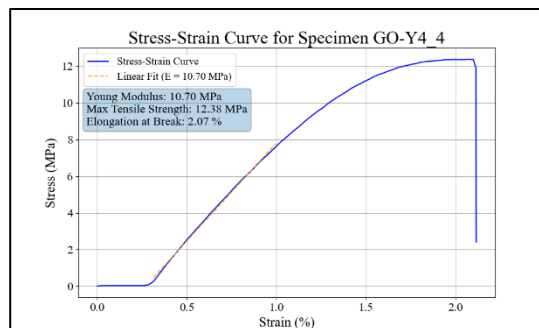
rGO resin, y-orientation, 4s exposure time, sample No.1



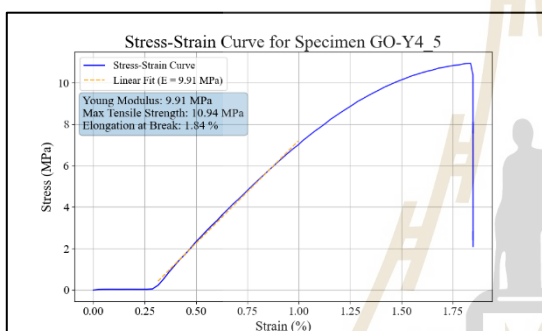
rGO resin, y-orientation, 4s exposure time, sample No.2



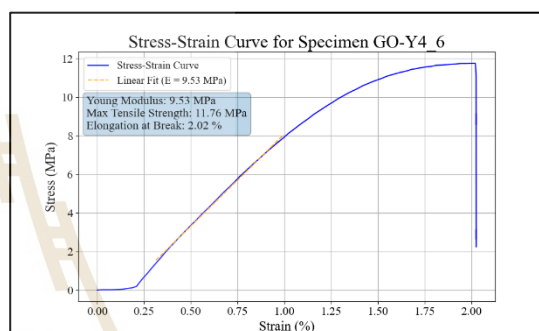
rGO resin, y-orientation, 4s exposure time,
sample No.3



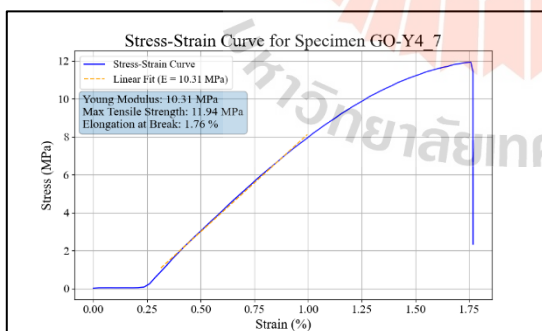
rGO resin, y-orientation, 4s exposure time,
sample No.4



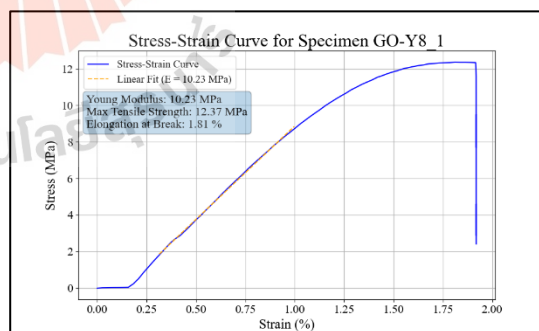
rGO resin, y-orientation, 4s exposure time,
sample No.5



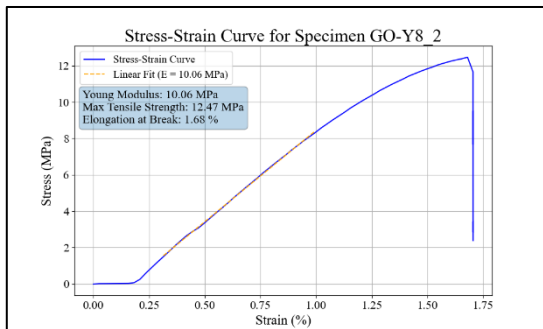
rGO resin, y-orientation, 4s exposure time,
sample No.6



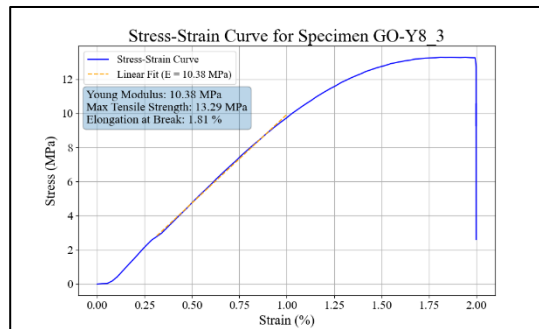
rGO resin, y-orientation, 4s exposure time,
sample No.7



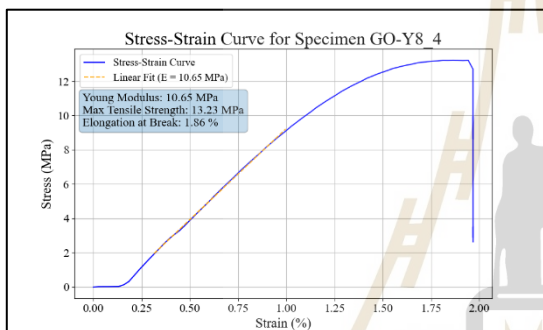
rGO resin, y-orientation, 8s exposure time,
sample No.1



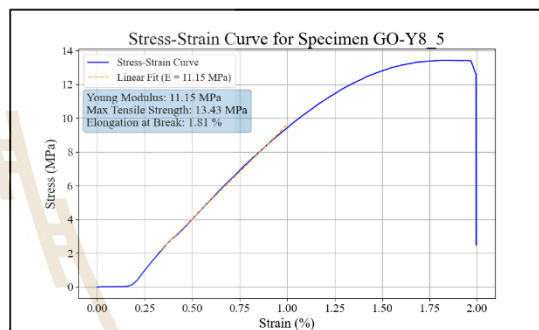
rGO resin, y-orientation, 8s exposure time, sample No.2



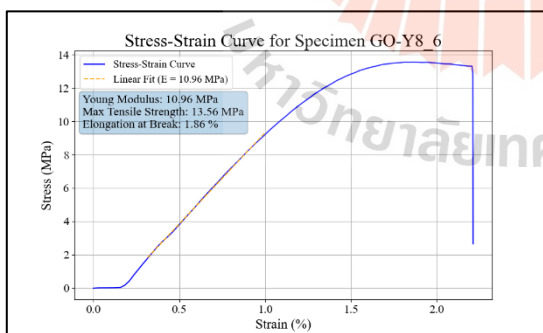
rGO resin, y-orientation, 8s exposure time, sample No.3



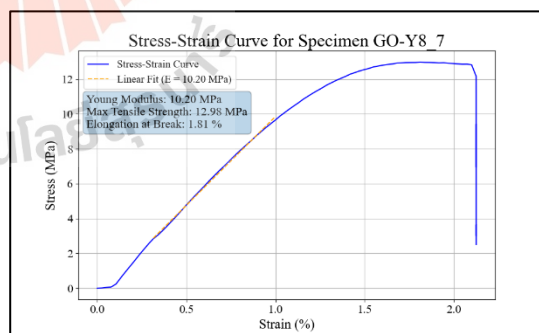
rGO resin, y-orientation, 8s exposure time, sample No.4



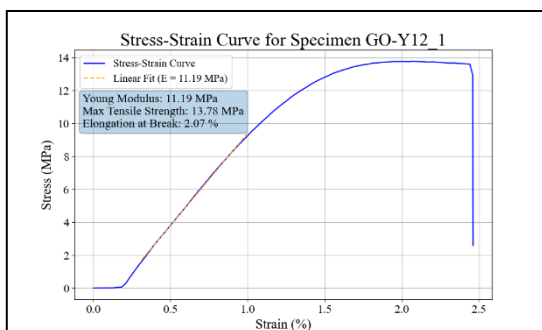
rGO resin, y-orientation, 8s exposure time, sample No.5



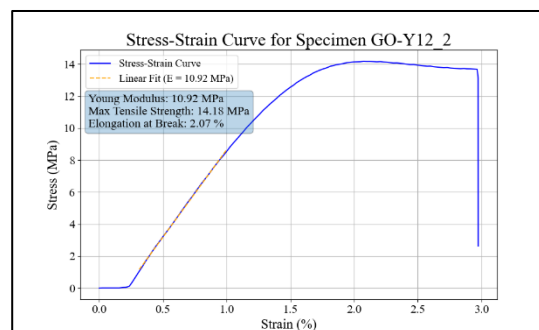
rGO resin, y-orientation, 8s exposure time, sample No.6



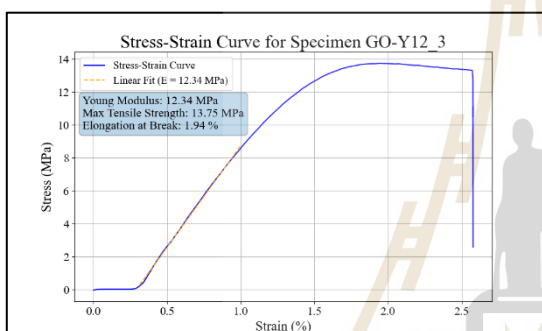
rGO resin, y-orientation, 8s exposure time, sample No.7



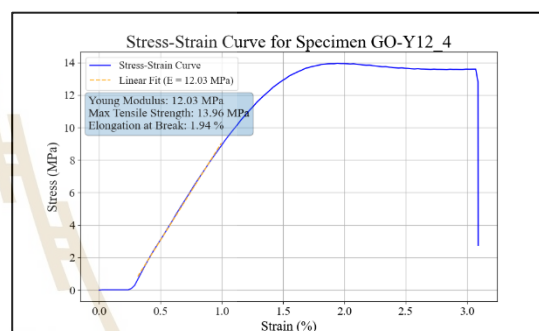
rGO resin, y-orientation, 12s exposure time,
sample No.1



rGO resin, y-orientation, 12s exposure time,
sample No.2



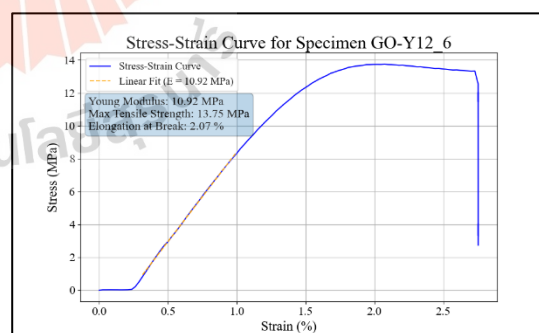
rGO resin, y-orientation, 12s exposure time,
sample No.3



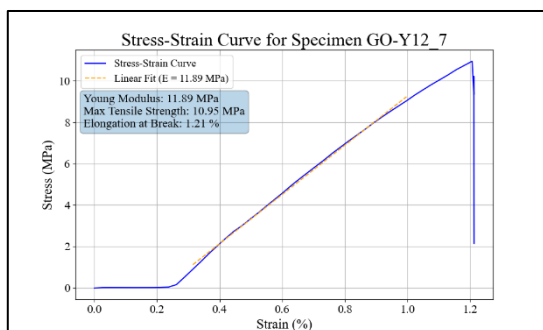
rGO resin, y-orientation, 12s exposure time,
sample No.4



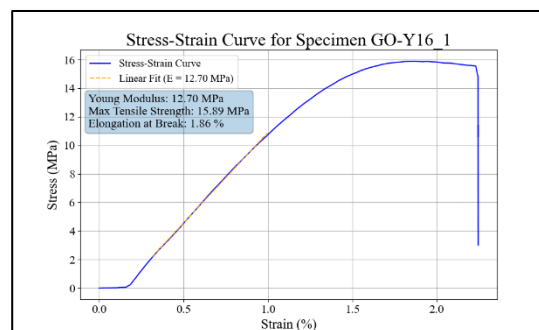
rGO resin, y-orientation, 12s exposure time,
sample No.5



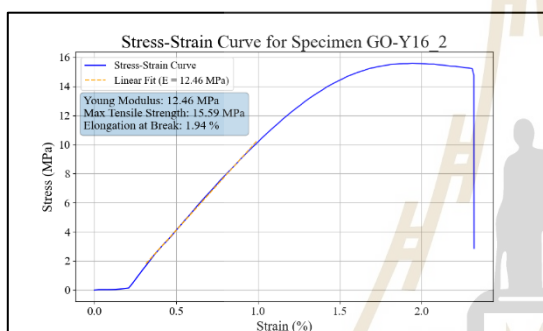
rGO resin, y-orientation, 12s exposure time,
sample No.6



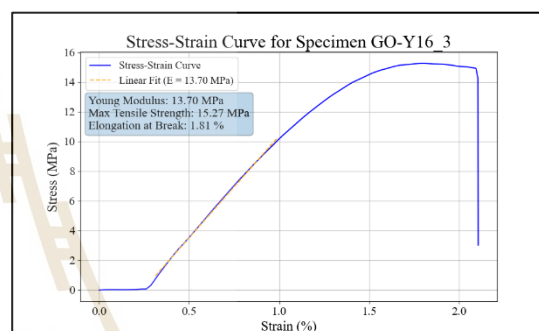
rGO resin, y-orientation, 12s exposure time,
sample No.7



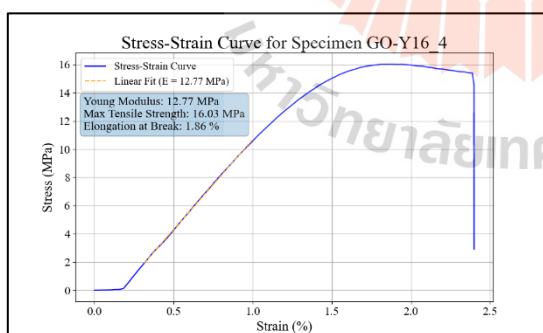
rGO resin, y-orientation, 16s exposure time,
sample No.1



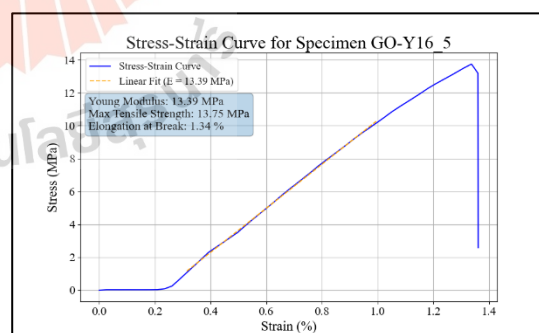
rGO resin, y-orientation, 16s exposure time,
sample No.2



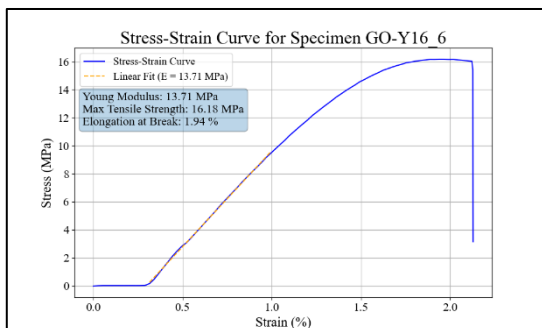
rGO resin, y-orientation, 16s exposure time,
sample No.3



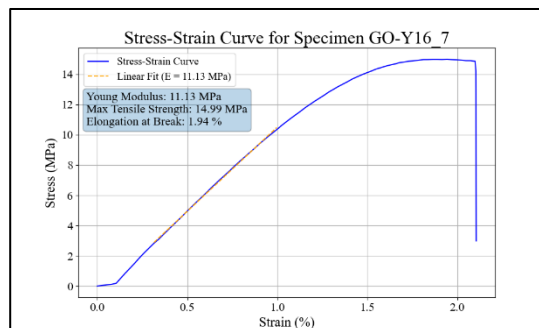
rGO resin, y-orientation, 16s exposure time,
sample No.4



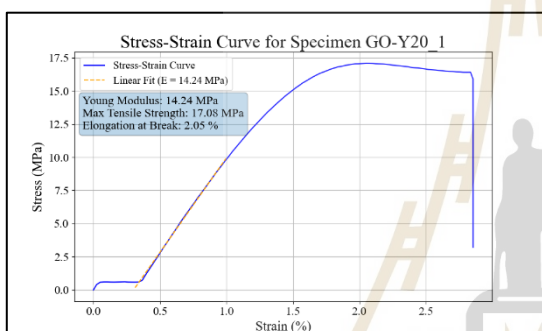
rGO resin, y-orientation, 16s exposure time,
sample No.5



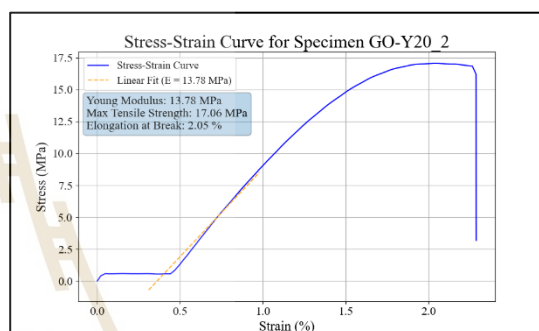
rGO resin, y-orientation, 16s exposure time,
sample No.6



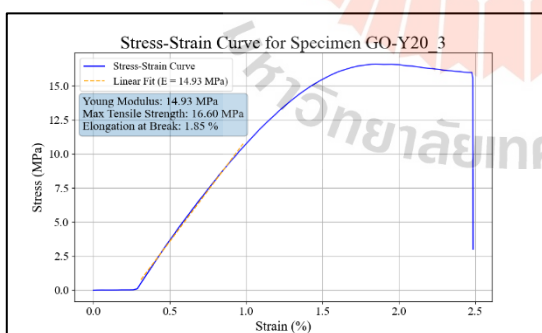
rGO resin, y-orientation, 16s exposure time,
sample No.7



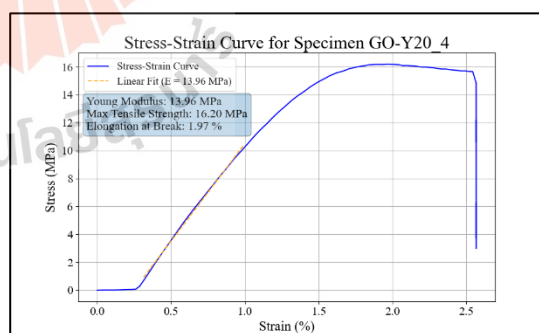
rGO resin, y-orientation, 20s exposure time,
sample No.1



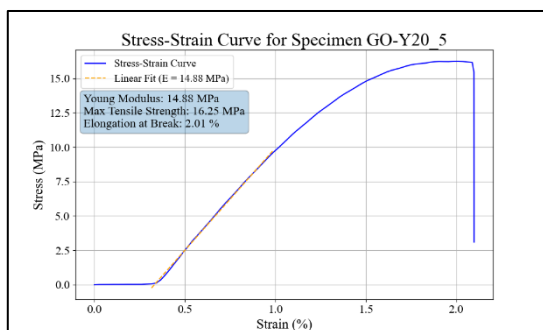
rGO resin, y-orientation, 20s exposure time,
sample No.2



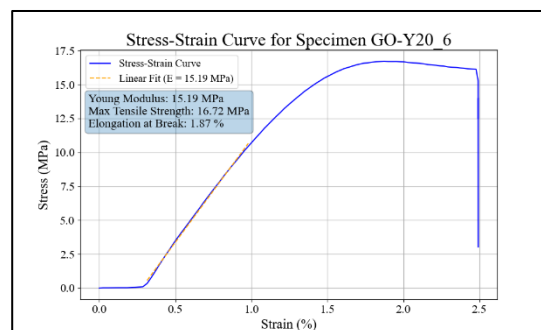
rGO resin, y-orientation, 20s exposure time,
sample No.3



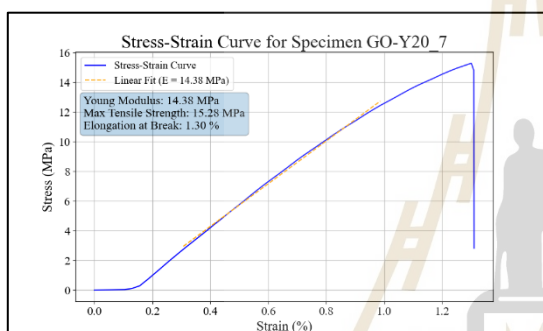
rGO resin, y-orientation, 20s exposure time,
sample No.4



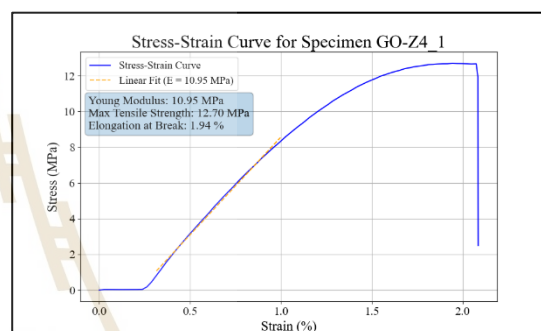
rGO resin, y-orientation, 20s exposure time,
sample No.5



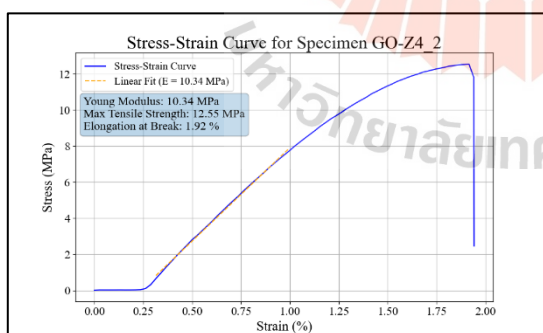
rGO resin, y-orientation, 20s exposure time,
sample No.6



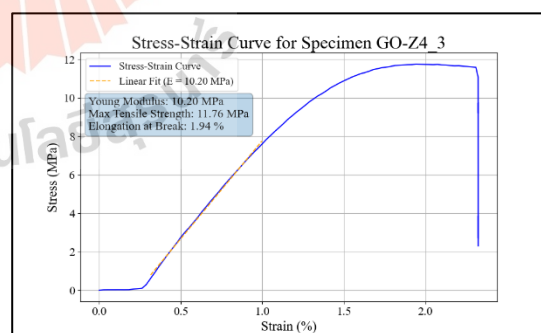
rGO resin, y-orientation, 20s exposure time,
sample No.7



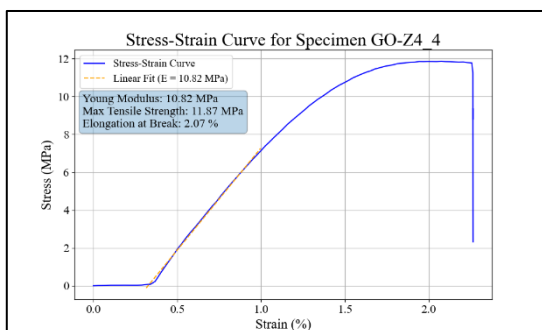
rGO resin, z-orientation, 4s exposure time,
sample No.1



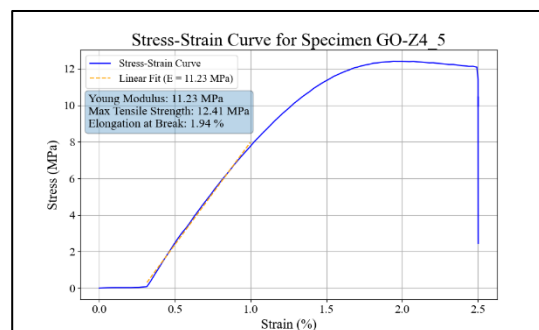
rGO resin, z-orientation, 4s exposure time,
sample No.2



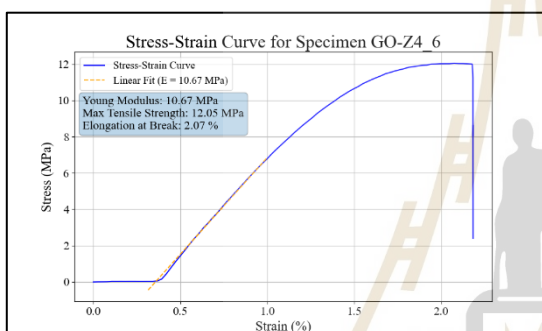
rGO resin, z-orientation, 4s exposure time,
sample No.3



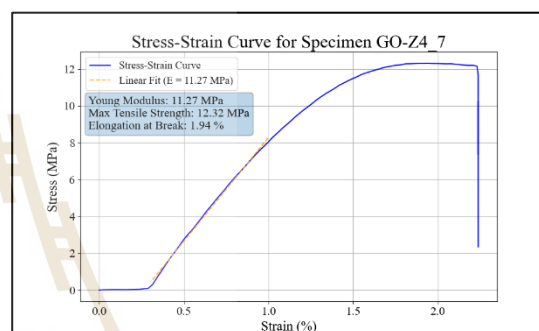
rGO resin, z-orientation, 4s exposure time,
sample No.4



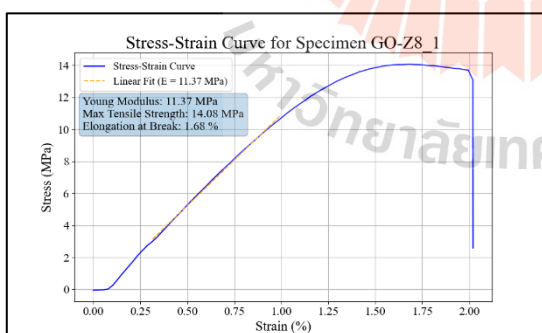
rGO resin, z-orientation, 4s exposure time,
sample No.5



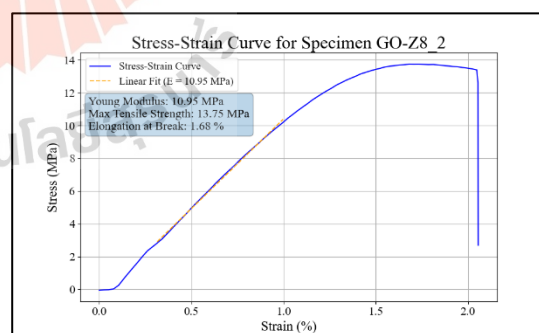
rGO resin, z-orientation, 4s exposure time,
sample No.6



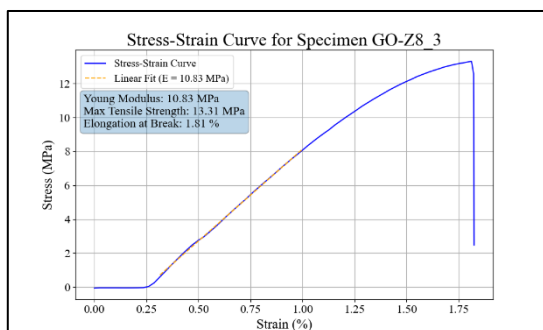
rGO resin, z-orientation, 4s exposure time,
sample No.7



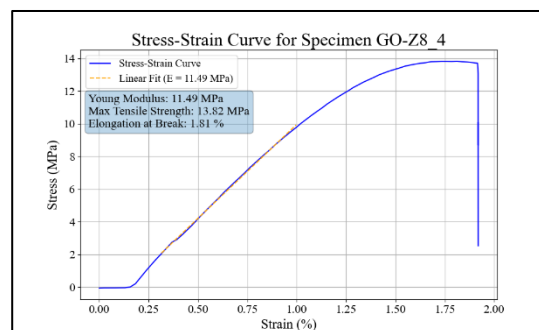
rGO resin, z-orientation, 8s exposure time,
sample No.1



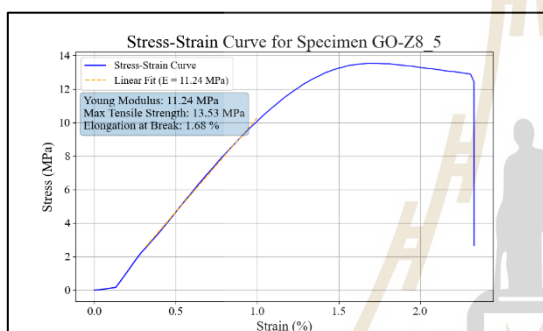
rGO resin, z-orientation, 8s exposure time,
sample No.2



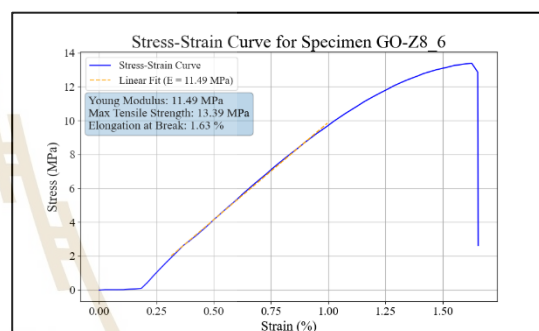
rGO resin, z-orientation, 8s exposure time,
sample No.3



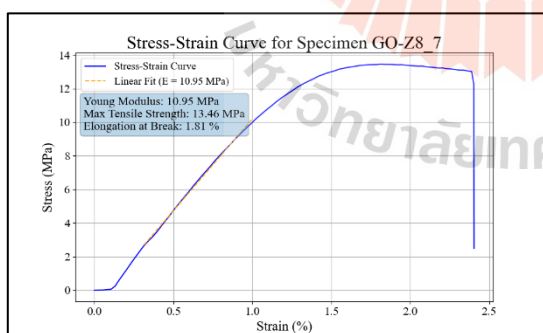
rGO resin, z-orientation, 8s exposure time,
sample No.4



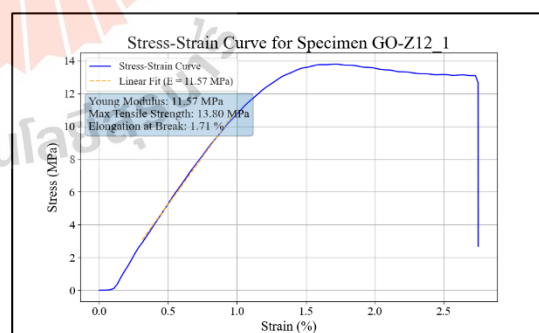
rGO resin, z-orientation, 8s exposure time,
sample No.5



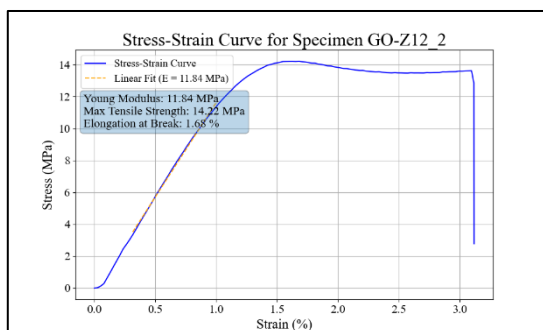
rGO resin, z-orientation, 8s exposure time,
sample No.6



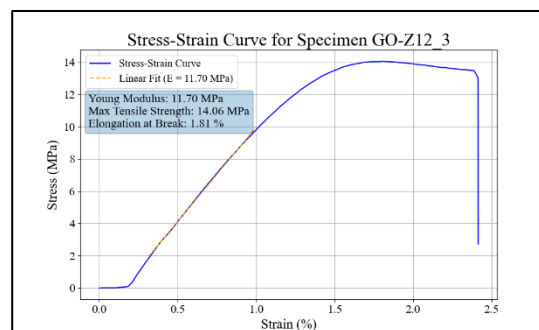
rGO resin, z-orientation, 8s exposure time,
sample No.7



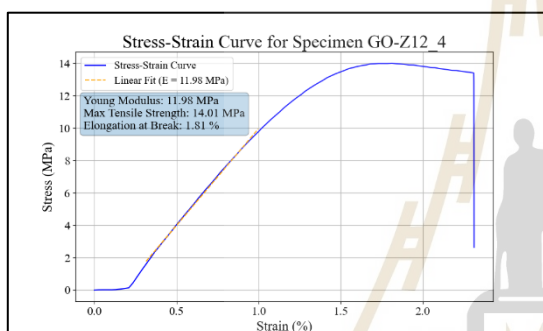
rGO resin, z-orientation, 12s exposure time,
sample No.1



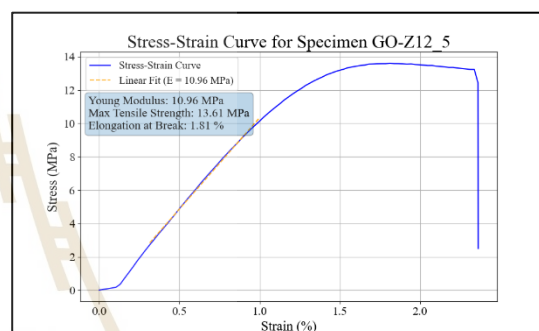
rGO resin, z-orientation, 12s exposure time,
sample No.2



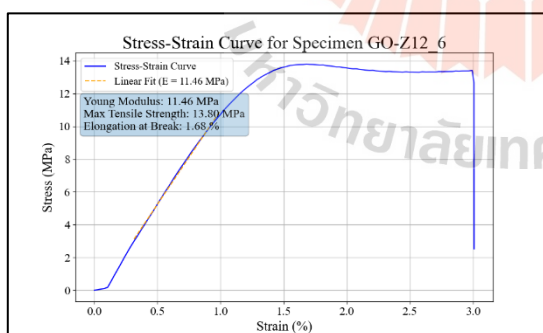
rGO resin, z-orientation, 12s exposure time,
sample No.3



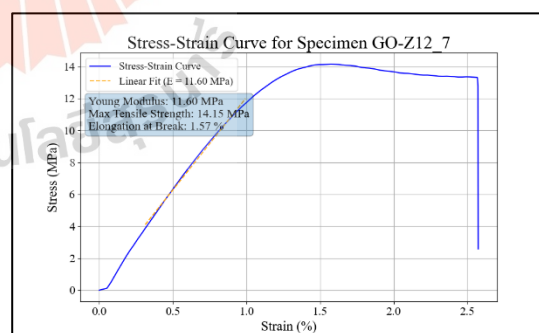
rGO resin, z-orientation, 12s exposure time,
sample No.4



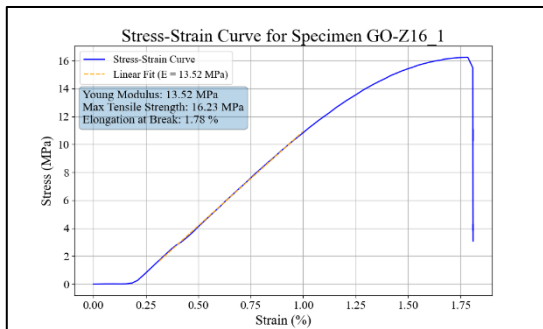
rGO resin, z-orientation, 12s exposure time,
sample No.5



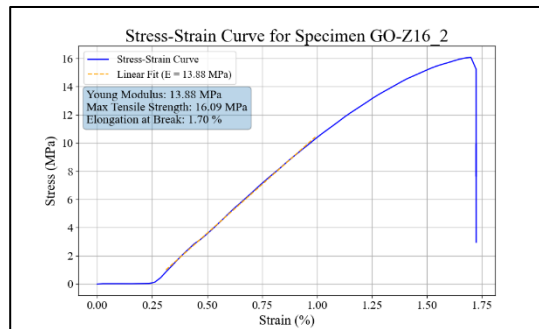
rGO resin, z-orientation, 12s exposure time,
sample No.6



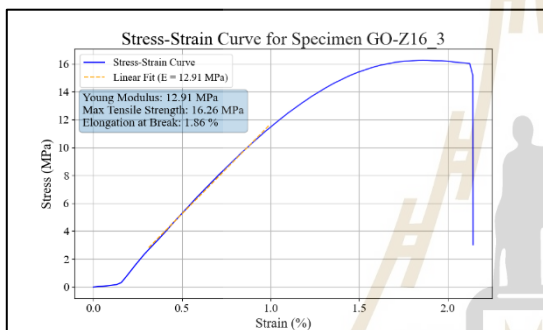
rGO resin, z-orientation, 12s exposure time,
sample No.7



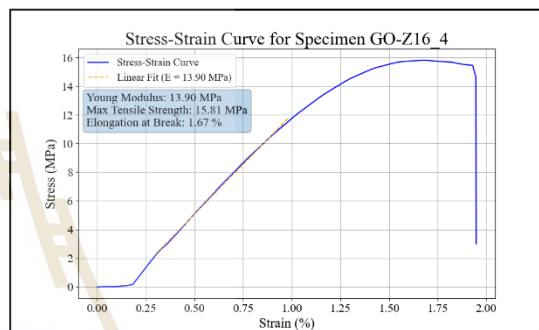
rGO resin, z-orientation, 16s exposure time, sample No.1



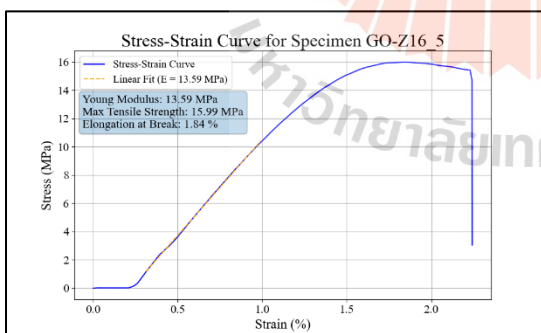
rGO resin, z-orientation, 16s exposure time, sample No.2



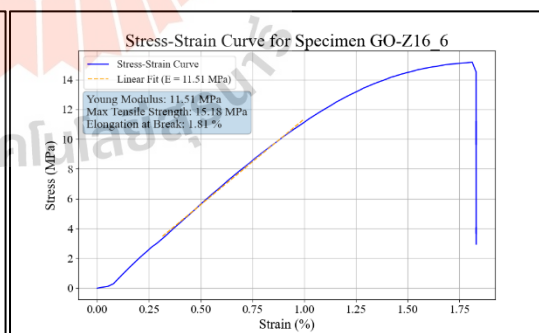
rGO resin, z-orientation, 16s exposure time, sample No.3



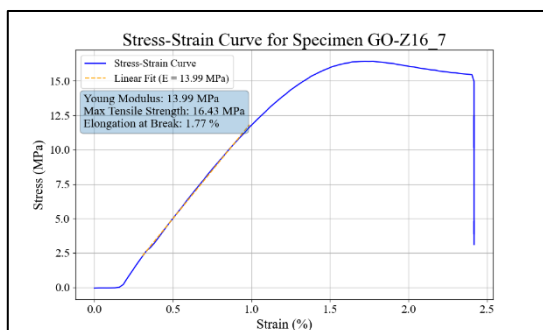
rGO resin, z-orientation, 16s exposure time, sample No.4



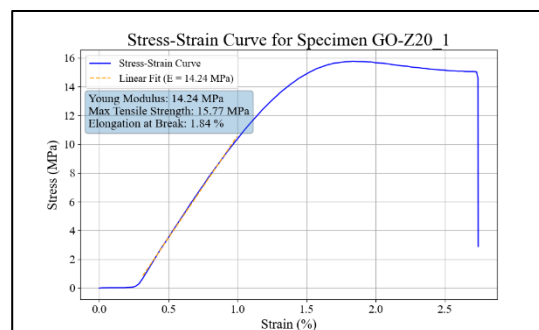
rGO resin, z-orientation, 16s exposure time, sample No.5



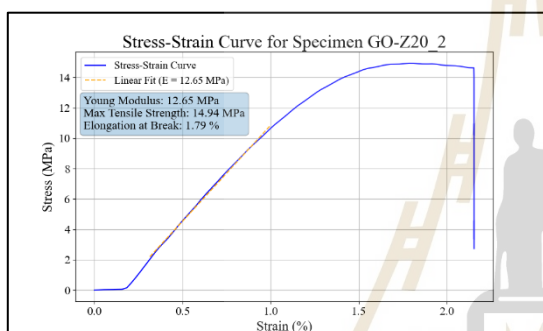
rGO resin, z-orientation, 16s exposure time, sample No.6



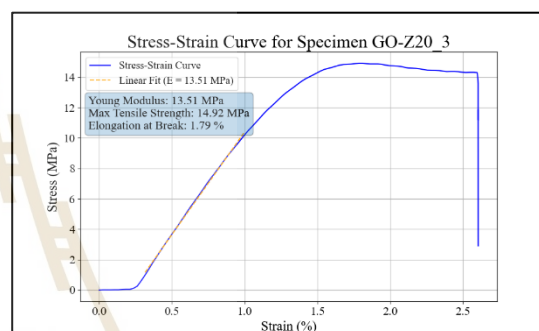
rGO resin, z-orientation, 16s exposure time,
sample No.7



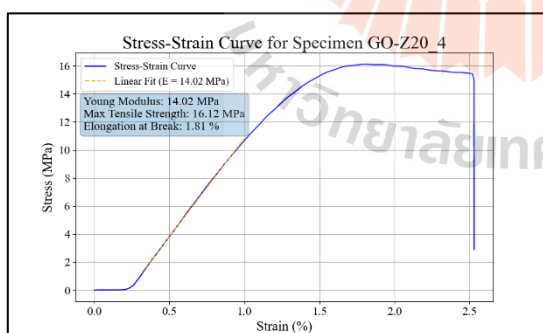
rGO resin, z-orientation, 20s exposure time,
sample No.1



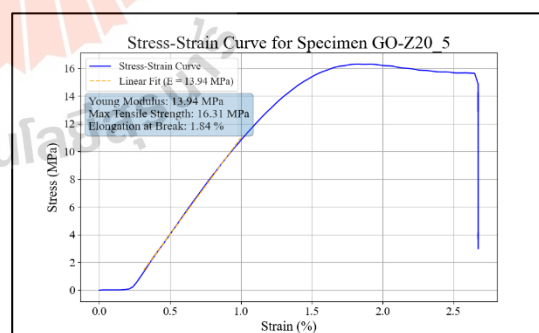
rGO resin, z-orientation, 20s exposure time,
sample No.2



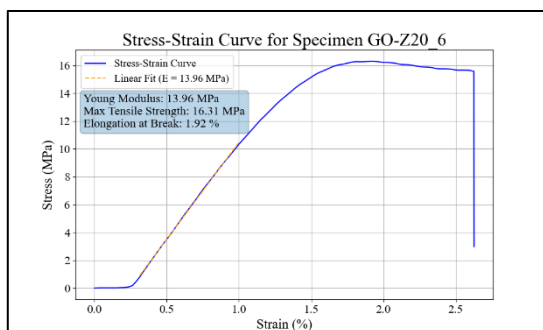
rGO resin, z-orientation, 20s exposure time,
sample No.3



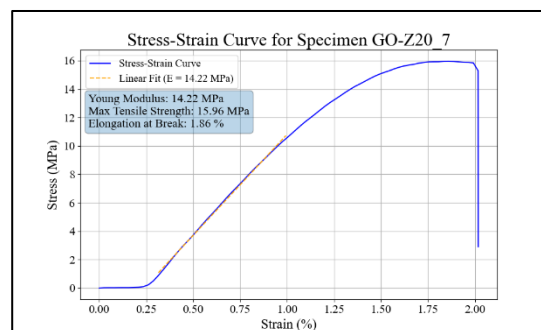
rGO resin, z-orientation, 20s exposure time,
sample No.4



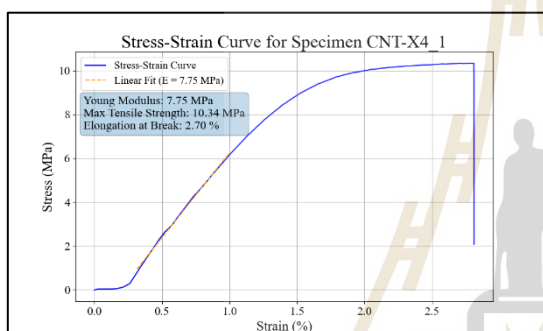
rGO resin, z-orientation, 20s exposure time,
sample No.5



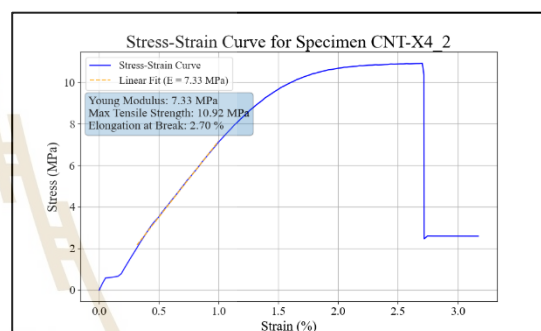
rGO resin, z-orientation, 20s exposure time,
sample No.6



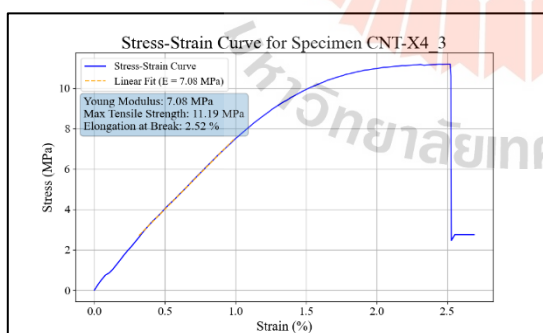
rGO resin, z-orientation, 20s exposure time,
sample No.7



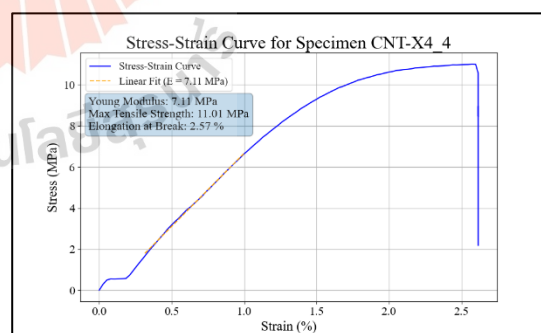
CNT resin, x-orientation, 4s exposure time,
sample No.1



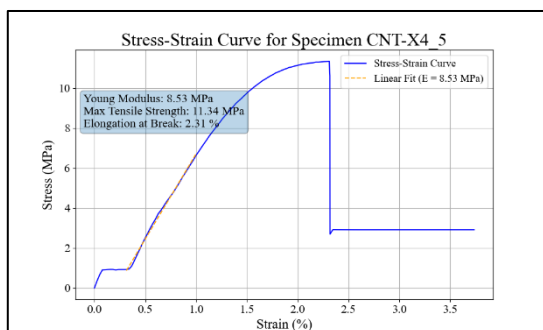
CNT resin, x-orientation, 4s exposure time,
sample No.2



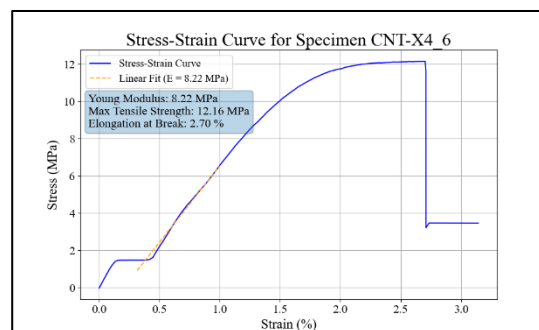
CNT resin, x-orientation, 4s exposure time,
sample No.3



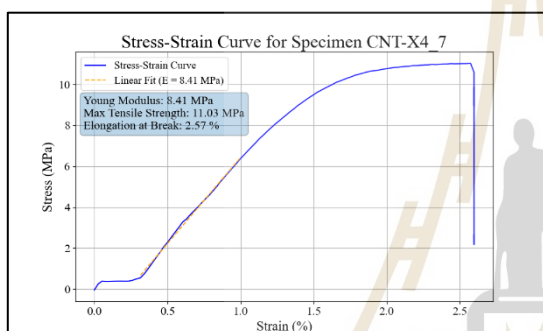
CNT resin, x-orientation, 4s exposure time,
sample No.4



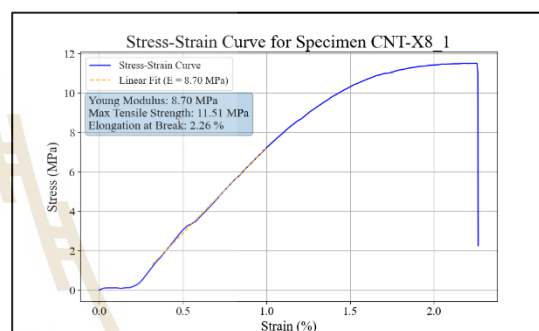
CNT resin, x-orientation, 4s exposure time,
sample No.5



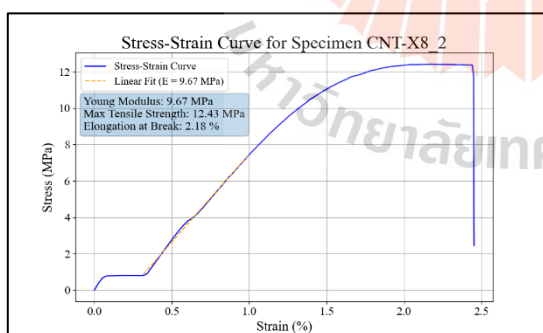
CNT resin, x-orientation, 4s exposure time,
sample No.6



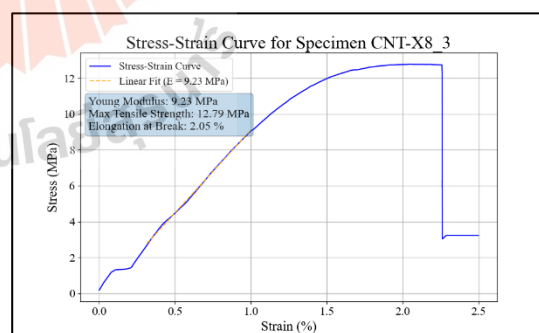
CNT resin, x-orientation, 4s exposure time,
sample No.7



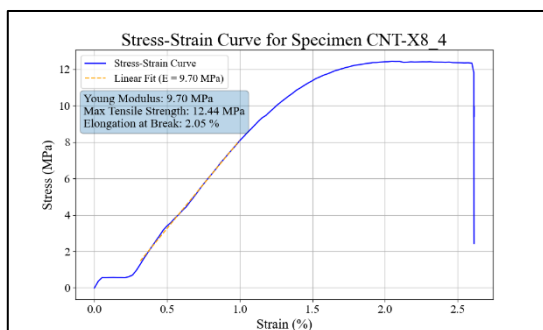
CNT resin, x-orientation, 8s exposure time,
sample No.1



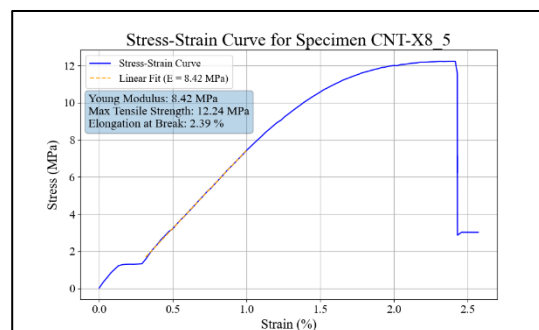
CNT resin, x-orientation, 8s exposure time,
sample No.2



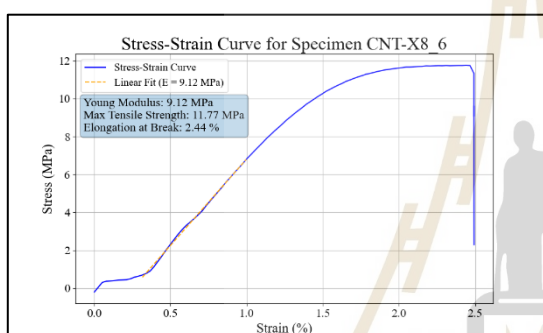
CNT resin, x-orientation, 8s exposure time,
sample No.3



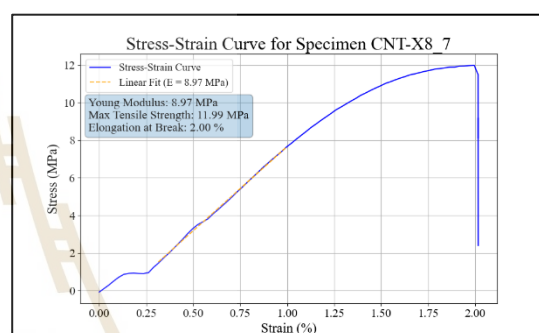
CNT resin, x-orientation, 8s exposure time,
sample No.4



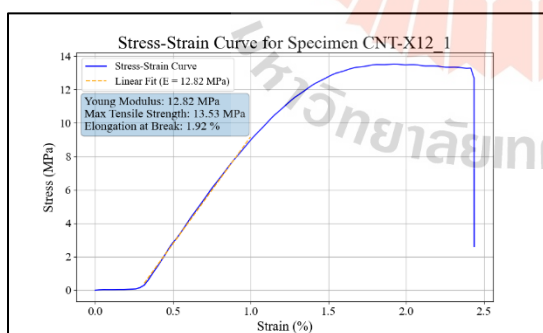
CNT resin, x-orientation, 8s exposure time,
sample No.5



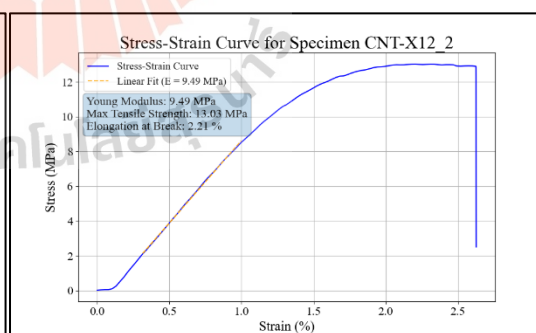
CNT resin, x-orientation, 8s exposure time,
sample No.6



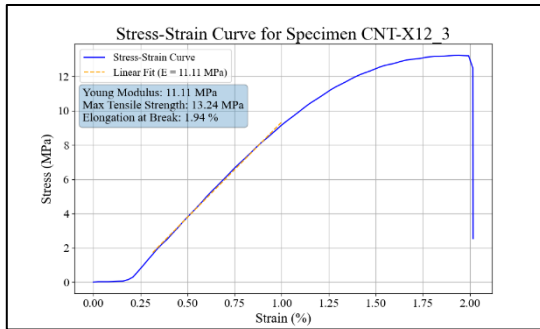
CNT resin, x-orientation, 8s exposure time,
sample No.7



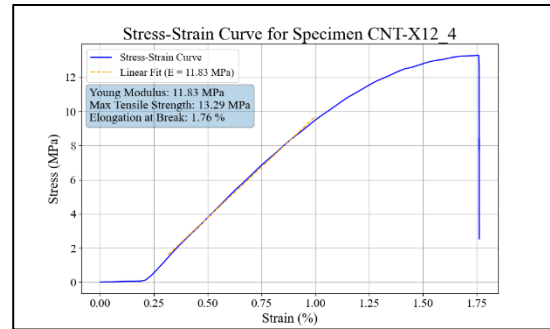
CNT resin, x-orientation, 12s exposure time,
sample No.1



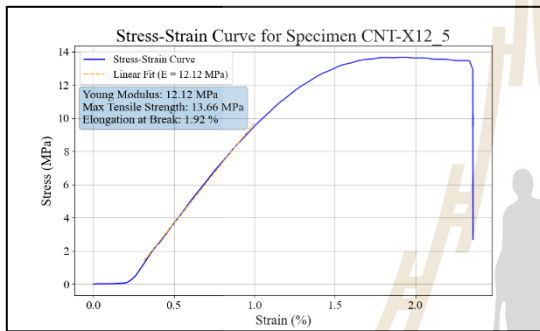
CNT resin, x-orientation, 12s exposure time,
sample No.2



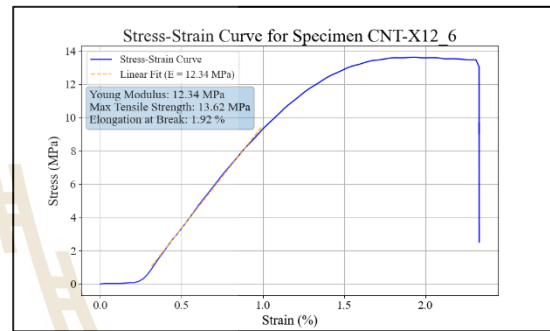
CNT resin, x-orientation, 12s exposure time, sample No.3



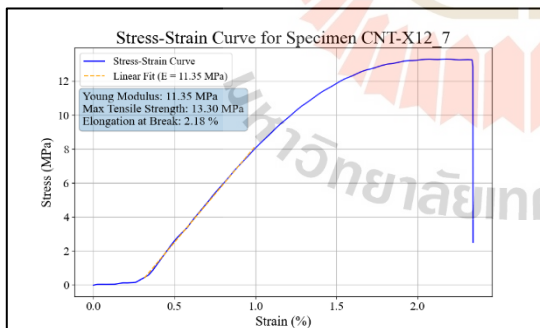
CNT resin, x-orientation, 12s exposure time, sample No.4



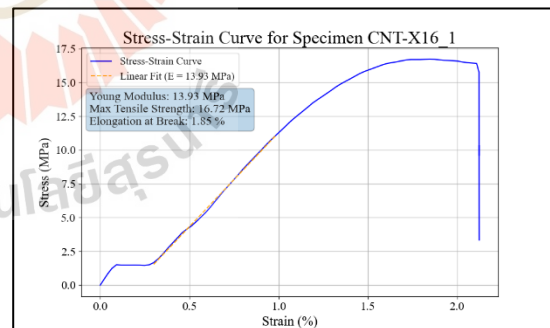
CNT resin, x-orientation, 12s exposure time, sample No.5



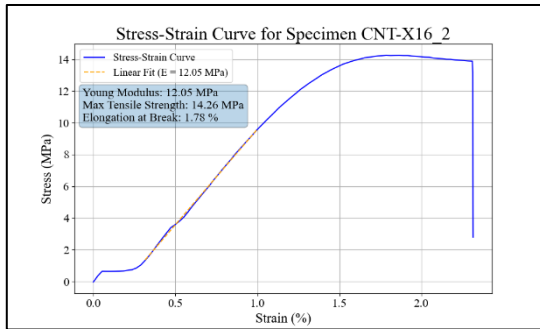
CNT resin, x-orientation, 12s exposure time, sample No.6



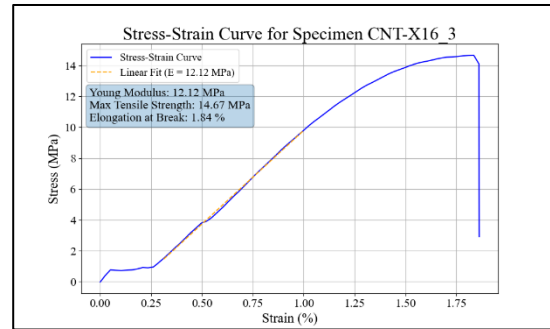
CNT resin, x-orientation, 12s exposure time, sample No.7



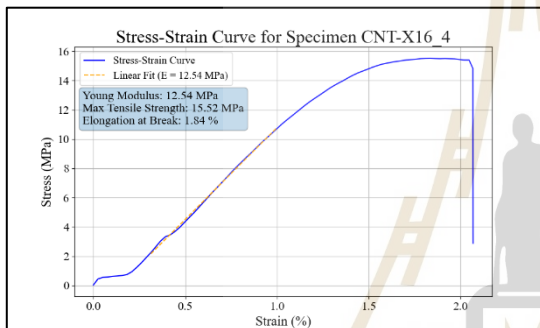
CNT resin, x-orientation, 16s exposure time, sample No.1



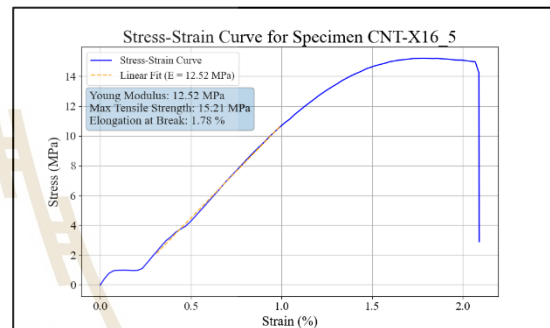
CNT resin, x-orientation, 16s exposure time, sample No.2



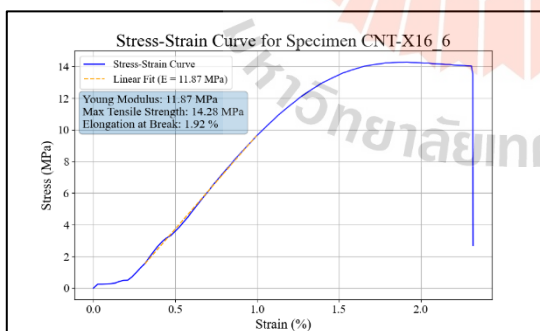
CNT resin, x-orientation, 16s exposure time, sample No.3



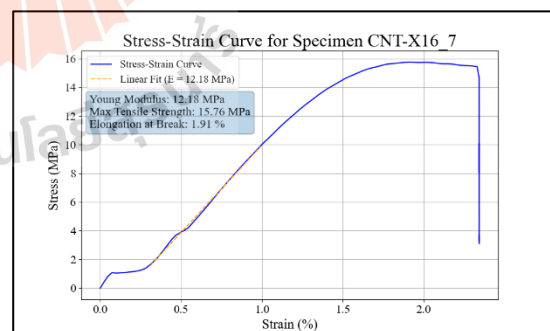
CNT resin, x-orientation, 16s exposure time, sample No.4



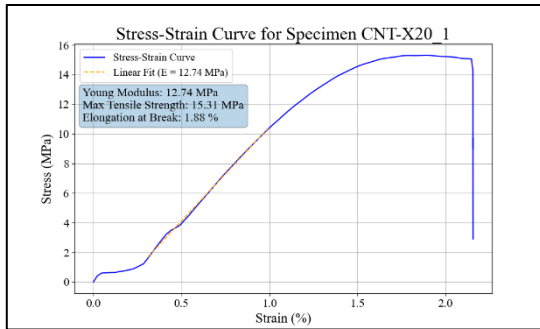
CNT resin, x-orientation, 16s exposure time, sample No.5



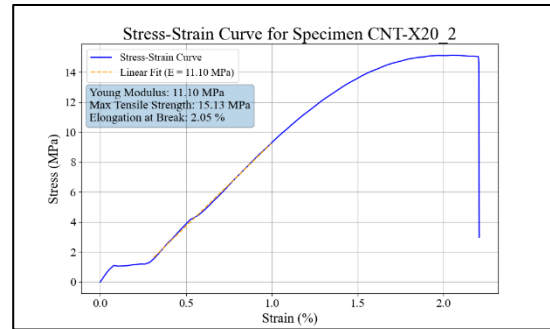
CNT resin, x-orientation, 16s exposure time, sample No.6



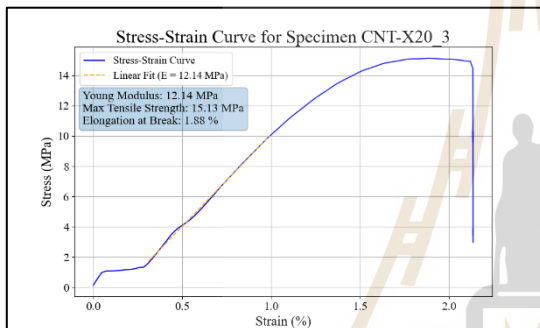
CNT resin, x-orientation, 16s exposure time, sample No.7



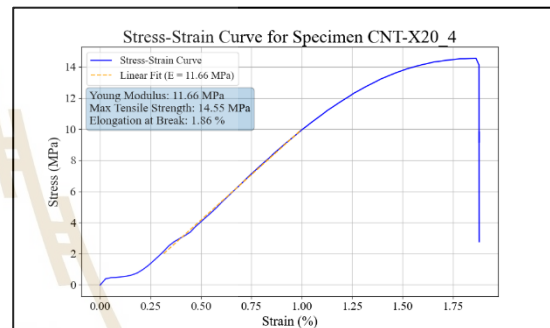
CNT resin, x-orientation, 20s exposure time, sample No.1



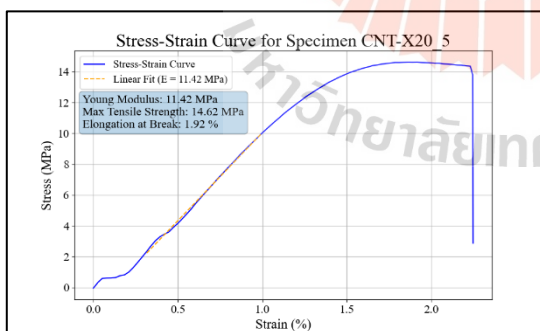
CNT resin, x-orientation, 20s exposure time, sample No.2



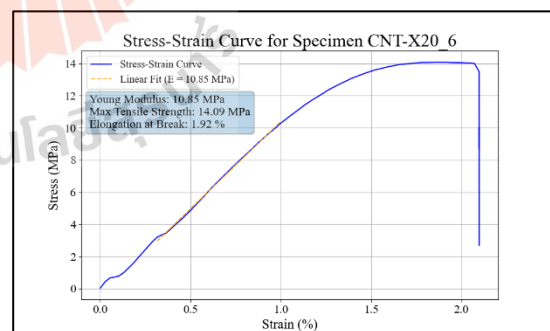
CNT resin, x-orientation, 20s exposure time, sample No.3



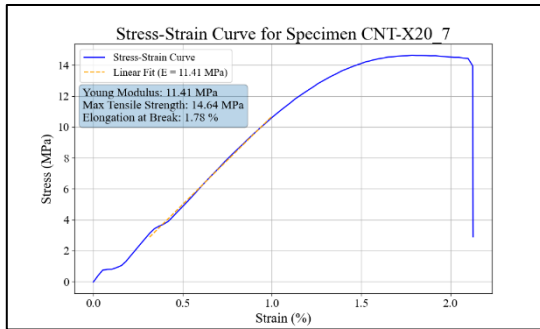
CNT resin, x-orientation, 20s exposure time, sample No.4



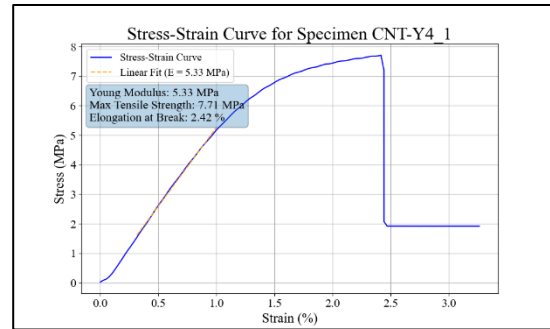
CNT resin, x-orientation, 20s exposure time, sample No.5



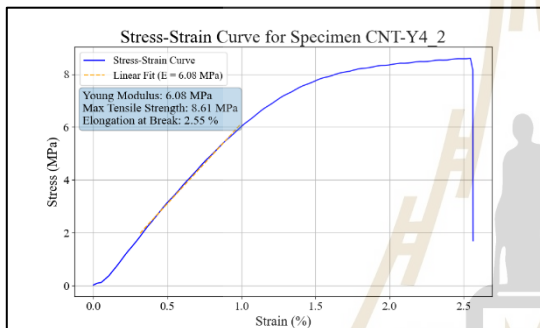
CNT resin, x-orientation, 20s exposure time, sample No.6



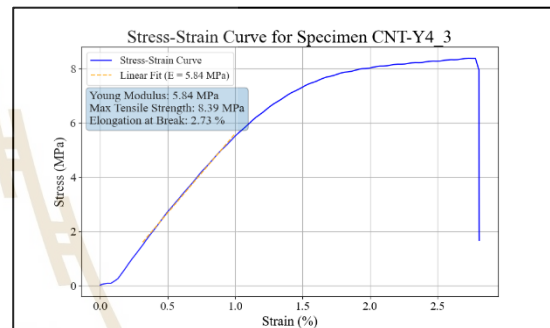
CNT resin, x-orientation, 20s exposure time, sample No.7



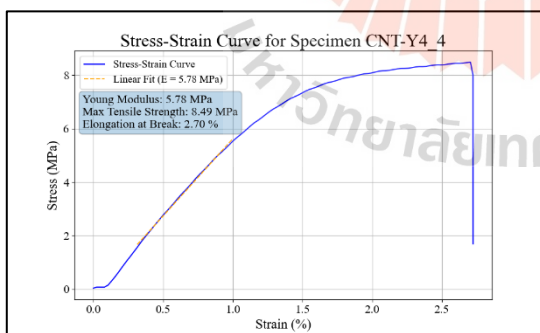
CNT resin, y-orientation, 4s exposure time, sample No.1



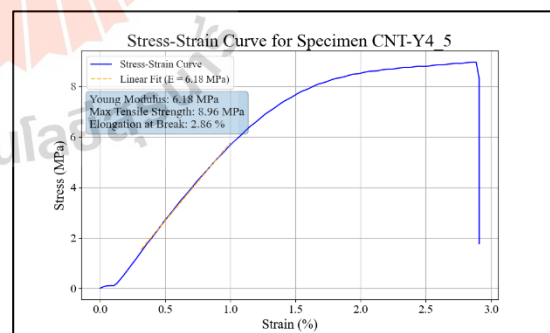
CNT resin, y-orientation, 4s exposure time, sample No.2



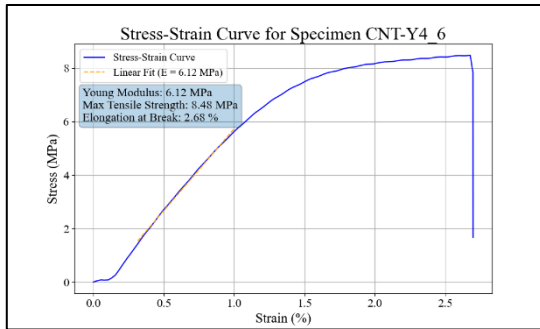
CNT resin, y-orientation, 4s exposure time, sample No.3



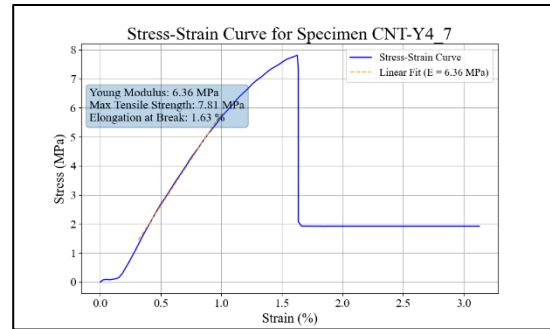
CNT resin, y-orientation, 4s exposure time, sample No.4



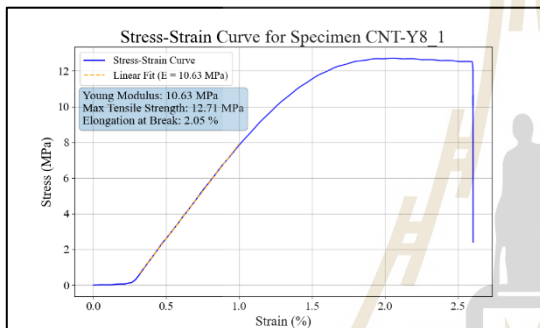
CNT resin, y-orientation, 4s exposure time, sample No.5



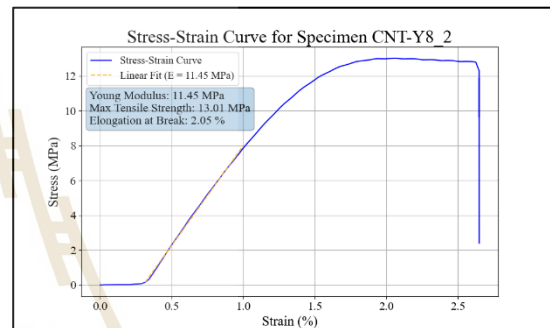
CNT resin, y-orientation, 4s exposure time, sample No.6



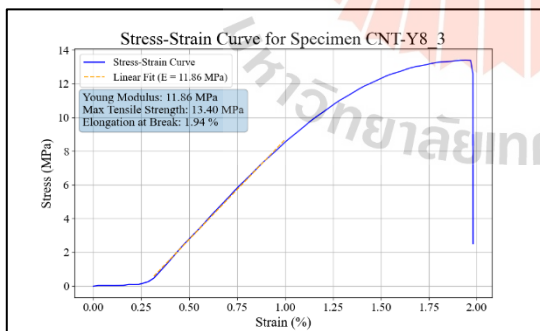
CNT resin, y-orientation, 4s exposure time, sample No.7



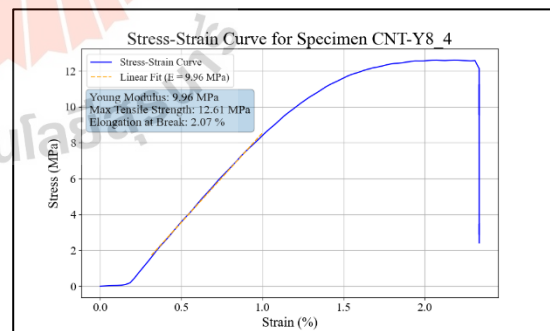
CNT resin, y-orientation, 8s exposure time, sample No.1



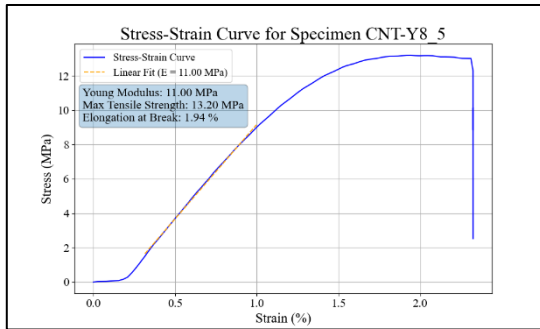
CNT resin, y-orientation, 8s exposure time, sample No.2



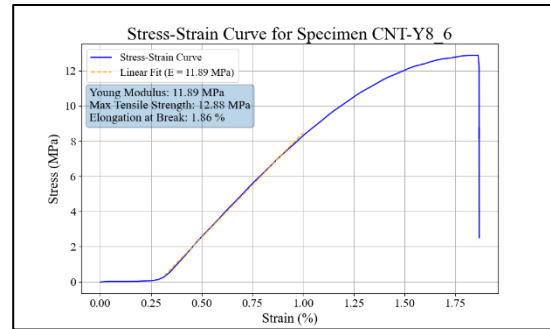
CNT resin, y-orientation, 8s exposure time, sample No.3



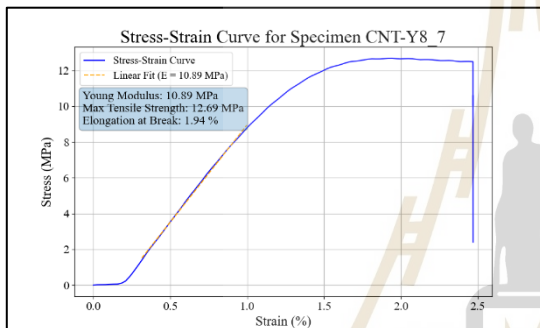
CNT resin, y-orientation, 8s exposure time, sample No.4



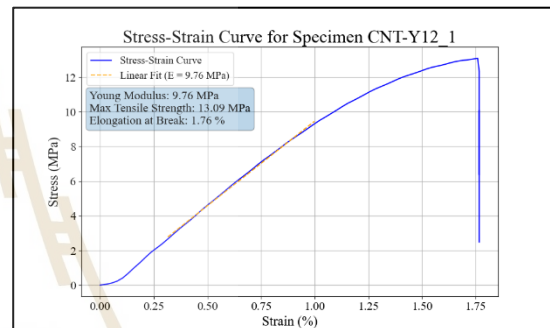
CNT resin, y-orientation, 8s exposure time, sample No.5



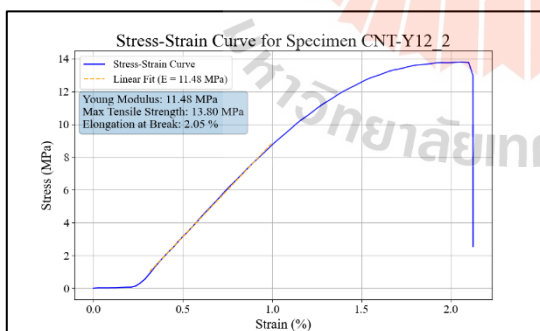
CNT resin, y-orientation, 8s exposure time, sample No.6



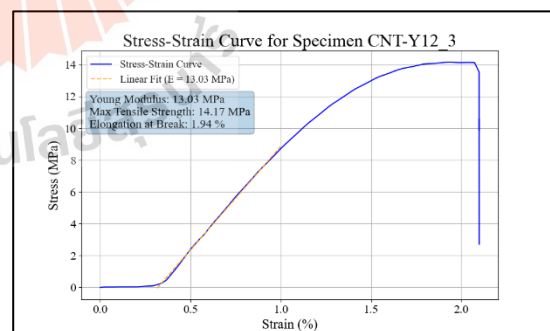
CNT resin, y-orientation, 8s exposure time, sample No.7



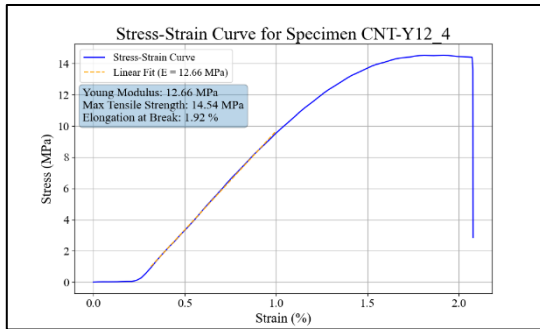
CNT resin, y-orientation, 12s exposure time, sample No.1



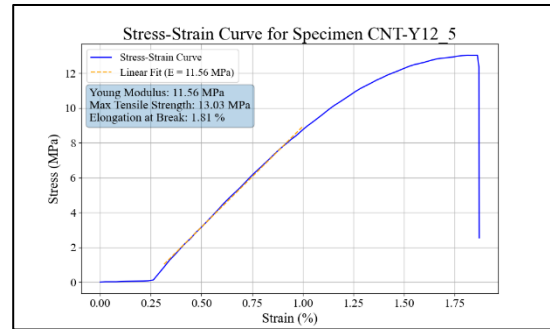
CNT resin, y-orientation, 12s exposure time, sample No.2



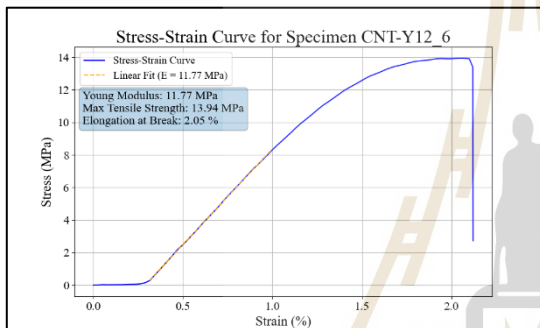
CNT resin, y-orientation, 12s exposure time, sample No.3



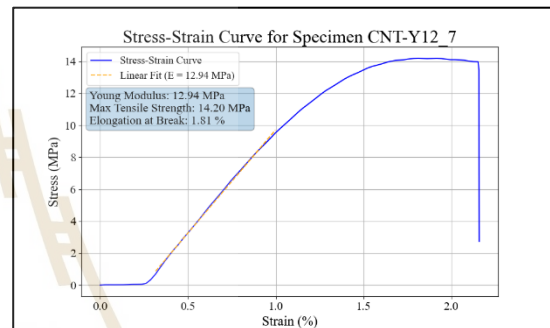
CNT resin, y-orientation, 12s exposure time, sample No.4



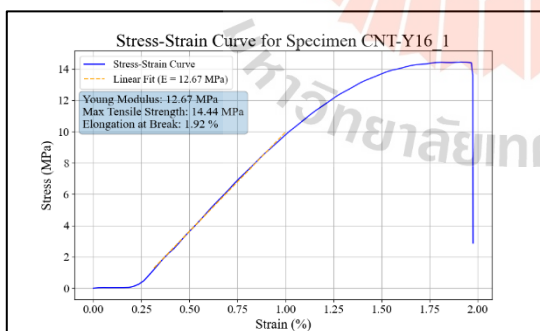
CNT resin, y-orientation, 12s exposure time, sample No.5



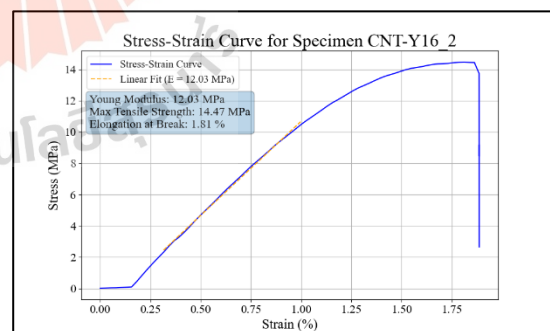
CNT resin, y-orientation, 12s exposure time, sample No.6



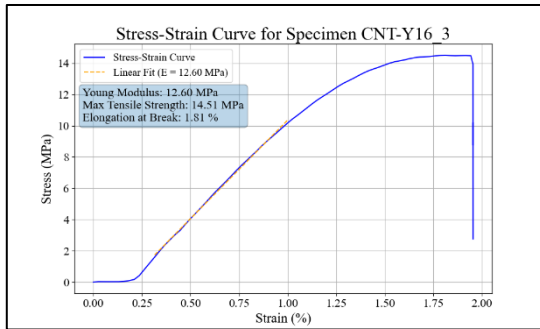
CNT resin, y-orientation, 12s exposure time, sample No.7



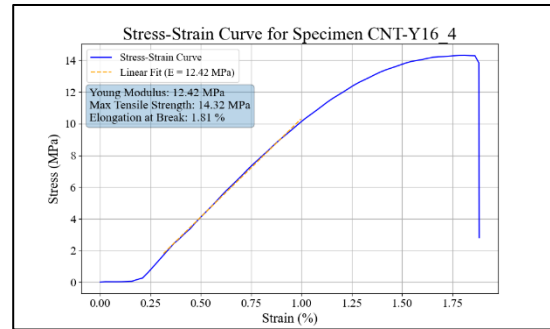
CNT resin, y-orientation, 16s exposure time, sample No.1



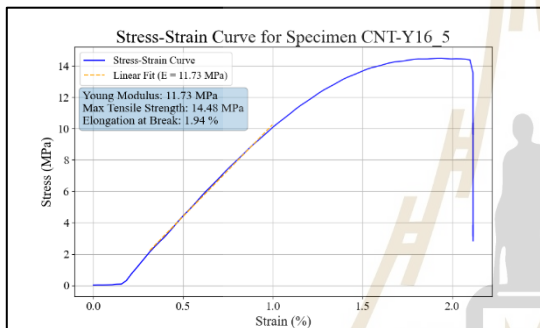
CNT resin, y-orientation, 16s exposure time, sample No.2



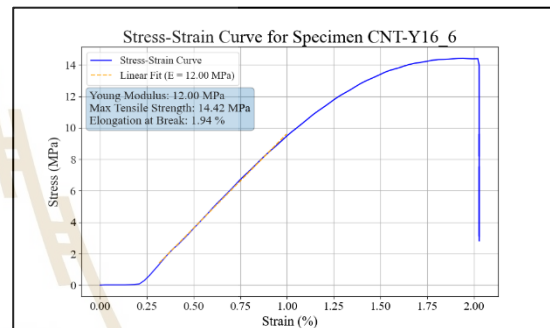
CNT resin, y-orientation, 16s exposure time, sample No.3



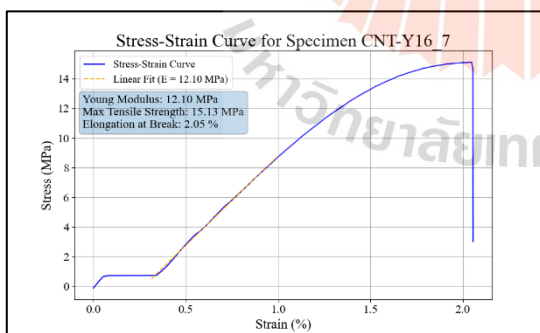
CNT resin, y-orientation, 16s exposure time, sample No.4



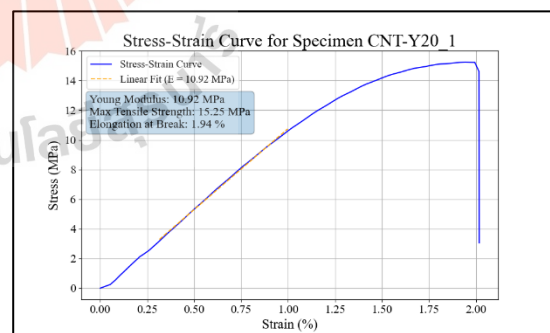
CNT resin, y-orientation, 16s exposure time, sample No.5



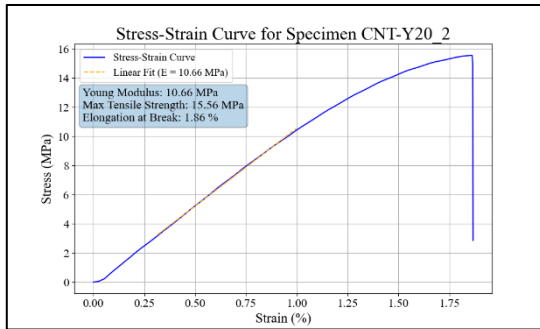
CNT resin, y-orientation, 16s exposure time, sample No.6



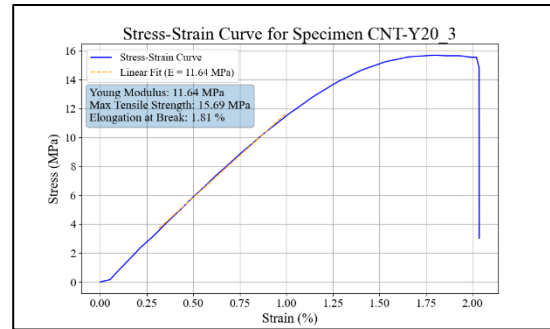
CNT resin, y-orientation, 16s exposure time, sample No.7



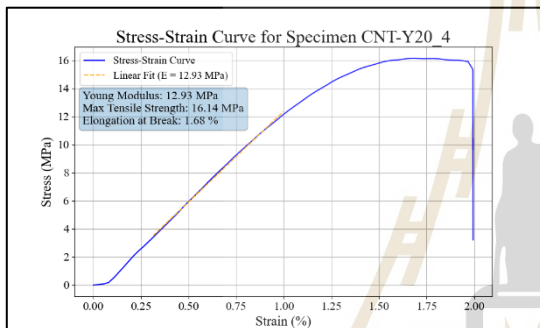
CNT resin, y-orientation, 20s exposure time, sample No.1



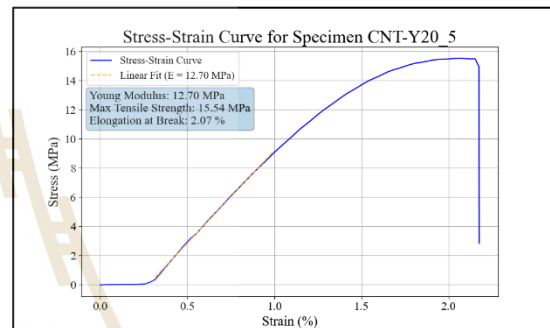
CNT resin, y-orientation, 20s exposure time, sample No.2



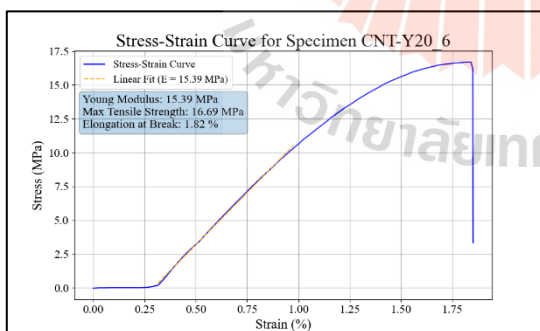
CNT resin, y-orientation, 20s exposure time, sample No.3



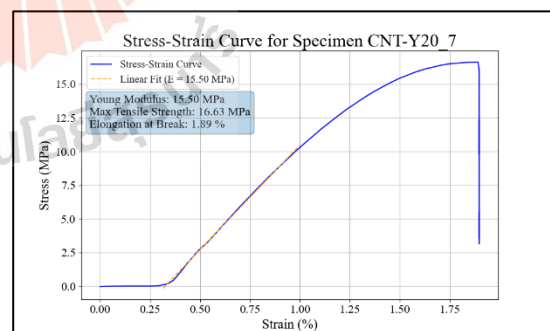
CNT resin, y-orientation, 20s exposure time, sample No.4



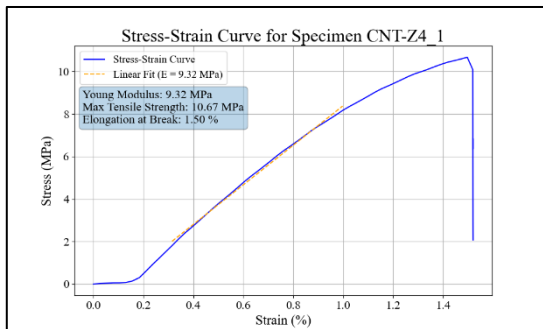
CNT resin, y-orientation, 20s exposure time, sample No.5



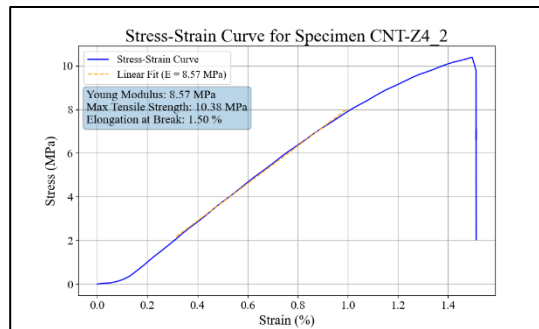
CNT resin, y-orientation, 20s exposure time, sample No.6



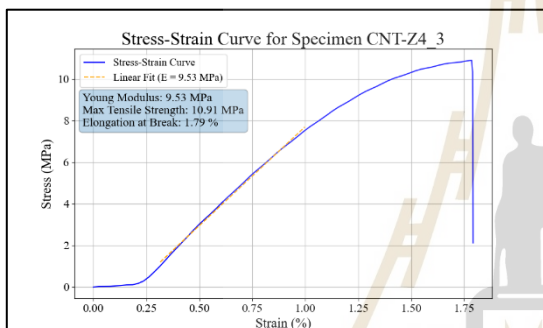
CNT resin, y-orientation, 20s exposure time, sample No.7



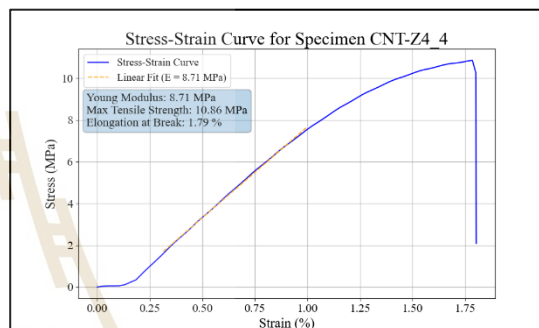
CNT resin, z-orientation, 4s exposure time, sample No.1



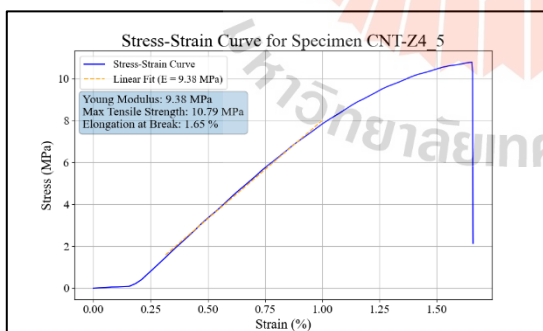
CNT resin, z-orientation, 4s exposure time, sample No.2



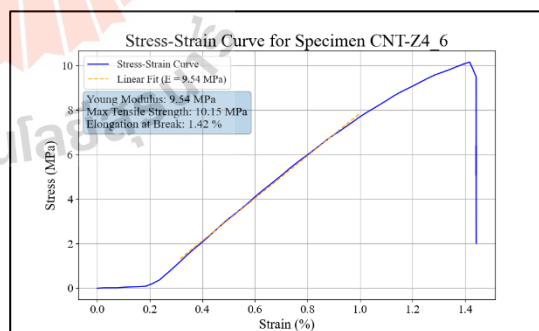
CNT resin, z-orientation, 4s exposure time, sample No.3



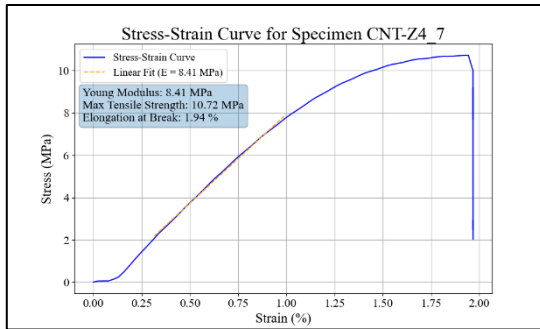
CNT resin, z-orientation, 4s exposure time, sample No.4



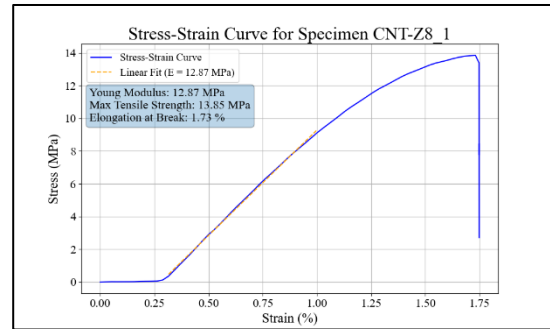
CNT resin, z-orientation, 4s exposure time, sample No.5



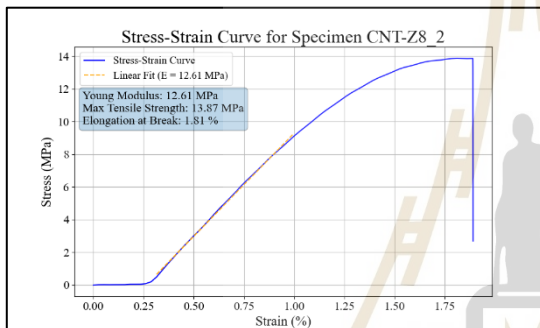
CNT resin, z-orientation, 4s exposure time, sample No.6



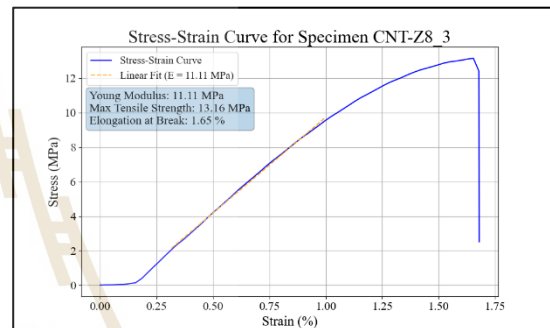
CNT resin, z-orientation, 4s exposure time, sample No.7



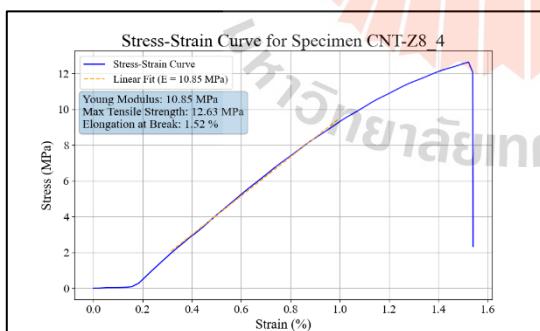
CNT resin, z-orientation, 8s exposure time, sample No.1



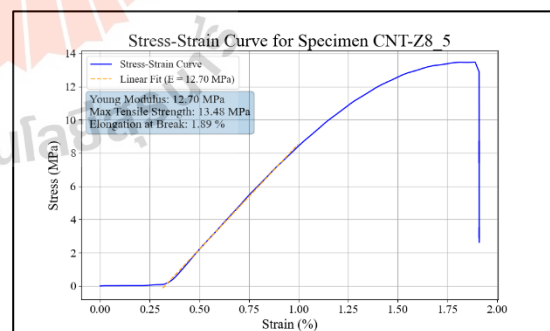
CNT resin, z-orientation, 8s exposure time, sample No.2



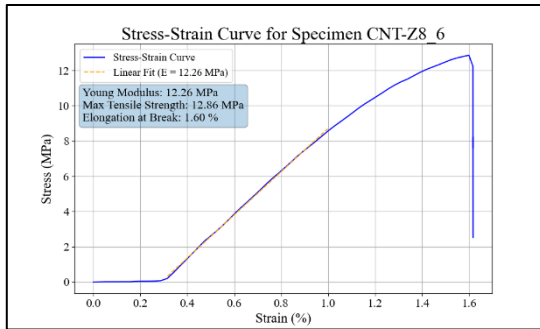
CNT resin, z-orientation, 8s exposure time, sample No.3



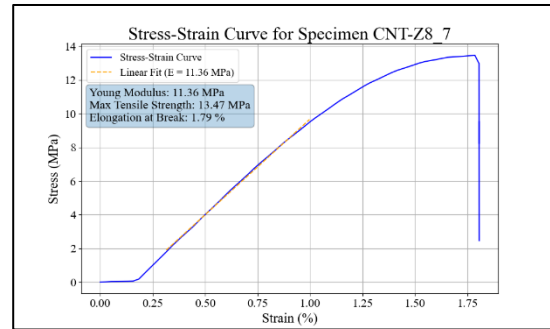
CNT resin, z-orientation, 8s exposure time, sample No.4



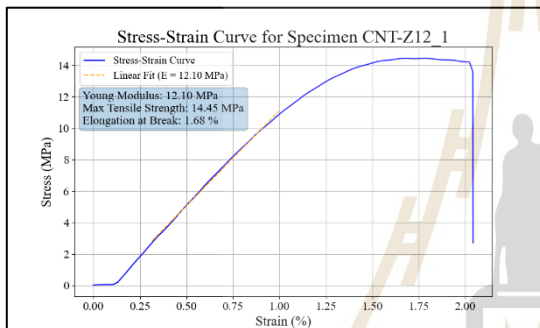
CNT resin, z-orientation, 8s exposure time, sample No.5



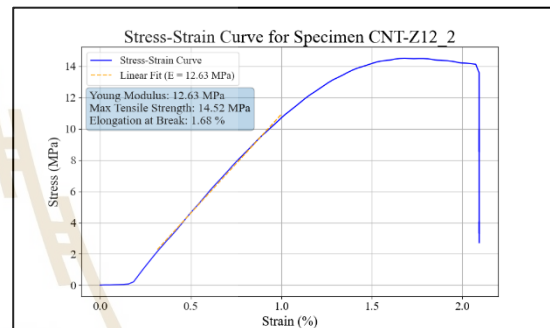
CNT resin, z-orientation, 8s exposure time, sample No.6



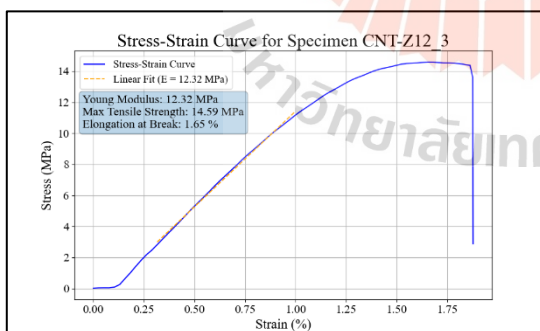
CNT resin, z-orientation, 8s exposure time, sample No.7



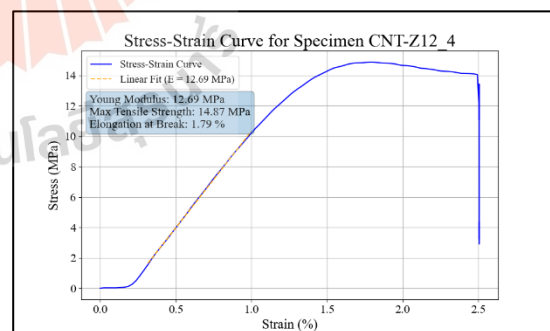
CNT resin, z-orientation, 12s exposure time, sample No.1



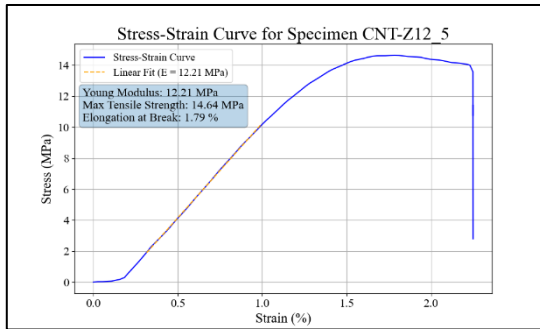
CNT resin, z-orientation, 12s exposure time, sample No.2



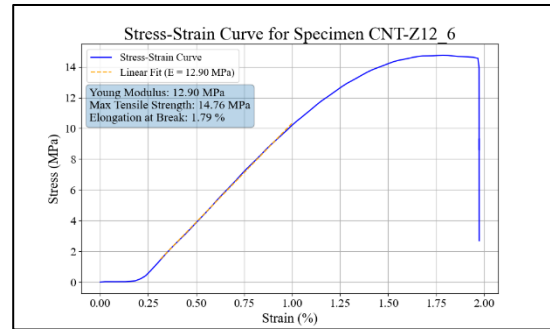
CNT resin, z-orientation, 12s exposure time, sample No.3



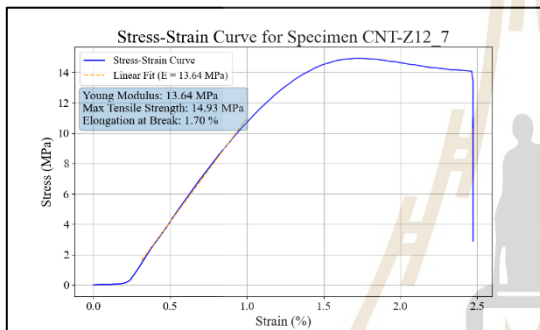
CNT resin, z-orientation, 12s exposure time, sample No.4



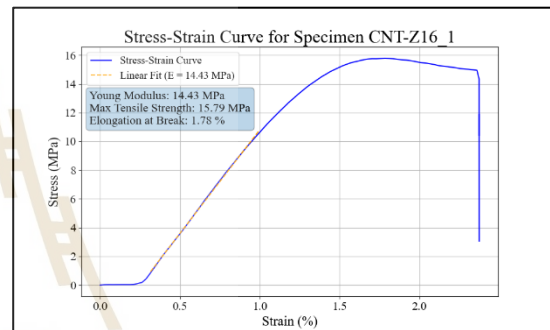
CNT resin, z-orientation, 12s exposure time, sample No.5



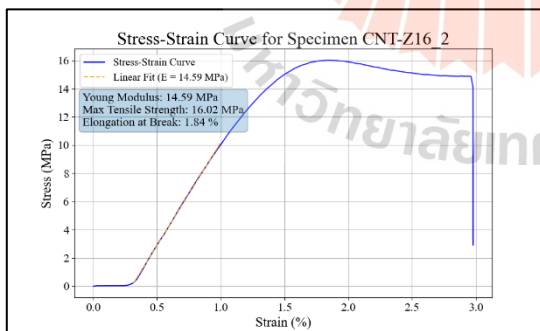
CNT resin, z-orientation, 12s exposure time, sample No.6



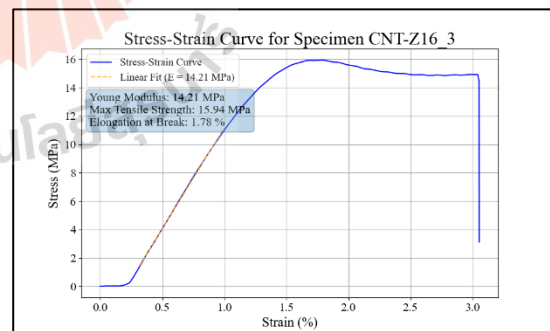
CNT resin, z-orientation, 12s exposure time, sample No.7



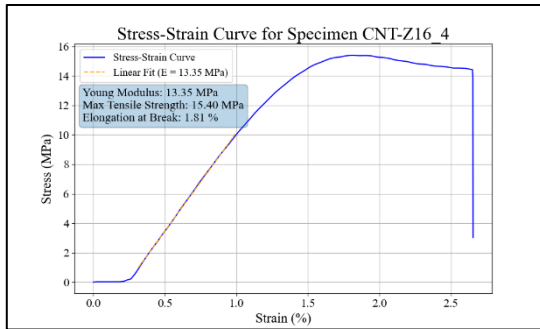
CNT resin, z-orientation, 16s exposure time, sample No.1



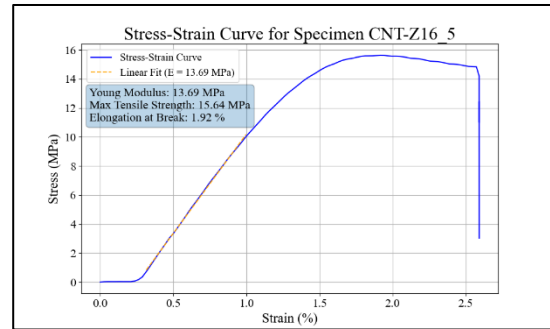
CNT resin, z-orientation, 16s exposure time, sample No.2



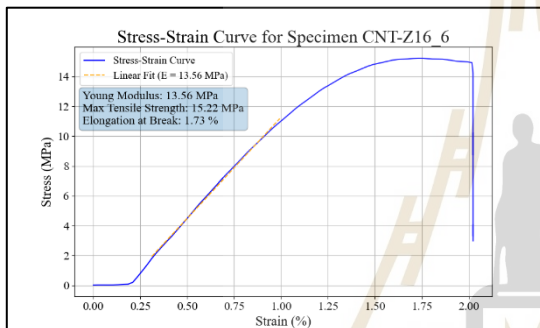
CNT resin, z-orientation, 16s exposure time, sample No.3



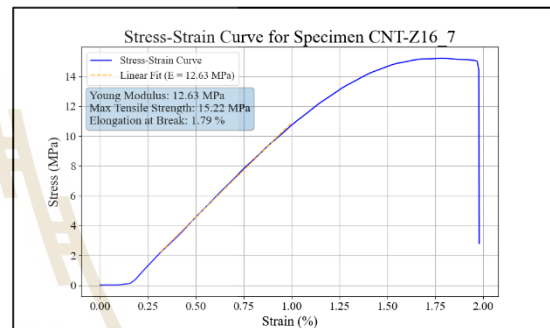
CNT resin, z-orientation, 16s exposure time, sample No.4



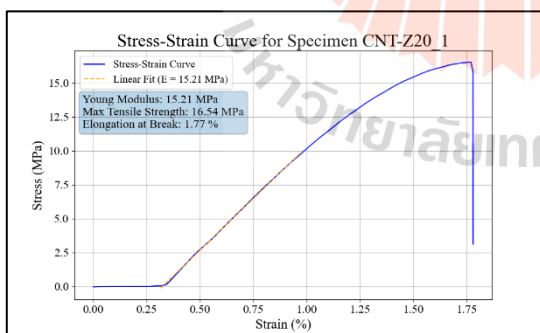
CNT resin, z-orientation, 16s exposure time, sample No.5



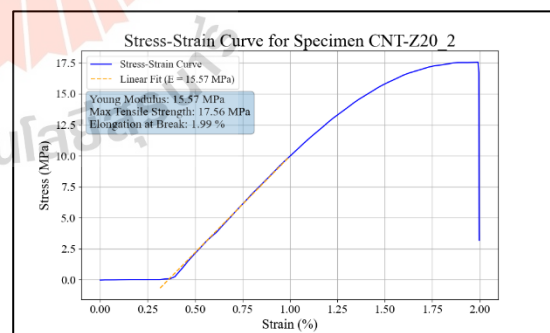
CNT resin, z-orientation, 16s exposure time, sample No.6



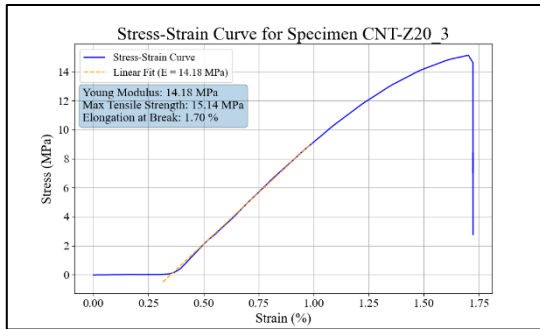
CNT resin, z-orientation, 16s exposure time, sample No.7



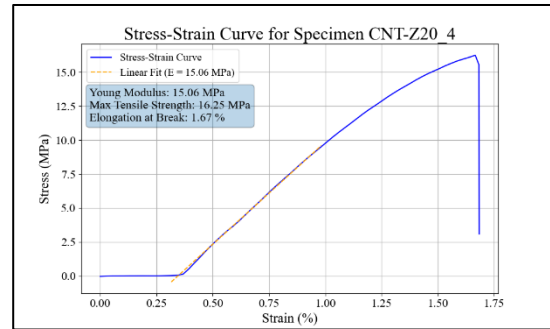
CNT resin, z-orientation, 20s exposure time, sample No.1



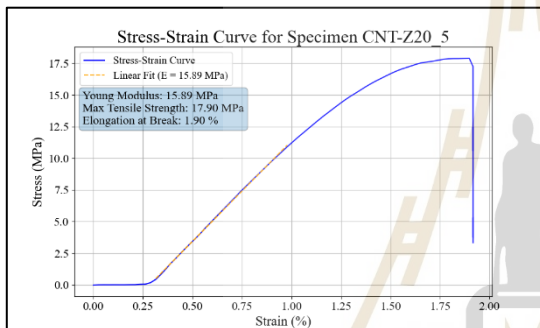
CNT resin, z-orientation, 20s exposure time, sample No.2



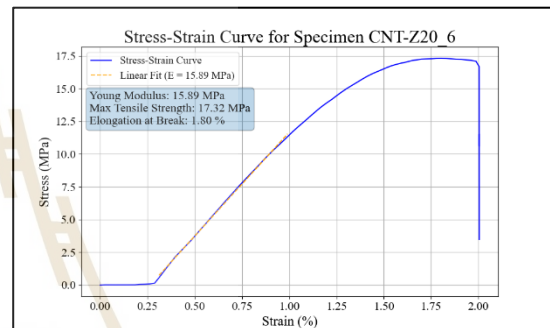
CNT resin, z-orientation, 20s exposure time, sample No.3



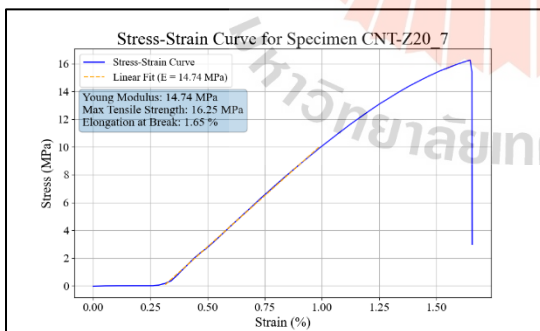
CNT resin, z-orientation, 20s exposure time, sample No.4



CNT resin, z-orientation, 20s exposure time, sample No.5



CNT resin, z-orientation, 20s exposure time, sample No.6



CNT resin, z-orientation, 20s exposure time, sample No.7

APPENDIX B

PUBLICATION AND PRESENTATION

B.1 List of publication

Pa-art, C. and Nuansing, W. (2023). Mechanical Properties of Graphene Nanoplatelets Composite Resin Fabricated by 3D Printing Technique. *Suranaree Journal of Science and Technology*, 30(5), 030149. doi: 10.55766/sujst-2023-05-e03020

B.2 List of presentation

Pa-art, C. and Nuansing, W. (2023). Three-dimensional Printing of Carbon-based Composite Resin and Mechanical Properties. *The 4th Materials Research Society of Thailand International Conference (MRS-Thailand 2023)*.



MECHANICAL PROPERTIES OF GRAPHENE NANOPATELETS COMPOSITE RESIN FABRICATED BY 3D PRINTING TECHNIQUE

Chanwit Pa-art^{1,*} and Wiwat Nuansing^{1,2}

Received: May 04, 2023; Revised: July 03, 2023; Accepted: August 17, 2023

Abstract

Vat photopolymerization 3D printing, including LCD 3D printing, is a versatile method for the fabrication of complex structures with numerous applications. The aim of this study was to investigate the potential of graphene nanoplatelets (GNP) as an additive for improving the mechanical properties of carbon-filled composite resin for LCD 3D printing. Tensile testing was conducted on the 3D printed samples using the ASTM D638 type V standard model. The results indicated that adding 0.1% w/w GNP with 20 sec of exposure time increased the elastic modulus of the specimen from 7.31 ± 1.02 MPa to 9.38 ± 0.37 MPa for x-orientation (horizontal) and from 7.62 ± 0.93 MPa to 9.58 ± 0.61 MPa for y-orientation (vertical). Furthermore, the maximum tensile strength increased from 3.87 ± 1.13 MPa to 5.28 ± 0.73 MPa for y-orientation and from 4.06 ± 0.92 MPa to 5.49 ± 0.49 MPa for x-orientation. These results demonstrate the efficacy of GNP as an effective additive for enhancing the mechanical properties of carbon-based composite resin in LCD 3D printing.

Keywords: Composite resin; graphene nanoplatelets; LCD 3D printing; mechanical properties; vat photopolymerization

Introduction

Three-dimensional (3D) printing, also known as additive manufacturing, has emerged as a transformative technology in the manufacturing industry due to its capability of producing complex geometries with high precision and accuracy (Abdollahi *et al.*, 2018; Shahrubudin *et al.*, 2019). Among the different 3D printing technologies, liquid crystal display (LCD) 3D printing, also known as mask stereolithography (MSLA), has gained significant attention due to its high resolution and accuracy (Lee *et al.*, 2017; Malas *et al.*, 2019). However, the mechanical properties of the printed objects using LCD 3D printing are often limited by the brittleness of the resins used. To address this challenge, researchers have been exploring the incorporation of various additives into the resins

¹ School of Physics, Institute of Science, Suranaree University of Technology, 111 University Ave, Muang District, Nakhon Ratchasima, 30000 Thailand. E-mail: Chanwit.paart@gmail.com; w.nuansing@g.sut.ac.th

² Center of Excellence on Advanced Functional Materials, Suranaree University of Technology, 111 University Ave, Muang District, Nakhon Ratchasima, 30000 Thailand.

* Corresponding author

DOI: <https://doi.org/10.55766/sujst-2023-05-e03020>

Suranaree J. Sci. Technol. 30(5):030149(1-5)

to improve the mechanical properties of the printed objects. In particular, the incorporation of carbon-based nanomaterials, such as graphene nanoplatelets (GNP), has shown great promise in enhancing the mechanical properties of various materials, including polymers, metals, and ceramics.

Graphene, a single layer of carbon atoms arranged in a hexagonal lattice, is known for its exceptional mechanical, thermal, and electrical properties (Lim *et al.*, 2017; Hanon *et al.*, 2021). GNP, a form of graphene produced by exfoliating graphene layers from graphite, possesses many advantages over other forms of graphene, such as high aspect ratio, low cost, and ease of production (Feng *et al.*, 2019; Markandan *et al.*, 2020). The incorporation of GNP into the resins used in LCD 3D printing has the potential to significantly enhance the mechanical properties of the printed objects.

In this study, we investigate the effectiveness of incorporating GNP into a UV-curable resin used in LCD 3D printing to enhance the mechanical properties of the printed objects. UV-curable resins are widely used in LCD 3D printing due to their fast-curing time, low shrinkage, and high resolution. However, the mechanical properties of the printed objects using UV-curable resins are often limited. Through a systematic characterization of the mechanical properties of the GNP-reinforced UV-curable resin, we aim to provide insights into the underlying mechanisms of the reinforcement effect and identify optimal processing conditions for the LCD 3D printing of high-performance objects. The study contributes to the field of vat photopolymerization by providing valuable insights into the enhancement of mechanical properties, specifically the elastic modulus and tensile strength, of 3D printed parts. Understanding the impact of GNPs on the resin matrix helps in the development of optimal printing parameters and conditions for composite materials, thereby advancing the application of vat photopolymerization 3D printing technology.

Methodology

This section provides a detailed account of the materials and equipment used in this research, along with the sample preparation, experimental and testing methodologies.

Material and Printer

The material used in this study was Puffermer3D resin (Hard) as the base material and Graphene nanoplatelets (GNP) obtained from Graphene Technology Co. Ltd. (Thailand) as the

reinforcing material. The resin was stored in a cool, dry place to prevent contamination. The 3D printer used in this study was the Elegoo Mars LCD 3D printer. The printer was calibrated and the build platform was leveled prior to printing.

Preparation and Printing Conditions

The printing conditions were varied to investigate their effects on the mechanical properties of the printed samples. The layer height was set to 0.05 mm, which is the highest resolution available on the Elegoo Mars LCD 3D printer. The exposure time was varied between 10, 20, and 30 sec for both the normal and GNP added resins. The concentration of GNP in the resin was 0.1% w/w. As shown in Figure 1, the printing orientation was varied between horizontal (x) and vertical (y) for each exposure time. After printing, the samples were post-exposed for 90 sec to ensure complete curing.

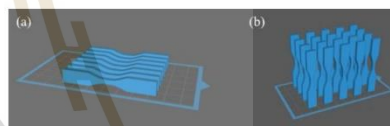


Figure 1. Printing orientation of specimens in horizontal (x) and vertical (y) axes, as shown in (a) and (b), respectively

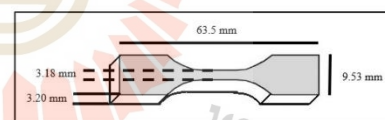


Figure 2. Demonstration of the dimensional schematic of the ASTM D638 Type V model utilized for tensile testing

Tensile Testing

Tensile testing was performed on an UTM Instron 5565 machine, which is capable of applying forces up to 100 kN. ASTM D638 type V standard model was used for the tensile testing, as in Figure 2. ASTM D638 is a standardized test method that outlines the procedures for evaluating the tensile properties of plastics and other resin materials (Kumar and Narayan, 2018). The test method provides guidelines for the preparation of the specimens, including their shape and size, as well as the testing apparatus and conditions. Specifically, the test involves using a dumbbell-shaped specimen. The test procedure involves subjecting the specimen

to a tensile force until it fractures, while monitoring the load and displacement. The test measures a range of mechanical properties including ultimate tensile strength, yield strength, elongation at break, and elastic modulus. These properties can be used to assess the strength, stiffness, and ductility of the material, and can be useful for material selection, design, and quality control purposes (Harding and Welsh, 1983). The accuracy requirements for the test frames and accessories used are also outlined in the standard, ensuring that the results obtained from different laboratories are comparable. In this work, the samples were placed in the UTM Instron 5565 machine and tested at the speed of 1 mm/min. The tensile testing was conducted until the sample broke, and the maximum load and elongation at break were recorded.

Result and Discussion

The obtained results revealed that the elastic modulus of the resin composite increased with exposure time, as illustrated in Figure 3(a). The solid and stripe plots in Figure 3(b) represent

the printing orientation of the specimens in the x and y axes, respectively. Interestingly, no significant difference was observed in the elastic modulus between the two printing orientations. These findings suggest that exposure time is a more critical factor than printing orientation in enhancing the elastic modulus of the resin composite. Furthermore, the data from this study provides valuable insights for the development of optimal printing parameters and conditions for the fabrication of composite materials using 3D printing technologies. Additional experiments can be conducted to further validate these findings and optimize the printing parameters for different composite materials.

Moreover, the effect of adding 0.1% w/w graphene mixed resin on the mechanical properties of 3D printed specimens was investigated. The results, as shown in Figures 4(a) and 4(b), indicate that there was a significant increase in elastic modulus and maximum tensile strength for specimens printed in the x-axis with 20 sec of exposure time.

The elastic modulus of the specimens increased by 28.3% while the maximum tensile

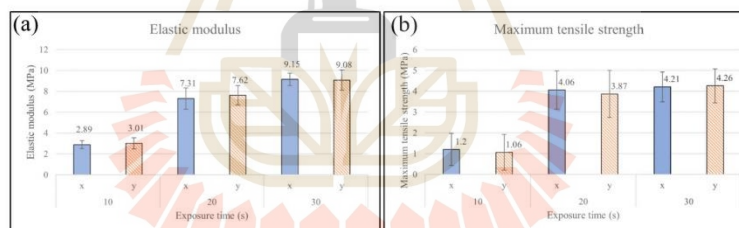


Figure 3. Plot of (a) elastic modulus and (b) maximum tensile strength over exposure time for both horizontal (x) and vertical (y) printing orientation

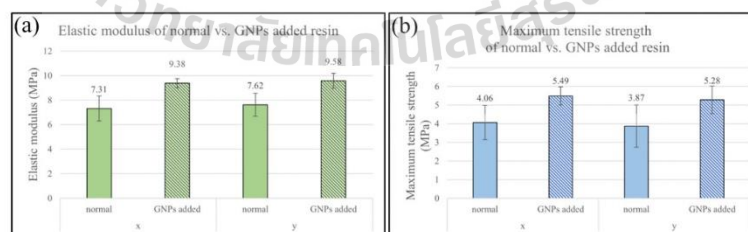


Figure 4. (a) Comparison of elastic modulus between normal resin and resin with added GNP, with 20 sec of exposure time, for horizontal (x) and vertical (y) printing orientations. (b) Comparison of maximum tensile strength between normal resin and resin with added GNP, with 20 sec of exposure time, for horizontal (x) and vertical (y) printing orientations

strength increased by 36.4%. This suggests that graphene nanoplatelets have a reinforcing effect on the composite material, resulting in improved mechanical properties.

The results also showed that there was no significant difference in mechanical properties observed between the x-axis and y-axis printing orientations. However, some studies have reported that printing orientation can indeed have an impact on the mechanical properties of 3D printed parts. The observed increase in load-bearing capacity before ultimate failure can be attributed to the angled arrangement of the print layers relative to the applied load. This structural configuration enhances the ability of the printed parts to withstand higher loads, resulting in improved mechanical performance (Saini *et al.*, 2020). While our study did not observe a significant difference in mechanical properties between the x-axis and y-axis printing orientations, it is worth noting that printing orientation can play a role in certain cases. The effect of printing orientation on mechanical properties can be influenced by factors such as the part geometry, layer adhesion, and anisotropic material behavior. It is possible that the specific resin matrix and GNPs used in our study mitigated the influence of printing orientation on the elastic modulus of the composite material. However, further investigations and specific experimental conditions may be required to fully understand the interplay between printing orientation and the mechanical properties of 3D printed parts in the context of resin composites with GNPs.

Overall, the addition of graphene nanoplatelets to the resin can be an effective method for improving the mechanical properties of 3D printed parts, which can be useful in various applications including aerospace, automotive, and biomedical industries. For instance, in the aerospace industry, these improved characteristics can contribute to the development of lightweight and durable components, leading to increased fuel efficiency and overall performance of aircraft systems. In the automotive sector, the augmented mechanical properties enable the production of stronger and more reliable parts, enhancing the safety and longevity of vehicles. Similarly, in the biomedical field, the heightened mechanical properties offer opportunities for fabricating patient-specific implants with superior strength and durability, thereby improving the success rates and longevity of medical interventions. The enhanced performance of these 3D printed parts holds great promise for advancing technological innovations and meeting the stringent requirements of these industries.

Conclusions

In conclusion, this study investigated the effect of adding graphene nanoplatelets (GNPs) to the resin for 3D printing of carbon-based composite materials using vat photopolymerization. The results showed that the addition of GNPs led to an increase in both elastic modulus and maximum tensile strength of the printed specimens. Specifically, the specimens printed in the x-axis with 0.1% w/w graphene mixed resin and 20 sec of exposure time showed the highest increase in both elastic modulus and maximum tensile strength. These findings demonstrate the potential of vat photopolymerization 3D printing for the production of graphene nanoplatelets composite materials with improved mechanical properties.

References

- Abdollahi, S., Davis, A., Miller, J.H., and Feinberg, A.W. (2018). Expert-guided optimization for 3D printing of soft and liquid materials. *PLOS ONE*, 13(4):e0194890 <https://doi.org/10.1371/journal.pone.0194890>
- Feng, Z., Li, Y., Xin, C., Tang, D., Xiong, W., and Zhang, H. (2019). Fabrication of graphene-reinforced nanocomposites with improved fracture toughness in net shape for complex 3d structures via digital light processing. *Journal of Carbon Research C*, 5(2):25. <https://doi.org/10.3390/c5020025>
- Hanon, M., Ghaly, A., Zsidai, L., Szakál, Z., Szabó, I., and Kátai, L. (2021). Investigations of the mechanical properties of dlp 3d printed graphene/resin composites. *Acta Polytechnica Hungarica*, 18(8):143-161. <https://doi.org/10.12700/APH.18.8.2021.8.8>
- Harding, J. and Welsh, L.M. (1983). A tensile testing technique for fibre-reinforced composites at impact rates of strain. *Journal of Materials Science*, 18:1810-1826. <https://doi.org/10.1007/BF00542078>
- Kumar, S.A. and Narayan, Y.S. (2018). Tensile testing and evaluation of 3d printed pla specimens as per astm d638 type-iv standard. In: *Innovative Design, Analysis and Development Practices in Aerospace and Automotive Engineering (I-DAD 2018)*. Chandrasekhar, U., Yang, L.J., and Gowthaman, S. (eds). Lecture Notes in Mechanical Engineering, Springer, Singapore. https://doi.org/10.1007/978-981-13-2718-6_9
- Lee, J.-Y., An, J., and Chua, C.K. (2017). Fundamentals and applications of 3D printing for novel materials. *Applied Materials Today*, 7:120-133. <https://doi.org/10.1016/j.apmt.2017.02.004>
- Lim, S.M., Shin, B.S., and Kim, K. (2017). Characterization of products using additive manufacturing with graphene/photopolymer-resin nano-fluid. *Journal of Nanoscience and Nanotechnology*, 17(8):5492-5495. <https://doi.org/10.1166/jnn.2017.14159>
- Malas, A., Isakov, D., Couling, K., and Gibbons, G.J. (2019). Fabrication of high permittivity resin composite for vat photopolymerization 3d printing: morphology, thermal, dynamic mechanical and dielectric properties. *Materials*, 12(23):3818. <https://doi.org/10.3390/ma12233818>

- Markandan, K. and Lai, C.Q. (2020). Enhanced mechanical properties of 3D printed graphene-polymer composite lattices at very low graphene concentrations. *Composites Part A: Applied Science and Manufacturing*, 129:105726. <https://doi.org/10.1016/j.compositesa.2019.105726>
- Saini, J., Dowling, I., Kennedy, J., and Trimble, D. (2020). Investigations of the mechanical properties on different print orientations in SLA 3D printed resin. In: *Proceedings of the Institution of Mechanical Engineers, Part C: Journal of Mechanical Engineering Science*, 234(11):2279-2293. <https://doi.org/10.1177/0954406220904106>
- Shahrubudin, N., Lee, T.C., and Ramlan, R. (2019). An overview on 3d printing technology: technological, materials, and applications. *Procedia Manufacturing*, 35:1286-1296. <https://doi.org/10.1016/j.promfg.2019.06.089>



CURRICULUM VITAE

Name : Chanwit Pa-art

Date of Birth : 18 September 1994

Place of Birth : 19 Moo 20, Muangdet, Det Udom, Ubon Ratchathani 34160

Education :

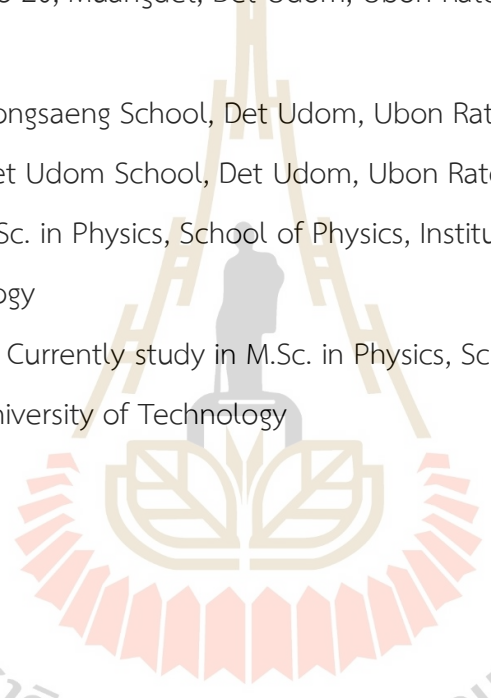
2001-2006 : Nongsaeng School, Det Udom, Ubon Ratchathani

2007-2013 : Det Udom School, Det Udom, Ubon Ratchathani

2014-2017 : B.Sc. in Physics, School of Physics, Institute of Science, Suranaree

University of Technology

2018-present : Currently study in M.Sc. in Physics, School of Physics, Institute of Science, Suranaree University of Technology



มหาวิทยาลัยเทคโนโลยีสุรนารี